Observer-based Fault Detection of Technical Systems over Networks

Von der Fakultät für Ingenieurwissenschaften

der Universität Duisburg-Essen

zur Erlangung des akademischen Grades eines

Doktor-Ingenieurs

genehmigte Dissertation

von

Wei Li

aus Jiangsu, V.R. China

Referent: Prof. Dr.-Ing Steven X. Ding

Korreferent: Prof. PhD Qing Zhao

Tag der mündlichen Prüfung: 28.05.2009

Acknowledgements

Behind every doctoral thesis lie years of hard work. It is therefore a great pleasure for me to thank those now who have given me the support and encouragement during all this time.

This thesis was written while the author was with the Institute for Automatic Control and Complex Systems (AKS) in the Faculty of Engineering at the University of Duisburg-Essen in Germany. I would like to thank Prof. Dr.-Ing. Steven X. Ding, the head of the institute, for his assistance in preparation of this thesis. His permanent support and interest enabled the presentation of this work. I would also like to thank Prof. PhD Qing Zhao from the University of Alberta for being my second supervisor.

I would like to express my gratitude to Prof. Dr.-Ing. Andreas Czylwik and M.Sc. Oliver Bredtmann from the Department of Communication Systems at the University of Duisburg-Essen for the cooperation and discussion in our research project.

Many thanks to all colleagues from the institute for making an inspiring and pleasant atmosphere. Special thanks to Dr.-Ing Ping Zhang, M.Sc. Cristian I. Chihaia, Dipl.-Ing Eberhard Goldschmidt, Dr.-Ing Ibrahim Al-Salami for valuable discussions and helpful suggestions, and many others who have been a great asset for me during my time in Duisburg and during the completion of this thesis.

Finally, I would like to express my gratitude to my family and to all friends for understanding and supporting me in whatever I decided to do - especially to my parents and Huihui, for their patience, love.

Duisburg, June 2009
Wei Li

To my parents

Contents

Notation and Symbols

Acronyms

FAR	false alarm rate
A/D	analog to digital
ARQ	automatic repeated request
BER	bit error rate
BSC	binary symmetric channel
FD	fault detection
FEC	forward error correction
LMI	linear matrix inequality
LTI	linear time invariant
MAC	medium access control
MJLS	Markov jumping linear system
MMP	model matching problem
NCS	networked control system
TDMA	time division multiple access

Mathematical Symbols

$\mathcal{RH}_\infty$	set of stable transfer functions
$co\{.\}$	convex set
$\|\|.\|\|_E$	l_2-norm of a stochastic vector signal
$\|\|.\|\|_e$	residual evaluation function
$\|\|.\|\|_2$	l_2-norm of a vector signal
$\|\|.\|\|_{peak}$	$peak$-norm of a vector signal
$E[.]$	expectation of a stochastic variable
$[.]_j$	the j-th row of a matrix
Pr	probability
X^T	transpose of X
A	system matrix
B	input matrix

C	output matrix
D	direct feedthrough matrix
E_d, F_d	disturbance distribution matrix
E_f, F_f	fault distribution matrix
$K(z)$	control law
L	observer gain
W	post filter
$\Delta(k)$	uncertainty in technical systems
T	length of residual evaluation window
u	control input
y_{dec}	decoded measurement
d	system disturbances
f	fault vector
y	output vector
r_j	the j-th residual signal
r	residual signal
x	state vector
e	estimation error of an observer
η_i	mean of the transmission error of the i-th measurement
$\sigma_{i,2}$	the second moment of the transmission error of the i-th measurement
$\sigma_{i,4}$	the fourth moment of the transmission error of the i-th measurement
Δ_i	transmission error of the i-th measurement
Δ_q	quantization error of a uniform quantizer, the coefficient of quantization error in a logarithmic quantizer
Δ_t	transmission error caused by bit errors and quantization errors
$\delta_{d,2}$	upper bound of the l_2-norm of disturbances
$\delta_{d,\infty}$	upper bound of the *peak*-norm of disturbances
J_{th}	threshold
Φ	transition matrix of a Markov Chain
$P(k)$	mode distribution of a Markov Chain
λ_{ij}	transition probability of a Markov Chain
N	number of modes of a Markov chain
ψ	mode space of a Markov chain or the state space of a switching system
θ_k	mode of a Markov jumping linear system
$p_i(k)$	the i-th mode probability of a Markov Chain
$\bar{p}_{i,b}$	upper bound of BER of the i-th measurement
p_b	BER vector
$p_{i,b}$	BER of the i-th measurement
T_s	sampling time
C_i^r	received code of the i-th measurement
C_i^t	transmitted code of the i-th measurement
τ	transmission delay in NCSs

N_k	distribution matrix of unknown inputs caused by bit errors and quantization errors
$\mathbb{L}(n_c, k_c)$	binary labeling
δ_q	parameter of a logarithmic quantizer
k_c	number of information bits in an (n_c, k_c) codeword
n_c	length of an (n_c, k_c)-codeword
$s(k)$	reliability class of the communication channel at the k-th time step
Y_i	quantized value belonging to the i-th partition cell
ϕ	decoding operator

Abstract

The introduction of networks into technical systems for facilitating remote data transmission, low complexity in wiring and easy diagnosis and maintenance, raises new challenges in fault detection (FD), such as how to handle network-induced time-varying transmission delays, packet dropouts, quantization errors and bit errors. These factors lead to increasing interest in developing new structures and design schemes for FD of technical systems over networks.

In this thesis all network-induced effects are analyzed and modeled systematically at first. By observing the stochastic inheritance of networks, an FD framework of Markov jumping linear systems is presented as a basis for the later developments. Then two observer-based schemes for the purpose of FD over networks with guaranteed false alarm rate (FAR) are proposed: a remote FD system and an FD system of networked control systems (NCSs). The remote FD scheme is for detecting faults in technical systems at a remote site, where system measurements are transmitted via networks. In this scheme, the coding mechanism of communication channels is investigated from the view point of control engineering and new methods are developed for optimal residual generation and evaluation by considering network-induced data loss and corruption. A novel design scheme of FD system is also developed for NCSs, where the technical system is networked, i.e. controllers, actuators and sensors are connected with communication channels. In this scheme, network-induced transmission delays, packet dropouts, quantization errors are taken into account for the design of the optimal FD system. The linear matrix inequalities (LMIs) and convex optimization techniques are applied for assisting the design procedures. The developed schemes are tested with numerical examples and implemented in a three-tank system benchmark, and their superiority to existing solutions is demonstrated.

Existing restrictions are overcome and new observer-based FD schemes over networks are introduced having the following characteristics: (1) the residual generators in both schemes are optimal in the sense of achieving the best trade-off between sensitivity to system faults and robustness against system disturbances and network-induced effects; (2) the proposed schemes can provide reliability information of rising fault alarms by analyzing the mean and variance of residual signals. Such information is very useful for practical applications in industries; (3) the design of residual generators and computation of thresholds can be efficiently solved by means of existing LMI-solvers.

1 Introduction

Due to growing demands on system performance and cost efficiency, the complexity and automation degree of modern technical systems are continuously increasing. In such complex systems, faults or abnormal changes of individual parts, e.g. actuators, sensors and components, can occur and result in economic dropout, system damage or even catastrophe. Hence guaranteeing the system safety and reliability becomes a critical issue on the design of automatic systems, and is often prescribed by authorities. For this purpose, the most important thing is to detect the faults in technical systems as early as possible. Motivated by these facts, the model-based FD technology has been intensively developed since the early 70's [3, 18, 30, 31, 87], which can provide valuable information about system faults. This technology has been fully integrated into many industrial processes and automatic control systems, e.g. vehicle control systems, robots, process control, power systems, transport systems, manufacturing processes. Among these existing model-based FD schemes, the observer-based technique has received more attention since 1990's, which has been developed in the framework of the well-established modern control theory.

Nowadays modern networks are widely used to link data points, which enable remote data transmission, reduce the complexity in wiring connection and the costs of media and provide ease in system diagnosis and maintenance. Because of these benefits, networks have been introduced into technical systems in last decades and new industrial network protocols have also been developed for the purposes of remote control and factory automation, e.g. Controller Area Network (CAN), Profibus, Foundation Fieldbus, ControlNet, Industrial Ethernet. With the decreasing price, increasing bandwidth, widespread usages, numerous software and applications and well-established infrastructure, general-purpose networks become major competitors to the mentioned industrial networks [102], such as Ethernet and Internet, which are originated from Slotted ALOHA [97] and ARPANET [80], respectively. The so-called NCSs, where the control loops are closed via networks, have been intensively investigated recently. On one side, new architectures of control systems are under research in order to take the advantages of the flexibility of networks. On the other side, there could be time varying transmission delays, packet dropouts, quantization errors and bit errors, as networks are with digital, shared mediums and have only limited bandwidth. Hence for the purpose of control over networks, a number of advanced control/filtering methodologies have been developed in order to handle these network-induced effects [102].

Very recently, the merger of techniques from FD and networks received more attention. Several new design schemes have been proposed for FD of technical systems over networks by considering the network-induced effects [1]. This thesis is going to answer the following two questions: how to design an observer-based remote FD system where the required data by the FD system are transmitted via networks and how to design an observer-based FD system for NCSs where the technical system itself is networked.

1.1 State of the art

In this section, the current state of the research in related fields, i.e. observer-based FD technique, control and FD over communication networks, will be given.

1.1.1 Observer-based FD

The basic idea of model-based FD system for a process is demonstrated by Fig. 1.1, where a process model is running parallel to the physical process and driven by the same inputs. In fault-free cases, if the process model is perfect and has no disturbances, the process outputs estimated by the model should follow the measured process outputs. In these cases the so-called *residual*, which is the difference between the estimated values and the measured values, should be zero. If there is a fault, the residual will be divergent from zero. Hence the residual presents important information about faults of the process. The procedure of creating the estimation and building the residual is called *residual generation*, and the process model including the comparison function is called *residual generator*. In fact, no technical systems can be modeled exactly and there are always different kinds of disturbances. Hence the residual is always influenced by the model uncertainties and disturbances. In order to extract the useful fault information from the residual signals, two strategies have been developed:

- replacing the process model with other advanced residual generators which are robust against model uncertainties and disturbances.
- evaluating the generated residual signals in order to distinguish the faults from disturbances. This procedure is call *residual evaluation* as shown in Fig. 1.1. The residual postprocessing and decision logic unit is called *residual evaluator*.

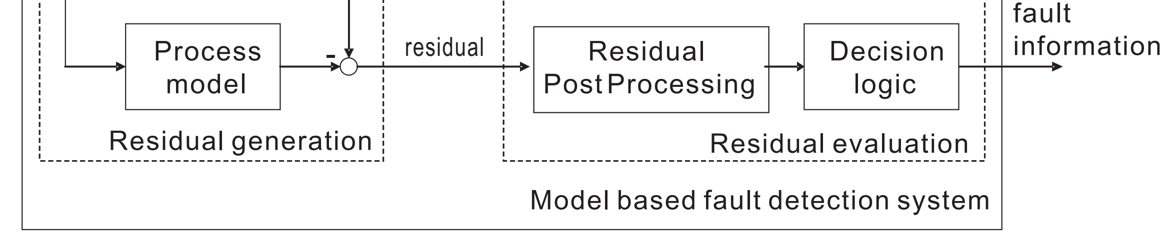

Figure 1.1: The model-based fault detection system.

Residual generation

The observer-based residual generator is one of the most important techniques developed for replacing the process model based one, which was initialized by Beard and Jones in the 1970's [2, 59]. The observer was first developed in the area of advanced control theory and can be used to reconstruct the system states with increased robustness against model uncertainties and disturbances. Since then the advanced control theory has been introduced into the development of FD techniques. But even with an observer, there could be estimation errors and thus the residual is still corrupted. With the development of unknown input decoupling control methods in the 1990's, a number of techniques were then developed to design observers which are decoupled from disturbances, such that the residual can directly indicate the faults (when there is no model uncertainties). The existence conditions of perfect unknown inputs decoupling observers have been given in different terms in [11, 21, 23, 48]. The frequency domain approach of designing such a decoupling observer has been proposed in [19, 32], which is based on simple multiplications and additions of transfer functions. In [88], the eigenstructure assignment approach has been presented. A geometric approach has also been given in [18, 79] for the decoupling observer design, in which the observer gain is selected to generate maximal uncontrollable subspace of the process and observers with low or minimum order can be obtained. There were also a number of contributions on unknown inputs decoupling observer (UIDO) technique and unknown inputs observer (UIO) technique, e.g. [41, 47], which have proposed different approaches to achieve disturbance decoupling. Recently, null matrix formulation has been applied for disturbance decoupling observer design and corresponding numerical solutions have been given in [34, 103].

Although there are a great number of approaches in the design of disturbance decoupling observers for residual generation, these techniques are restricted by their strong existence conditions and they are not optimal in the sense of fault detection. Many approaches concentrate on designing the residual generator with minimized H_∞ disturbance attenuation [60]. But simply reducing the influence of disturbances does not lead to an optimal performance of fault detection. For example when the disturbance decoupling is achieved, some faults may also be decoupled from the residual and thus can not be detected. Hence as mentioned in [31], the residual generator should be designed to maximize the robustness against model uncertainties as well as disturbances and simultaneously maximize the sensitivity to faults. A performance index was firstly proposed in [11] and [75] for an optimal design of parity vector in the parity space approach if a perfect disturbance decoupling is not achievable. Later a ratio index, i.e. H_2/H_2, has been introduced in [20] based on the system induced norm for the optimal design of observer-based residual generators, where the numerator represents the H_2-norm of the transfer function from faults to residuals and the denominator represents the H_2-norm of the transfer function from disturbances to residuals. Based on it, the time-frequency domain approach has been developed in [112]. Then residual generators have been designed to optimize the index H_∞/H_∞ in [22, 32, 91] and H_-/H_∞ in [73, 90, 104]. In [19] and [118] unified solutions to optimizing H_i/H_∞ have been proposed in a factorization approach for continuous-time system and discrete-time system, respectively, where H_i represents the i-th nonzero singular value of the transfer matrix from faults to residuals. Similar solutions to sampled-data systems and periodic systems can be found in [54, 116].

For the technical systems with both model uncertainties and disturbances, reference residual model strategies were applied to design an optimal residual generator, in which the original residual generation problem is transformed into a standard model matching problem (MMP). In most early works [9, 33], only faults were considered in the reference models. Hence the obtained residual generators were only sensitive to faults and may not be robust against system disturbances and model uncertainties. In [121] the residual generator has been designed to minimize the H_∞-norm of the difference between the residual generator and the reference model, where the reference model is an optimal solution for the robust fault detection under assumption that there is no model uncertainties. This approach can achieve an optimal trade-off between the sensitivity to faults and the robustness against model uncertainties and disturbances. Another way to handle residual generation with uncertainties is to extend the mentioned H_-/H_∞ or H_∞/H_∞ solutions in the H_∞/μ framework [46].

Until now the results of observer-based FD for systems with uncertainties are limited. Especially when the technical system has stochastic parameters, there are only few publications available. In [18] and [122], the residual generation of special classes of stochastic systems has been presented by applying the reference model strategy. The FD of uncertain systems and stochastic systems is one of the most interesting topics.

Residual evaluation

It is clear that if there is no model uncertainty in the process model and no disturbance in the process, faults can be detected when the residual is not equal to zero. But the residual is generally corrupted with model uncertainties and disturbances. To achieve successful fault detection based on available information, a norm-based residual evaluation strategy was proposed initially by [26] in the early stage of the development of model-based FD technologies. The basic idea is to distinguish the faults from uncertainties and disturbances by generating special features of the residual. For this purpose, the root-mean-square norm of the residual was used as the evaluation function and a threshold regarding to all possible model uncertainties and disturbances was selected to compare with the evaluated residual. Exceeding the threshold indicates a fault in the process and a *fault alarm* will be released. Based on this pioneering work, residual evaluation problems have been formulated in the H_∞-framework [22, 32, 58, 90], where the l_2-norm measuring the energy level of a signal is adopted as the residual evaluation function. The absolute value and the *peak*-norm of the residual were also used as the evaluation functions [18]. For different application purposes, different residual evaluation functions should be employed.

The major tools for the threshold selection are the robust control theory and the linear matrix inequality (LMI) technique [4, 94]. The norm-based residual evaluation strategies consider the worst case and thus may lead to a conservative threshold selection, but they provide a reliable and reasonable estimate of the threshold, such that false detections of faults are prevented and at the same time the missing detections of faults are reduced.

When the system parameters are stochastic, proper residual evaluation methods are still missing. By simply applying existing results from deterministic systems can result in poor fault detection performance. Hence the design of suitable residual evaluation methods for stochastic systems is also attracting more and more interests.

1.1.2 Control and filtering over networks

In the past few years, one of the important topics in control society is NCSs. Fig. 1.2 shows a typical structure of NCSs, where networks are used to establish the connection between the controller and the technical system (also called process) including sensors, plants and actuators [102]. The controller and process are physically located in different sites. The control signals are encapsulated in a packet and sent to the process via the network. The process then returns the process outputs to the controller by putting the sensor sampling into a packet as well.

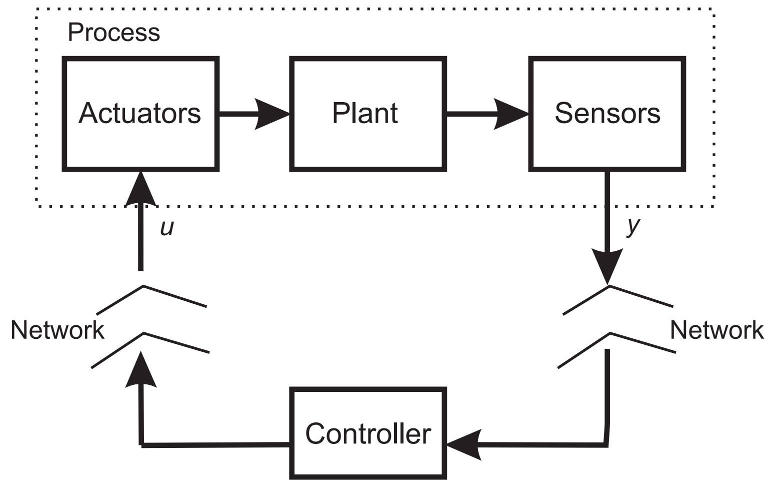

Figure 1.2: The structure of NCS.

Regardless of the type of networks applied, the overall performance of NCSs is always affected by *transmission delays* in the control loop since the network is connected with the control system [70]. Delays can degrade the performance of control systems. Existing constant time-delay control theory can not be directly used for NCSs, as the transmission delay is usually time varying and random. In the field of networking, random transmission delays have been modeled by using various formulations, such as Poisson process and Markov chain [93], fluid flow model [28] and Autoregressive moving average model [62]. These techniques have been brought into NCS formulations with modifications. For instance, Markov chain was firstly applied in [61, 82] and the stochastic stability of NCSs with transmission delays has been analyzed. In some early work, the time varying transmission delays have also been transformed into deterministic delays by using augmentation and queuing techniques; See [76, 77] and [8]. Then the conventional time-delayed system theory can be applied. With the development of robust control theory, a number of robust control approaches of NCSs have been proposed in last ten years which require only the upper (and lower) bound of transmission delays rather than their probability distributions [24, 49]. The main idea is to construct a suitable Lyapunov-Krasovskii function and then reformulate it in terms of LMIs. The controller design syntheses of NCSs have also been proposed. In [83], the controller design has been formulated as an linear-quadratic-Gaussian optimization problem. Later robust controllers have been obtained in the H_∞-framework [38].

Transmission failure is another rising challenge in NCSs. When the network applies medium access control (MAC), e.g. CSMA/CD, there could be packet collisions which can result in failures of data transmissions when the network load is high. Besides, disturbances from the environment and networks themselves can also result in failures of data transmissions, especially in wireless LAN and Internet. Usually the failure of data transmission is called *packet dropout*. Similar with transmission delays, packet dropouts can also degrade control performance. Markov chain is a reasonable model of the packet delivery characteristic in communication channels and it is widely used in literature. In [108, 111], stochastic stability conditions for NCSs with packet dropouts have been derived, where the NCSs have been formulated as Markov jumping linear systems (MJLSs) with some differences among these approaches. In [50, 57, 96] and [27, 109], the Kalman filtering problems with packet dropouts have been studied, where the packet dropouts have been modeled as a Bernoulli process or a Markov process.

Since modern networks are digital, analog signals are quantized with a limited resolution and then transformed into a sequence of binary bits, and finally transmitted via networks. The number of bits is interpreted as data rate from the view point of control engineering. Since the data rate is limited, there are always *quantization errors*. Besides, due to the noises in communication channels, there could also be *bit errors* [72]. The fundamental minimum data rate for the system stability has been intensively studied in [81, 99, 100]. In [100] the necessary and sufficient minimum data rate for the asymptotic observability and stability with noiseless channels (no bit errors in transmissions) has been derived. In [99], a necessary condition for the system stability with noisy channels (with bit errors in transmissions) has been studied. The influence of communications over noisy channels on linear quadratic Gaussian problem has been investigated in [101]. The main idea of these works is combining the dynamics of the system with the information theory [36] in order to derive the fundamental requirements of the information transmission. In [81] a similar result has been presented for the exponential stability. Besides, quantized feedback control systems have been analyzed and designed with different techniques in [5, 25, 43, 52, 71]. These works indicated that the feedback information can be useful with different levels of resolutions for different levels of system performances. In order to stabilize the system the minimum feedback information must be enough to compensate for the increase in the uncertainty due to the quantization.

Some papers addressing the analysis or synthesis problems with simultaneous consideration of the mentioned network-induced effects, i.e. transmission delays, packet dropouts and quantization errors, have been published very recently [37]. This is also the state-of-the-art of the research on NCSs.

1.1.3 FD over networks

Recently, the FD over communication networks has also attracted more attention. There are two kinds of schemes considered: the remote FD system and the FD system of NCSs. The first one is used to monitor technical systems at a remote site, where the data transmission from technical systems to the FD system is via networks. The second one is used to detect faults in technical systems where the technical systems themselves are NCSs.

There is a few literature contributed to the remote FD system design. In [68], bit errors appearing in wireless communication channels have been analyzed in the design of an observer-based residual generator of remote FD system where bit errors have been transformed into system uncertainties. In [69], a new kind of residual evaluation method has been proposed for remote FD with bit errors, in which the stochastic properties of bit errors have been investigated in order to compute thresholds. In [66], an observer-based remote FD system has been designed in a framework of stochastic uncertain systems by considering packet dropouts and quantization errors.

There are many works contributed to designing FD system of NCSs. A number of results have been obtained to deal with network-induced transmission delays. In [105, 106, 113, 114], the structure matrix of transmission delays has been extracted through Taylor approximation [113], eigendecomposition and Pade approximation [105], and Cayley-Hamilton theorem [106, 114]. Then conventional robust fault detection methods have been applied to achieve robustness against transmission delays. In [44, 45, 92], transmission delays have been modeled as Makrov processes. A deadbeat filter has been designed in [92] for the purpose of fault isolation. Robust filters minimizing the error between residuals and faults have been proposed in [44] and [45]. In [74] transmission delays have been estimated and compensated under a persistent excitation condition such that false alarms can be avoided in the residual evaluation. The FD problems of NCSs with packet dropouts have also attracted a lot of interests. In [117] the FD system for NCSs has been designed by modeling packet dropouts as a Markov process. In [39] the FD problem for uncertain systems with missing measurements modeled as a Bernoulli process has been studied. See also [44, 45]. The quantization errors have been considered in the FD design in [67] where the quantizer has been optimized for the purpose of FD.

To the author's best of knowledge, most of these approaches concentrated on the residual generator design and less attention has been paid to the residual evaluation for NCSs, especially when there are packet dropouts and bit errors. Due to the uncertain and stochastic properties of NCSs, the residual signals usually can not be well evaluated through existing methods. One of the current focuses of FD over networks is to find an optimal residual generator and a suitable residual evaluation approach.

1.2 Objectives

The main objective of this thesis is to develop new observer-based FD technologies, where networks are used for the purpose of data transmissions. Following problems are addressed:

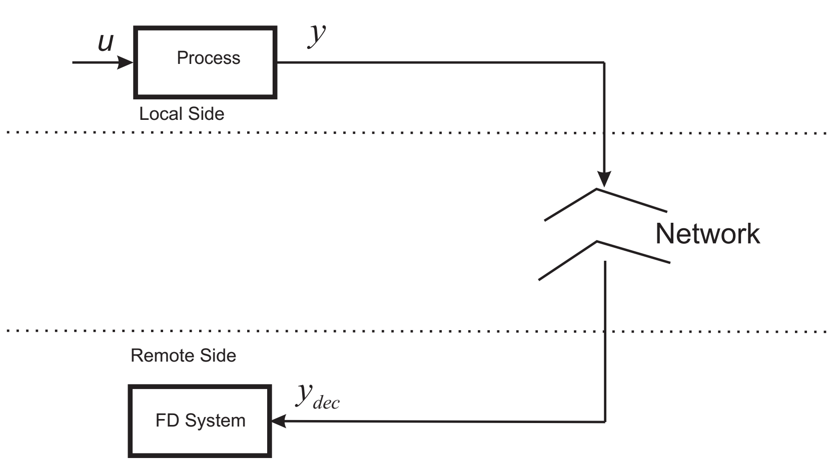

Figure 1.3: The structure of remote FD system.

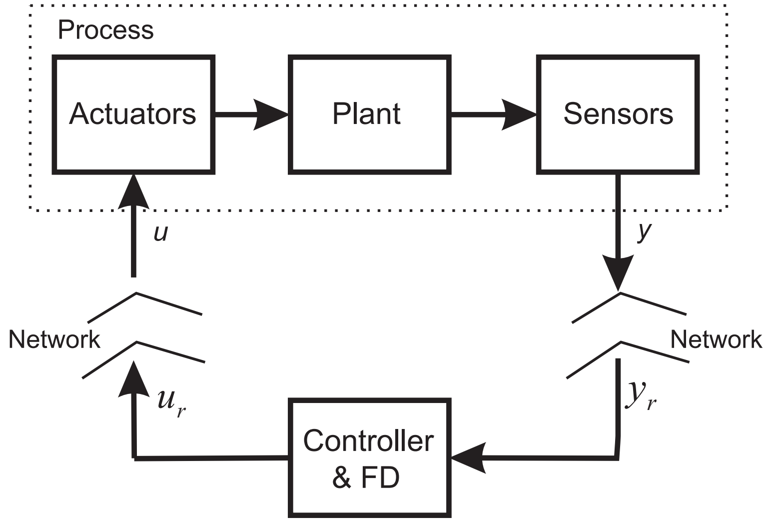

Figure 1.4: The structure of FD system of NCSs.

- modeling of technical systems and communication networks from the view point of control engineering. The network-induced transmission delays, packet dropouts, quantization errors as well as bit errors should be described in a systematic way.

- developing technologies of observer-based FD over networks. Two types of FD schemes are of interests:
  - Remote FD system (Fig. 1.3): The FD system is located at the remote side and connected to the process via communication channels, i.e. the process outputs are transmitted over networks to the FD system.
  - FD system of NCSs (Fig. 1.4): The FD system is designed for the purpose of detecting faults in the NCSs, i.e. the controller is connected to actuators and sensors with networks and the FD system is located together with the controller.

  Both of them include two parts: residual generation and residual evaluation. The design procedures should take the network-induced effects into consideration. The obtained residual generator should be robust against system disturbances and networked-induced effects and simultaneously sensitive to system faults. New residual evaluation methods should be developed, which can deal with stochastic residual signals.

The first scheme is useful for a long distance monitoring of technical systems. The second scheme is preferred when the technical systems are NCSs. In fact, the second scheme is more complicated than the first one, as the network-induced effects will influence the dynamics of the technical system, while it is not the case in the first scheme. Hence the focuses and the design procedures of two schemes are quite different.

1.3 Outline

After the introduction, the nominal and faulty behaviors of technical systems are described in the state-space form in chapter 2. In this chapter, communication networks are mathematically modeled from the view point of control engineering with which network-induced effects can be easily integrated into the description of technical systems.

In chapter 3, some definitions and preliminary theoretical background on residual generation and evaluation are given and then a new approach for designing observer-based FD system of MJLSs is proposed. These are the basis for the results presented in later chapters. The proposed FD system of MJLSs consists of: (1) an optimal residual generator which is sensitive to system faults and robust against system disturbances; (2) a novel residual evaluator with which residuals are evaluated by considering their statistical properties, such that the probability of the occurrences of false alarms is upper bounded and at the same time the missing detections of faults are also reduced. Numerical examples are given to illustrate the feasibility and effectiveness of the proposed approach.

In chapter 4, the remote FD system is presented where the applied communication channel could be either constant or time varying and the transmissions of measurements could be either centralized or decentralized. By employing a proper error control strategy in communications, the design procedure focuses on dealing with bit errors and quantization errors during transmissions. Their influence is first transformed into stochastic unknown inputs, and then their statistical properties are used for the design of the optimal residual generators and evaluators, which can bound the probability of false alarms with an adaptive threshold. To demonstrate the results, numerical examples are also given.

In chapter 5, the design approach of FD system of NCSs is proposed. The focus is how to deal with transmission delays, packet dropouts and quantization errors, which influence not only the FD system but also the dynamics of the NCS. The design problem is formulated in the framework of MJLSs with uncertainties. The results presented in chapter 3 are extended here. The obtained optimal residual generator has network-dependent parameters, and it is robust against network-induced effects and sensitive to system faults. The threshold in residual evaluation is also adaptive to the network-induced effects. A numerical example is used to illustrate the results.

In Chapter 6, the proposed schemes of FD over networks are applied in a three-tank system benchmark where the networks are simulated with Truetime toolbox and MATLAB/SIMULINK. The sensor faults, actuator faults and components faults are used to demonstrate the proposed schemes.

Chapter 7 gives the summary of the results and the outlook of future work.

2 Models of Technical Systems and Networks

The objective of this chapter is to model communication networks and technical systems from the view point of control engineering. The technical system is described in the input-output description and the state-space form. Different kinds of system uncertainties and disturbances are introduced. The network-induced effects, i.e. time varying transmission delays, packet dropouts, quantization errors and bit errors, are then described in a systematic way which can be integrated into the state-space form of technical systems.

2.1 Description of technical systems

In this thesis, the technical systems are assumed to be linear time invariant (LTI) and their nominal (disturbance-free and fault-free) behaviors can be described with the following state-space form:

$$\begin{aligned} x(k+1) &= Ax(k) + Bu(k), x(0) = x_0 \\ y(k) &= Cx(k) + Du(k) \end{aligned} \tag{2.1}$$

where $x \in \mathbb{R}^n$ is the state vector, x_0 the initial condition of the system, $u \in \mathbb{R}^{k_u}$ the input vector and $y \in \mathbb{R}^m$ the output vector. Matrices A, B, C, D are real constant matrices with appropriate dimensions.

The transfer matrix is an input-output description of the dynamic behavior of an LTI system in the frequency domain. The system (2.1) can be written as

$$y(z) = G_{yu}(z)u(z).$$

Here $G_{yu}(z) \in \mathcal{RH_\infty}^{m \times k_u}$ is the transfer matrix and it can be written as

$$G_{yu}(z) = C(zI - A)^{-1}B + D.$$

The system (2.1) is a state-space realization of $G_{yu}(z)$, and it is assumed that (2.1) is a minimal realization.

Remark 2.1 The technical systems can also be continuous-time systems. Since the communication networks are digital, the system outputs must be sampled with a given sampling rate at first, then quantized and transmitted. Such systems are called sampled-data systems and they can be equivalently written as a discrete-time system [53, 119]. Hence in this thesis, the discrete-time LTI system is used to describe the technical systems.

2.1.1 Representation of disturbances and uncertainties

In practice, the environmental interferences, measurements and process noises always exist in technical systems. These effects are usually modeled as system disturbances. By denoting $d \in \mathbb{R}^{k_d}$ as the disturbance vector, the description of the system (2.1) including disturbances can be written as

$$\begin{aligned} x(k+1) &= Ax(k) + Bu(k) + E_d d(k), x(0) = x_0 \\ y(k) &= Cx(k) + Du(k) + F_d d(k) \end{aligned} \tag{2.2}$$

where E_d, F_d are known disturbance distribution matrices of compatible dimensions. The corresponding input-output representation is

$$y(z) = G_{yu}(z)u(z) + G_{yd}(z)d(z)$$

where $G_{yd}(z)$ is the disturbance transfer matrix and

$$G_{yd}(z) = C(zI - A)^{-1}E_d + F_d.$$

Usually, it is difficult to obtain an exact model of a technical system due to unknown changes within the system or in the environment around the system. Hence there is always difference between the system model and the reality, which is called the model uncertainty. The representation of uncertainties is given in the state-space form. Consider the extended form of the system (2.2) given by

$$\begin{aligned} x(k+1) &= \tilde{A}x(k) + \tilde{B}u(k) + \tilde{E}_d d(k), x(0) = x_0 \\ y(k) &= \tilde{C}x(k) + \tilde{D}u(k) + \tilde{F}_d d(k) \end{aligned}$$

with

$$\begin{aligned} &\tilde{A} = A + \Delta A, \tilde{B} = B + \Delta B, \tilde{C} = C + \Delta C, \\ &\tilde{D} = D + \Delta D, \tilde{E}_d = E_d + \Delta E, \tilde{F}_d = F_d + \Delta F \end{aligned}$$

where $\Delta A, \Delta B, \Delta C, \Delta D, \Delta E$ and ΔF are the model uncertainties. There are two types of uncertainties widely accepted in literature:

- the norm bounded type

$$\begin{bmatrix} \Delta A & \Delta B & \Delta E \\ \Delta C & \Delta D & \Delta F \end{bmatrix} = \begin{bmatrix} E \\ F \end{bmatrix} \Delta(k) \begin{bmatrix} G & H & J \end{bmatrix} \tag{2.3}$$

  where E, F, G, H, J are known matrices of appropriate dimensions and $\Delta(k)$ is unknown but bounded by

$$\Delta(k)^T \Delta(k) \leq I$$

- the polytopic type

$$\begin{bmatrix} \Delta A & \Delta B & \Delta E \\ \Delta C & \Delta D & \Delta F \end{bmatrix} = co \left\{ \begin{bmatrix} \Delta A_1 & \Delta B_1 & \Delta E_1 \\ \Delta C_1 & \Delta D_1 & \Delta F_1 \end{bmatrix}, \dots, \begin{bmatrix} \Delta A_l & \Delta B_l & \Delta E_l \\ \Delta C_l & \Delta D_l & \Delta F_l \end{bmatrix} \right\} \tag{2.4}$$

where $\Delta A_i, \Delta B_i, \Delta C_i, \Delta D_i, \Delta E_i, \Delta F_i, i = 1, \cdots, l$, are known matrices of appropriate dimensions and $co\{.\}$ denotes a convex set defined by

$$co\left\{\begin{bmatrix} \Delta A_1 & \Delta B_1 & \Delta E_1 \\ \Delta C_1 & \Delta D_1 & \Delta F_1 \end{bmatrix}, \cdots, \begin{bmatrix} \Delta A_l & \Delta B_l & \Delta E_l \\ \Delta C_l & \Delta D_l & \Delta F_l \end{bmatrix}\right\}$$
$$= \sum_{i=1}^{l} \alpha_i \begin{bmatrix} \Delta A_i & \Delta B_i & \Delta E_i \\ \Delta C_i & \Delta D_i & \Delta F_i \end{bmatrix}, \sum_{i=1}^{l} \alpha_i = 1, \alpha_i \geq 0.$$

2.1.2 Representation of faults

The system faults can be divided into three categories:

- sensor faults which cause the abnormal changes on process measurements,
- actuator faults which cause the abnormal changes in the actuators, and
- component faults which are the malfunctions within the plant.

The widely used way to model faults is to extend the system (2.2) as follows:

$$\begin{aligned} x(k+1) &= Ax(k) + Bu(k) + E_d d(k) + E_f f(k), x(0) = x_0 \\ y(k) &= Cx(k) + Du(k) + F_d d(k) + F_f f(k) \end{aligned} \tag{2.5}$$

where $f \in \mathbb{R}^{k_f}$ is the vector of faults to be detected and E_f, F_f are the fault distribution matrices indicating the influence of faults on the system. Here f is assumed to be a deterministic time function. The corresponding input-output representation is

$$y(z) = G_{yu}(z)u(z) + G_{yd}(z)d(z) + G_{yf}(z)f(z) \tag{2.6}$$

where $G_{yf}(z)$ is the fault transfer matrix and

$$G_{yf}(z) = C(zI - A)^{-1}E_f + F_f.$$

Remark 2.2 According to the way how they affect the system dynamics, the faults described in (2.5) are called additive faults. There is another kind of faults called multiplicative fault. Generally, the multiplicative faults can be reformulated as additive faults [18]. Hence this thesis will focus on the detection of additive faults.

2.2 Model of network-induced effects

Recent development in communication theory has contributed toward achieving the reliability required by the high speed communication systems, and the use of coding and decoding has become an integral part in the design of modern communication systems [15]. Typically such a system may be represented by the block diagram shown in Fig. 2.1. In this case, a physical process is regarded as the information source and its outputs, which are going to be transmitted to the destination, are continuous variables, e.g. process outputs y. The source encoder transforms the source outputs into a sequence of k_c binary bits which is called the information sequence. This encoder usually uses a quantizer with

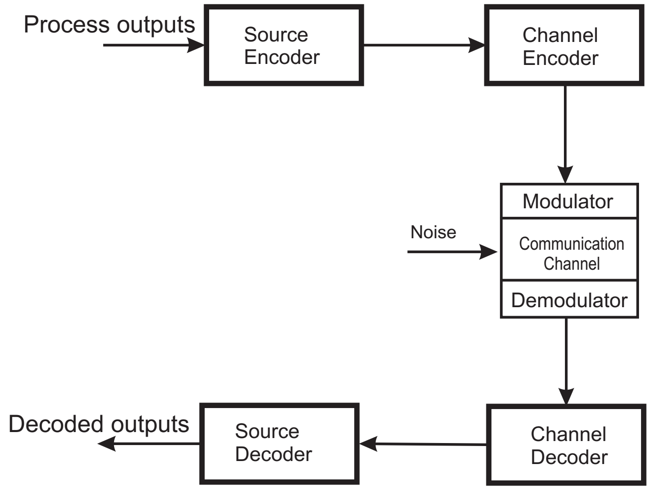

Figure 2.1: The scheme of communication systems.

a finite number of levels. The channel encoder transforms the information sequence into a discrete encoded sequence, called a codeword, of the length n_c ($n_c \geq k_c$) which is also a binary sequence. The channel encoders are designed and implemented to combat the noisy environment as the noise may cause some decoding errors. The generated codeword is encapsulated into a packet and then transmitted via the network channels. The channel decoder transforms the received sequence into a binary sequence called the estimated information sequence. The decoding strategies, e.g. hard-decision decoding and soft-decision decoding, are based on the rules of channel encoding and the noise characteristics of the channel. The channel decoders are designed and implemented to minimize the probability of decoding errors. The estimated information sequence can be completely correct or with detected but uncorrectable bit errors or with undetected bit errors. Bit errors are typical in wireless communication channels, while the probability of occurring bit errors in wired networks could be small. The source decoder transforms the estimated information sequence into an estimate of the source outputs which is called decoded outputs. The difference between the process outputs and the decoded outputs is defined as the *transmission error*.

The networks usually have shared medium with limited bandwidth. Therefore certain MAC methods are applied to arrange the network communication. For system with time division multiple access (TDMA), different time slots are assigned to different nodes for accessing the network. TDMA is used in Fieldbus, bluetooth, etc. The carrier sensing multiple access/collision avoidance (CSMA/CA) is applied in the standard IEEE 802.3 Protocol in which different nodes in the network compete for the access right in order to avoid packet collisions. Due to the applied MAC methods, network load and disturbances in the environment, the packets can be dropped and their arrivals at destination can be delayed. The transmission delay is the difference between the time instance of sampling measurement and the time instance of receiving the decoded outputs. It includes the preprocessing delay in encoding, the waiting time, frame time and propagation time in channels and the postprocessing time in decoding [70].

Before designing the FD system over networks, it is necessary to describe these features of networks from the view point of control engineering.

2.2.1 Quantization errors

The dictionary definition of quantization is the division of a quantity into a discrete number of small parts. In digital control systems, the quantization is usually understood as an analog to digital (A/D) conversion with a limited resolution. More generally, a quantizer is defined as consisting of a set of partition cells $\mathcal{S} = \{\mathcal{S}_i, i \in \mathcal{I}\}$, where the index set $\mathcal{I}$ is a collection of consecutive integers, together with a set of quantized values $\mathcal{C} = \{Y_i, i \in \mathcal{I}\}$, so that the quantizer is defined by $Q(v) = Y_i$ for $v \in \mathcal{S}_i$ [42]. The quantization error is defined as the difference between the real values and the quantized values.

There are two kinds of quantizers widely used in different applications: uniform quantizer and logarithmic quantizer. A quantizer is said to be uniform when the quantized values Y_i are equally spaced and the size of S_i is the same. Fig. 2.2 shows an example of the uniform quantizer. If Y_i is at the center of $\mathcal{S}_i$, then the quantization error, i.e. $\Delta_q = v - Q(v)$, is in $[-l/2, l/2]$ with the size of S_i being l.

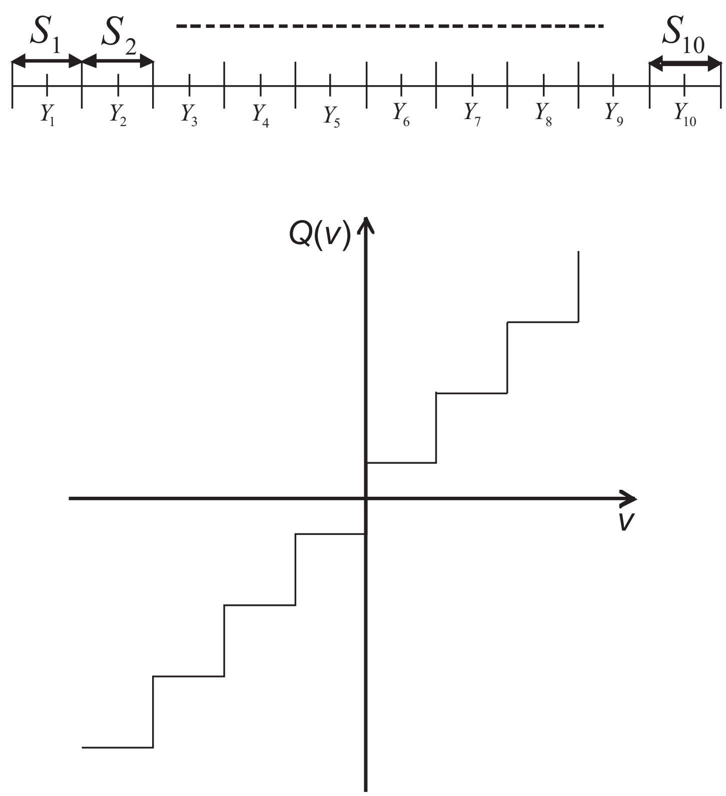

Figure 2.2: An example of uniform quantizer.

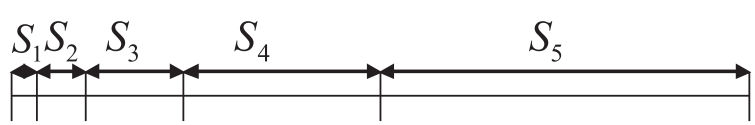

Figure 2.3: An example of logarithmic quantizer.

When the size of S_i obeys a logarithmic function as shown in Fig. 2.3, then the quantizer is called the logarithmic quantizer. The position of Y_i can be selected as the middle of S_i

or according to other criteria. One of the logarithmic quantizer widely accepted in control applications was proposed in [25], which is

$$Q(v) = \begin{cases} \rho^i v_0 & \text{if } \frac{1}{1+\delta_q}\rho^i v_0 < v \leq \frac{1}{1-\delta_q}\rho^i v_0, v > 0 \\ 0 & \text{if } v = 0 \\ -Q(-v) & \text{if } v < 0 \end{cases} \tag{2.7}$$

where $0 < \rho < 1$, $v_0 > 0$ is the maximum possible value of v and

$$\delta_q = \frac{1-\rho}{1+\rho}.$$

It is well known that [35], a suitable model for the logarithmic quantizer $Q(v)$ with parameter δ_q consists in the following multiplicative random map

$$Q(v) = (1 + \Delta_q)v$$

where $\Delta_q \in [-\delta_q, \delta_q]$. Hence the quantization error is $\Delta_q v$, which depends on v and the quantization parameter δ_q.

2.2.2 Bit errors

In this thesis, the communication channel in networks is assumed to a binary symmetric channel (BSC). A BSC is a practically important and simple channel model in communications [72]. For a BSC, as shown in Fig. 2.4, the received bit can be different from the transmitted one with a probability p_b, where p_b is called the bit error rate (BER). Bit errors in different positions of the codeword are independent. That means if an n_c-bit codeword is transmitted, each bit can be incorrectly received with the probability p_b. In other words, a binary error sequence of n_c-bit will be added to the transmitted codeword. Such a binary error sequence is called an error pattern. For n_c-bit codewords, there are 2^{n_c} different error patterns.

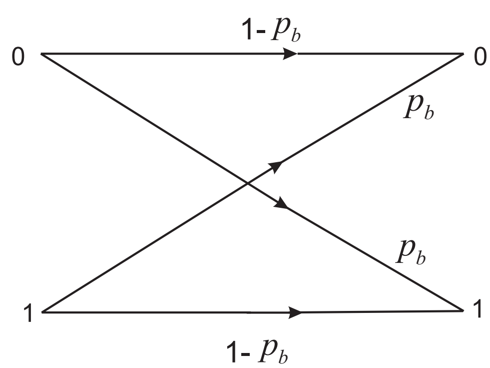

Figure 2.4: BSC bit error rate diagram

The probabilities of occurrences of different error patterns can be calculated based on p_b as follows

$$P_i^e = p_b^{w(i)}(1-p_b)^{n_c - w(i)}, \; i = 1, \cdots, 2^{n_c}. \tag{2.8}$$

Here $w(i)$ is the weight which is equal to the number of non-zero bits of each error pattern. Generally, the bit error probability p_b can be calculated from the knowledge of the modulator used and the statistical properties of the noise. In this case, the bit error rate is given by

$$p_b = \frac{1}{\sqrt{2\pi}} \int_{\sqrt{2E_s/N_0}}^{\infty} e^{-y^2/2} dy \tag{2.9}$$

where E_s is the symbol energy level and N_0 is the noise energy level [72].

2.2.3 Packet dropouts

The packet dropout is a typical feature of network communications. As shown in Fig. 1.4, when networks are introduced into technical systems for the purpose of control and FD, such packet dropouts can result in losses of process inputs or process outputs. The simple and popular method to model packet dropout behavior is using the i.i.d. Bernoulli model or the Gilber-Elliott model [107]. In the i.i.d Bernoulli model, a Bernoulli random variable α_k indicates whether the packet at the k-th time step is successfully received or not. If it is received, then $\alpha_k = 1$, otherwise $\alpha_k = 0$. For any k, α_k is i.i.d. distributed with the probability:

$$\Pr\{\alpha_k = 1\} = \lambda, \Pr\{\alpha_k = 0\} = 1 - \lambda, \lambda \in [0, 1].$$

The Gilbert-Elliott model considers the network as a discrete-time Markov chain with two possible states: "good" and "bad". In the "good" state, the packet is successfully received with a higher probability, and in the "bad" state, the packet is dropped with a higher probability. The network jumps between two states follow a Markov chain with transition probability matrix Φ as

$$\Phi = \begin{bmatrix} \lambda_{00} & \lambda_{01} \\ \lambda_{10} & \lambda_{11} \end{bmatrix},$$

where 1 is the "good" state, 0 is the "bad" state and λ_{ij} is the transition probability:

$$\lambda_{ij} = \Pr\{\text{current state} = j | \text{previous state} = i\}, i, j \in \{0, 1\}.$$

The Gilbert-Elliott is able to capture the dependence between consecutive packet dropouts, i.e. bursty packet dropping. The model can be easily extended to Markov chains with more possible states, but no significant improvement can be obtained to model the packet dropout behavior [107]. When the sampling period of the process is larger enough, the dependency between consecutive packet dropouts could be neglected. In this case, the Bernoulli model can be applied.

2.2.4 Transmission delays

Time-delay systems have been intensively investigated in the past. Hence the time varying transmission delay is not a completely new problem for control and FD. By extending the existing results and using existing tools, e.g. Lyapunov-Krasovskii functions, the transmission delay can be handled [24, 49].

In [44, 45, 92], transmission delays were modeled as a Markov chain, i.e.

$$\lambda_{ij} = \Pr\{\tau(k+1) = j | \tau(k) = i\},$$

where $\{\tau(k)\}$ is assumed to take values in the finite state space $\{-1, 0, \cdots, N\}$, N is a positive integer. In practice, λ_{ij} is difficult to obtain.

In [106, 113, 114], the structure matrix of transmission delays were derived and then the delays were transformed into unknown inputs or system uncertainties. This method requires only the upper bound and lower bound of transmission delays, which are usually available. In the rest of this thesis, this description of transmission delays is adopted.

3 Background and Some Preliminary Results

In this chapter, the background of FD with focus on the observer-based approach is introduced and then the FD problem of MJLSs is investigated. They are useful for the later analysis and design of FD system over networks. The key results on residual generation and residual evaluation for LTI systems are presented at first, including the unified solution to an optimal FD. Based on that, the FD problem of MJLSs is formulated. An optimal residual generator is designed by applying a new reference residual model and a novel residual evaluation method is proposed to detect the occurrences of faults with a guaranteed false alarm rate (FAR).

3.1 FD of linear time-invariant systems

Some standard results on FD problems will be briefly presented here. As mentioned in the first chapter, the observer-based FD technology includes two steps: residual generation and residual evaluation. Consider an LTI discrete-time system given in (2.5) and (2.6). Without loss of generality, the following assumptions are made throughout the thesis:

- (A3.1) (C, A) is detectable.
- (A3.2) $\begin{bmatrix} A - e^{j\theta}I & E_d \\ C & F_d \end{bmatrix}$ has full row rank for all $\theta \in [0, 2\pi)$.

The two assumptions are standard in robust control theory.

The following notations are used throughout the thesis: X^T is the transpose of a matrix X. $X > 0$ denotes a positive definite matrix. In a symmetric matrix

$$\begin{bmatrix} \ddots & X_1 \\ * & X_2 \end{bmatrix}$$

where $X_2 = X_2^T$, $*$ denotes the symmetric entry which is equal to X_1, and the empty entries are zeros. $[.]_j$ denotes the j-th row of a matrix or vector.

3.1.1 On residual generation

Let $(\hat{M}_u(z), \hat{N}_u(z))$ be a left coprime factorization pair of G_{yu} [123], i.e.

$$G_{yu} = \hat{M}_u(z)^{-1}\hat{N}_u(z), \hat{M}_u(z), \hat{N}_u(z) \in \mathcal{RH}_\infty.$$

With assumptions (A3.1) and (A3.2), $\hat{M}_u(z)G_{yd}(z), \hat{M}_u(z)G_{yf}(z) \in \mathcal{RH}_\infty$. In [21], a parametrization of all LTI residual generators was proposed as follows:

$$r(z) = R(z)(\hat{M}_u(z)y(z) - \hat{N}_u(z)u(z)) \tag{3.1}$$

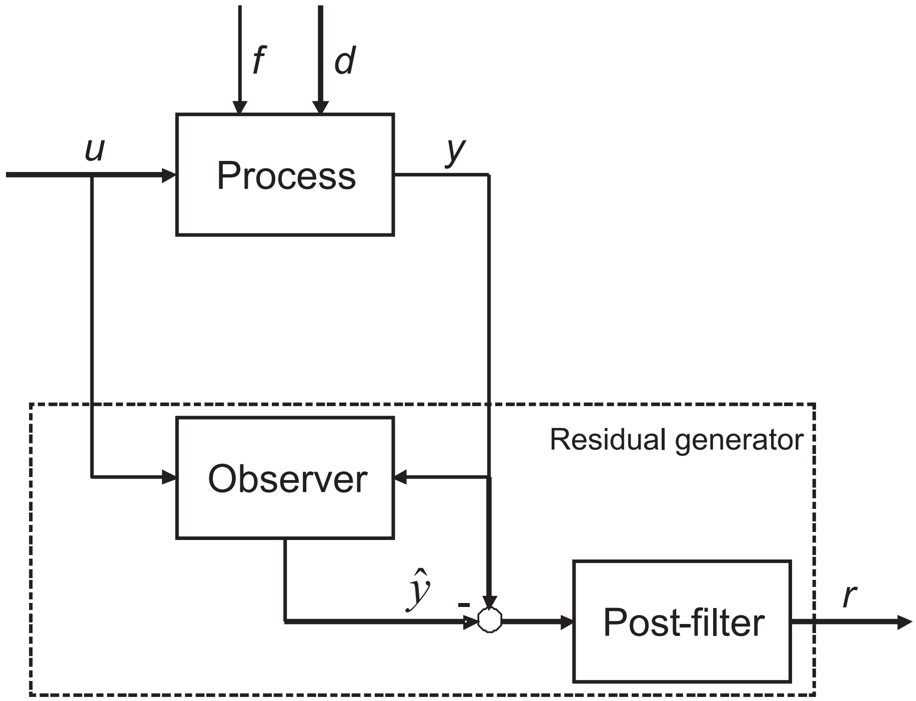

Figure 3.1: Observer-based residual generator

where $r(z)$ is the residual vector and $R(z) \in \mathcal{RH}_\infty$ is the so-called post-filter that is arbitrarily selectable. Obviously, the dynamics of (3.1) is governed by

$$r(z) = G_{rd}(z)d(z) + G_{rf}(z)f(z)$$

with

$$G_{rd}(z) = R(z)\hat{M}_u(z)G_{yd}(z), G_{rf}(z) = R(z)\hat{M}_u(z)G_{yf}(z).$$

The corresponding observer-based residual generator shown in Fig. 3.1 is given by

$$\begin{aligned} \hat{x}(k+1) &= A\hat{x}(k) + Bu(k) + L(y(k) - \hat{y}(k)) \\ \hat{y}(k) &= C\hat{x}(k) + Du(k) \\ r(k) &= W(y(k) - \hat{y}(k)) \end{aligned} \tag{3.2}$$

where $\hat{x}(k) \in \mathbb{R}^n$ is the estimated state vector and $\hat{y}(k) \in \mathbb{R}^m$ the estimated output vector. L, W are the observer gain and the post-filter, respectively, which are both design parameters.

Define $e(k)$ as the estimation error, i.e.

$$e(k) = x(k) - \hat{x}(k).$$

The dynamics of (3.2) in the state-space form can be described through

$$\begin{aligned} e(k+1) &= (A - LC)e(k) + (E_d - LF_d)d(k) + (E_f - LF_f)f(k) \\ r(k) &= W(Ce(k) + F_d d(k) + F_f f(k)) \end{aligned} \tag{3.3}$$

and the coprime factors can be expressed as

$$\begin{aligned} \hat{M}_u(z) &= I - C(zI - A + LC)^{-1}L, \\ \hat{N}_u(z) &= D + C(zI - A + LC)^{-1}(B - LD). \end{aligned}$$

The observer gain is a constant matrix and it should be selected such that the residual generator (3.2) is stable. The post-filter is arbitrarily selectable and it can be either constant or dynamic. The selection of W can be done independent of the selection of L. If W is constant, then $G_{rd}(z)$ and $G_{rf}(z)$ can be written as

$$\begin{aligned} G_{rd}(z) &= WF_d + WC(zI - A + LC)(E_d - LF_d), \\ G_{rf}(z) &= WF_f + WC(zI - A + LC)(E_f - LF_f). \end{aligned}$$

The design of a residual generator has been formulated as following typical fault detection, isolation and identification problems:

- Perfect disturbance decoupling problem (PDDP), in which $R(z)$ or L and W are selected such that
$$G_{rd}(z) = 0, G_{rf}(z) \neq 0.$$
That means the residual signals are only influenced by the faults. It is solvable, if and only if
$$rank \begin{bmatrix} G_{rd}(z) & G_{rf}(z) \end{bmatrix} > rank \begin{bmatrix} G_{rd}(z) \end{bmatrix}.$$

- Perfect fault isolation problem (PFIP), which is going to find $R(z)$ or L and W satisfying
$$G_{rd}(z) = 0, G_{rf}(z) = diag\{t_1(z), \cdots, t_{k_f}(z)\} \in \mathcal{RH}_\infty.$$
This problem can be reformulated as a set of PDDPs.

- Exact fault identification problem (EFIP), in which
$$G_{rd}(z) = 0, G_{rf}(z) = I_{k_f \times k_f}.$$
The strict existence condition of EFIP is that $G_{yf}(z)$ is left invertible in $\mathcal{RH}_\infty$.

- H_∞ optimal fault identification problem, in which $R(z)$ or L and W are selected such that β is minimized under a given γ, where
$$\|G_{rd}(z)\|_\infty < \gamma, \|I - G_{rf}(z)\|_\infty < \beta.$$
That means the residual signals will robustly reconstruct the faults.

The above formulated problems can not achieve the best trade-off between system robustness against unknown disturbances and system sensitivity to the faults. Hence the ratio-type performance index

$$J = \frac{\text{influence of faults}}{\text{influence of unknown disturbances}} \tag{3.4}$$

is suggested to address the influence of disturbances and faults on the residual signals simultaneously. The maximization of (3.4) leads to the optimal design of the residual generator (3.2), which is formulated as the following optimization problem:

- H_i/H_∞ optimal design problem, in which
$$\sup_{R(z)\in\mathcal{RH}_\infty} \frac{\sigma_i(G_{rf}(e^{j\theta}))}{\|G_{rd}(z)\|_\infty} = \sup_{L,W} \frac{\sigma_i(WF_f + WC(zI - A + LC)(E_f - LF_f))}{\|WF_d + WC(zI - A + LC)(E_d - LF_d)\|_\infty} \tag{3.5}$$
is maximized for all $\theta \in [0, 2\pi)$, where σ_i is the nonzero singular values measuring the influence of faults in each direction of the subspace spanned by $G_{rf}(e^{j\theta})$.

The following theorem gives the unified solution for optimizing the index (3.5).

Theorem 3.1 *[18] Given a residual generator*

$$r(z) = R(z)(\hat{M}_u(z)G_{yd}(z)d(z) + \hat{M}_u(z)G_{yf}(z)f(z))$$

for an LTI system

$$y(z) = G_{yu}(z)u(z) + G_{yd}(z)d(z) + G_{yf}(z)f(z)$$

where $G_{yu}(z) = \hat{M}_u(z)^{-1}\hat{N}_u(z)$. *If*

$$\hat{M}_u(e^{jw})G_{yd}(e^{jw})G^*_{yd}(e^{jw})\hat{M}^*_u(e^{jw}) > 0, \forall w \in [0, 2\pi),$$

then

$$R_{opt}(z) = G^{-1}_{do}(z)$$

solves the optimization problem (3.5), where

$$\hat{M}_u(z)G_{yd}(z) = G_{do}(z)G_{di}(z), \hat{M}_u(z), \hat{N}_u(z) \in \mathcal{RH}_\infty$$

and $G_{do}(z)$ *is the* $\mathcal{RH}_\infty$*-left-invertible co-outer of* $\hat{M}_u(z)G_{yd}(z)$*, and* $G_{di}(z)$ *is the co-inner containing all right half complex plane zeros of* $\hat{M}_u(z)G_{yd}(z)$ *and satisfying* $G_{di}(z)G^*_{di}(z) = I$.

The optimal post filter given above is in frequency domain. In order to compute the co-outer $G_{do}(z)$, the following lemma is introduced.

Lemma 3.2 *[51] Consider* $G(z)$ *realized by* (A, B, C, D)*, without zeros on the unit circle, and suppose that* (A, B, C, D) *is stabilizable and has no unreachable null modes and no unobservable modes on the unit circle. Then* $G(z)$ *has an inner-outer factorization as* $G(z) = G_i(z)G_o(z)$*, where*

$$G_i(z) = D\Gamma + (C + DF)(zI - (A + BF))^{-1}B\Gamma$$

is inner and

$$G_o(z) = \Theta - \Theta F(zI - A)^{-1}B$$

is outer, (X, F) *is the stabilizing solution to the following discrete-time algebraic Riccati system*

$$\begin{bmatrix} A^TXA - X + C^TC & A^TXB + C^TD \\ B^TXA + D^TC & D^TD + B^TXB \end{bmatrix} \begin{bmatrix} I \\ F \end{bmatrix} = 0$$

and $D^TD + B^TXB \geq 0$, Θ *is an appropriate surjective matrix satisfying* $\Theta^T\Theta = D^TD + B^TXB$, Γ *is the right inverse of* Θ.

Now it is the position to give the optimal post filter $R(z)$ in the state-space form.

Theorem 3.3 *[18] Consider system*

$$\begin{aligned} x(k+1) &= Ax(k) + Bu(k) + E_d d(k) + E_f f(k), x(0) = x_0 \\ y(k) &= Cx(k) + Du(k) + F_d f(k) + F_f f(k) \end{aligned} \tag{3.6}$$

with assumptions (A3.1) and (A3.2). Then the residual generator (3.2) with

$$L_o = -L_d, W_o = W_d$$

delivers the residual signal $r(k)$ *that is the optimum in the sense of maximizing (3.5), where* W_d *is the left inverse of a full column rank matrix* H_d *satisfying*

$$H_d H_d^T = C X_d C^T + F_d F_d^T,$$

and (X_d, L_d) *is the stabilizing solution to the discrete-time algebraic Riccati system*

$$\begin{bmatrix} A X_d A^T - X_d + E_d E_d^T & A X_d C^T + E_d F_d^T \\ C X_d A^T + F_d E_d^T & C X_d C^T + F_d F_d^T \end{bmatrix} \begin{bmatrix} I \\ L_d \end{bmatrix} = 0.$$

3.1.2 On residual evaluation

The residual evaluation problem of deterministic systems has been intensively studied. In ideal cases, the residual signals should be zero when there is no fault. But considering the system (3.3), it is clear that the residual signal $r(k)$ is always corrupted by $d(k)$. Hence the core task of residual evaluation is to distinguish the faults from the disturbances. The simplest way to evaluate the residual signal is computing its size at each time instant and then comparing it with threshold, where the threshold is computed considering all possible disturbances and uncertainties in the system.

Naturally, various norms of residual are used to measure its size, e.g. l_2-norm measuring the energy level and *peak*-norm measuring the maximum absolute value. The l_2-norm is widely accepted as the residual evaluation function [23, 32], which is

$$\|r(k)\|_2 = \left\{ \sum_{i=0}^{\infty} r(i)^T r(i) \right\}^{\frac{1}{2}}$$

where $||.||_2$ stands for the l_2-norm of a signal. Since an evaluation of residual over the whole time is usually unrealistic, the evaluation function is computed in a time window, which is

$$\|r(k)\|_e = \|r(k)\|_T = \sqrt{\sum_{j=k-T+1}^{k} r(j)^T r(j)} \tag{3.7}$$

with T being the length of the evaluation window and $||.||_e$ denoting the evaluation function of residual. In case of no fault, the residual is determined by $d(k)$. According to (3.3),

$$\|r(k)\|_2 \leq ||G_{rd}(z)||_\infty \|d(k)\|_2.$$

If $\|d(k)\|_2 \leq \delta_{d,2}$, in fault-free cases

$$\|r(k)\|_T \leq \|r(k)\|_2 \leq ||G_{rd}(z)||_\infty \delta_{d,2}.$$

Hence the threshold should be tolerant to disturbances. As widely accepted in literature, the threshold can be selected as

$$J_{th} = \min_{\gamma} \gamma \delta_{d,2}$$

subject to

$$\gamma > \sup_{d \in l_2} \frac{\|r(k)\|_2}{\|d(k)\|_2}.$$

The following theorem gives the method to select J_{th}.

Theorem 3.4 *[18] Given the system (3.6), the residual generator (3.2), the residual evaluation function (3.7) and $\|d(k)\|_2 \leq \delta_{d,2}$, then the threshold can be set as*

$$J_{th} = \check{\gamma}\delta_{d,2} \tag{3.8}$$

where $\check{\gamma}$ is the minimum of the optimization problem

$$\min_{P>0} \gamma$$

subject to the following LMI

$$\begin{bmatrix} -P & P(A-LC) & P(E_d - LF_d) & 0 \\ * & -P & 0 & (WC)^T \\ * & * & -\gamma^2 I & (WF_d)^T \\ * & * & * & -I \end{bmatrix} < 0.$$

With the optimal residual generator proposed in Theorem 3.3, it follows $J_{th} = \delta_{d,2}$.

Similarly, the peak value of the residual can be taken as the residual evaluation function as follows

$$\|r(k)\|_e = \|r(k)\|_{peak} = \sup_{k \geq 0} \left(r(k)^T r(k)\right)^{\frac{1}{2}} \tag{3.9}$$

with $||.||_{peak}$ standing for the *peak*-norm of a signal. The threshold can be set as

$$J_{th} = \sup_{\text{fault-free},\ k \geq 0} \|r(k)\|_{peak}$$

The following theorem gives the method to select J_{th}.

Theorem 3.5 *[18] Given the system (3.6), the residual generator (3.2), the residual evaluation function (3.9) and $\|d(k)\|_{peak} \leq \delta_{d,\infty}$, then the threshold can be set as*

$$J_{th} = \check{\gamma}\delta_{d,\infty} \tag{3.10}$$

where $\check{\gamma}$ is the minimum of the optimization problem

$$\min_{P>0, \kappa>0, \mu>0} \gamma$$

subject to the following matrix inequalities

$$\begin{bmatrix} -P & P(A-LC) & P(E_d - LF_d) \\ * & (\kappa-1)P & 0 \\ * & * & -\mu I \end{bmatrix} < 0,$$

$$\begin{bmatrix} -\kappa P & 0 & (WC)^T \\ * & (\mu-\kappa)I & (WF_d)^T \\ * & * & -\gamma I \end{bmatrix} < 0.$$

Then the occurrences of faults can be tested by a comparison between the residual evaluation function and the calculated threshold. It can be expressed as the following decision logic

$$\begin{aligned} \|r(k)\|_e &> J_{th} \Rightarrow \text{fault alarm}, \\ \|r(k)\|_e &\leq J_{th} \Rightarrow \text{fault-free}. \end{aligned} \tag{3.11}$$

For the residual evaluation, the notations of the false fault alarm and the false alarm rate (FAR) are defined as follows:

Definition A fault alarm is called the false fault alarm, when $\|r(k)\|_e > J_{th}, \|f\|_e = 0$. The probability of the occurrences of false alarms is called the FAR.

With the norm-based residual evaluation approaches for LTI systems, false alarms are prevented, i.e. $FAR = 0$, and the missing detections of faults are minimized.

3.2 FD of Markov jumping linear systems

The MJLS is one of the hybrid systems in which a state takes values in a countable finite set, referred to as the *mode*. It can be used to represent a class of linear systems subject to abrupt changes in their structures due to random components failures, repairs, sudden environment disturbances, change of the operation points of a linearized model of nonlinear systems, e.g. electric power systems, aircraft flight control and especially NCSs (for reasonable model of the packet delivery characteristic in communication channels). There are many theoretical works contributed in the field of MJLSs. The results on the stability of MJLSs have been presented in [12, 56]. The linear quadratic Gaussian control problem has been studied by [10, 55]. The bounded real lemma for MJLSs has been fully developed by [95] in the form of LMIs. The H_∞-control problems have been discussed in [14, 29], where a controller stabilizing a linear system ensures that the l_2 induced norm from disturbances to the outputs is bounded. In [13, 17], the H_∞ filtering for MJLSs has been studied as the dual problem of control. For NCSs, recently there were also many new results obtained by applying the MJLS theorem; see for example [57, 108, 111].

Although there is intensive research in FD and MJLS, the design of FD system for MJLSs has just begun. In [117], the packet dropout in NCSs was modeled as a Markov chain and an FD system has been designed in terms of LMIs. In [68], the FD system over noisy communication channels has also been described via an MJLS in order to model the transitions between different channel states. In [39], a fault detection filter has been proposed for systems whose measurements missing phenomenon is associated with a binary Bernoulli process. In [122], the design of FD system for MJLSs has been formulated as an H_∞-filtering problem. These approaches mainly concentrated on the residual generation, where residual generators have been designed to minimize the influence of disturbances [68, 117] or to minimize the difference between residual signals and (weighted) faults [39, 122], and the applied residual evaluation methods were similar to those for LTI systems. However, by only considering the disturbances or faults in the design, the residual generator usually can not achieve an optimal performance in the sense of the best trade-off between the robustness against disturbances and the sensitivity to faults [18]. Besides, further statistical properties of residual signals were not analyzed and considered in the design procedure and a proper residual evaluation methods for MJLSs is still missing to the best of author's knowledge. It will be shown that, the usual norm based residual evaluation methods in literature can not be directly applied in the FD design of MJLSs, and without taking the variance of residual signals into account the evaluation will result in a possible high FAR.

In this section, the FD system design of MJLSs is formulated as a set of optimization problems. The residual generator is designed to stochastically match a deterministic reference residual model which can achieve an optimal trade-off between the system robustness and the fault sensitivity. The reference residual model is selected according to the statistical properties of the MJLS. For the stationary MJLS, in which the distributions of Markov modes at different time instances remain the same, a new bounded real lemma is also derived. Then the stochastic model matching problem is solved by optimizing the H_∞-norm of an MJLS subject to variance constraints. In the residual evaluation, the absolute value of each residual signal is selected as the evaluation function and the corresponding thresholds are computed by considering their means and variances. These statistical properties of evaluated residual signals are calculated with the help of (iterative) LMIs based on convex optimization problems. An upper bound of the FAR is also derived in this evaluation method. The FD problem of non-stationary MJLSs is then addressed in a similar way. Finally a numerical example is given to illustrate the feasibility and effectiveness of the proposed design approaches.

3.2.1 Problem formulation

The considered MJLS is defined as follows

$$\begin{aligned} x(k+1) &= A(\theta_k)x(k) + B(\theta_k)u(k) + E_d(\theta_k)d(k) + E_f(\theta_k)f(k) \\ y(k) &= C(\theta_k)x(k) + D(\theta_k)u(k) + F_d(\theta_k)d(k) + F_f(\theta_k)f(k) \end{aligned} \tag{3.12}$$

where $x \in \mathbb{R}^n$ denotes the state vector, $u \in \mathbb{R}^p$ denotes the control inputs, $y \in \mathbb{R}^m$ denotes the measured output vector, $d \in \mathbb{R}^{n_d}$ denotes the disturbances and $f \in \mathbb{R}^{n_f}$ is the vector of faults to be detected. $\{\theta_k\}$ is a discrete homogeneous Markov chain taking values in a finite mode space $\psi = \{1, 2, \cdots, N\}$ with transition probability matrix $\Phi = [\lambda_{ij}]_{i,j\in\psi}$, and λ_{ij} is defined as

$$\lambda_{ij} = \Pr\{\theta_{k+1} = j | \theta_k = i\}$$

which are subject to the restriction $\lambda_{ij} \geq 0$, $\sum_{j=1}^N \lambda_{ij} = 1$ for any $i, j \in \psi$. For notation, define $P(k)$ as the vector of mode probabilities

$$P(k) = \begin{bmatrix} p_1(k) & p_2(k) & \cdots & p_N(k) \end{bmatrix}^T,$$

$$p_i(k) = \Pr\{\theta_k = i\}, i \in \psi.$$

The Markov chain with the following assumption is considered:

- (A3.3) $\{\theta_k\}$ is homogeneous and $\lambda_{ij} > 0$.

This assumption means that, in such a Markov chain it is possible to get to any mode from any mode. It is well known that,

$$\Phi^k \rightarrow constant, P(k) \rightarrow P(\infty), \text{ when } k \rightarrow \infty \tag{3.13}$$

where $P(\infty)$ is a unique constant vector called the stationary mode distribution of a Markov chain with the assumption (A3.3) and $P(\infty)$ can be computed according to

$$P(\infty) = \Phi P(\infty).$$

It is clear that, θ_k is asymptotically stationary with $P(0) \neq P(\infty)$. When $P(0) = P(\infty)$, then $P(0) = P(1) = \cdots = P(\infty)$, which means the mode probabilities are independent of time, i.e. the Markov chain is in the stationary state. According to the initial mode distribution $P(0)$, two kinds of MJLSs are defined:

Definition With assumption (A3.3) and $P(0) = P(\infty)$, system (3.12) is a stationary MJLS.

Definition With assumption (A3.3) and $P(0) \neq P(\infty)$, system (3.12) is a non-stationary MJLS.

For the FD purpose, it can be generally assumed that the MJLS under consideration is operating in its stationary state before a fault occurs. Hence the next subsection will first focus on the design of the FD system for stationary MJLSs and then an FD system for non-stationary MJLSs will also be given.

Residual generator design

Residual generation is the first step of FD. The following residual generator for the system (3.12) is proposed:

$$\begin{aligned} \hat{x}(k+1) &= A(\theta_k)\hat{x}(k) + B(\theta_k)u(k) + L(\theta_k)(y(k) - \hat{y}(k)) \\ \hat{y}(k) &= C(\theta_k)\hat{x}(k) + D(\theta_k)u(k) \\ r(k) &= W(\theta_k)(y(k) - \hat{y}(k)) \end{aligned} \tag{3.14}$$

where $\hat{x}(k)$ and $\hat{y}(k)$ are the estimated state vector and output vector, respectively. $r(k)$ is the residual. The matrices $L(\theta_k)$ and $W(\theta_k)$ are to be designed. For the convenience, denote the matrices associated with $\theta_k = i \in \psi$ by

$$\begin{aligned} &A_i = A(\theta_k), B_i = B(\theta_k), E_{d,i} = E_d(\theta_k), E_{f,i} = E_f(\theta_k), L_i = L(\theta_k), \\ &C_i = C(\theta_k), D_i = D(\theta_k), F_{d,i} = F_d(\theta_k), F_{f,i} = F_f(\theta_k), W_i = W(\theta_k). \end{aligned}$$

With $e(k) = x(k) - \hat{x}(k)$, the residual dynamics of (3.14) can be written as

$$\begin{aligned} e(k+1) &= A_L(\theta_k)e(k) + E_{d,L}(\theta_k)d(k) + E_{f,L}(\theta_k)f(k) \\ r(k) &= W(\theta_k)(C(\theta_k)e(k) + F_d(\theta_k)d(k) + F_f(\theta_k)f(k)) \end{aligned} \tag{3.15}$$

where

$$\begin{aligned} A_L(\theta_k) &= A(\theta_k) - L(\theta_k)C(\theta_k), \\ E_{d,L}(\theta_k) &= E_d(\theta_k) - L(\theta_k)F_d(\theta_k), \\ E_{f,L}(\theta_k) &= E_f(\theta_k) - L(\theta_k)F_f(\theta_k). \end{aligned}$$

The objective of the design is to generate residual signals which are robust against disturbances and sensitive to faults. It is clear that system (3.15) itself can be an MJLS instead of a deterministic system. The Markov mode θ_k is not known as a prerequisite. Hence a reference residual model which can achieve an optimal trade-off between system robustness and fault sensitivity, is proposed and then the residual generator is designed to match the reference residual model in a stochastic sense. In this approach the matrices $L(\theta_k)$ and $W(\theta_k)$ in (3.14) should be selected such that

$$\sup_{f,d} \frac{\|r_{ref} - r\|_E}{\| \begin{bmatrix} d \\ f \end{bmatrix} \|_2} \tag{3.16}$$

is minimized subject to

$$\|(r_{ref} - r) - E[r_{ref} - r]\|_E^2 = E\left[\sum_{k=0}^{\infty}\{(r(k) - \bar{r}(k))^T(r(k) - \bar{r}(k))\}\right] < \alpha^2 \| \begin{bmatrix} d \\ f \end{bmatrix} \|_2^2 \tag{3.17}$$

where $\alpha > 0$, $\bar{r}(k) = E[r(k)]$ with $E[.]$ denoting the expectation of a stochastic variable, $||.||_E$ represents the l_2-norm of a stochastic signal, i.e.

$$\|r_{ref} - r\|_E = \sqrt{E\left[\sum_{k=0}^{\infty}(r_{ref}(k) - r(k))^T(r_{ref}(k) - r(k))\right]},$$

and r_{ref} denotes the residual generated by the reference residual model in the form of

$$\begin{aligned} e_{ref}(k+1) &= (A_{ref} - L_oC_{ref})e_{ref}(k) + (E_{d,ref} - L_oF_{d,ref})d(k) + (E_{f,ref} - L_oF_{f,ref})f(k) \\ r_{ref}(k) &= W_oC_{ref}e_{ref}(k) + W_oF_{d,ref}d(k) + W_oF_{f,ref}f(k). \end{aligned} \tag{3.18}$$

Here L_o and W_o are chosen by applying the unified solution proposed in Theorem 3.3, such that

$$\begin{aligned} J(L_o, W_o) \geq J(L, W) &= \frac{\sigma_i(G_{rf}(e^{j\theta}))}{\|G_{r,d}\|_2} \\ &= \frac{\sigma_i(WF_{f,ref} + WC_{ref}(zI - A_{ref} + LC_{ref})^{-1}(E_{f,ref} - LF_{f,ref}))}{\|WF_{d,ref} + WC_{ref}(zI - A_{ref} + LC_{ref})^{-1}(E_{d,ref} - LF_{d,ref})\|_\infty} \end{aligned}$$

for any L, W and $\theta \in [0, 2\pi)$, where σ_i represents the i-th nonzero singular value of $G_{rf}(e^{j\theta})$. Since $r(k)$ is a stochastic vector, usually the expectation, $\|r_{ref} - r\|_E$, is not enough to characterize its behavior. Hence the constraint (3.17) is applied to ensure that the summation of variances of each residual signal over time is bounded by an expected value α^2.

Remark 3.1 A significant difference between the reference model for the purpose of FD adopted here and the one in literature is that disturbances $d(k)$ is included in the model such that an optimal trade-off between system robustness against disturbances and sensitivity to faults can be achieved. As mentioned before, simply reducing the influence of $d(k)$ or increasing the sensitivity to $f(k)$, does not automatically lead to an optimal trade-off. Hence it is necessary to take both of $d(k)$ and $f(k)$ into account in the reference model. It has been proved in [18] that, the reference model (3.18) does provide a better performance for the purpose of fault detection.

Recall (3.13), which means that as time goes by, the Markov chain forgets its initial condition and converges to its stationary distribution. Hence it is reasonable to set the following matrices

$$A_{ref} = \sum_{i=1}^{N} A_i p_i(\infty), E_{d,ref} = \sum_{i=1}^{N} E_{d,i} p_i(\infty), E_{f,ref} = \sum_{i=1}^{N} E_{f,i} p_i(\infty),$$
$$C_{ref} = \sum_{i=1}^{N} C_i p_i(\infty), F_{d,ref} = \sum_{i=1}^{N} F_{d,i} p_i(\infty), F_{f,ref} = \sum_{i=1}^{N} F_{f,i} p_i(\infty),$$

such that the reference residual model describes the optimal stationary expected behavior of the MJLS (3.15).

In fact, the MJLS (3.15) consists of two groups of states: the system states $e(k)$ and the Markov mode θ_k. In the robust control system design, the initial condition of system state is usually assumed to be zeros (so-called zero initial condition). Comparably, the following two assumptions are made for the MJLS:

- (A3.4) $e(0)$ is deterministic and $e(0) = 0$,
- (A3.5) θ_0 is independent of $e(0)$.

The problem of residual generator design of an MJLS is then summarized as follows.

Problem RGFD (Residual generator for FD): Given system (3.12) and the reference residual model (3.18), determine the matrices L_i and W_i, $i \in \psi$, of the residual generator in the form of (3.14) under assumption (A3.1)-(A3.5), such that the residual dynamics described by (3.15) minimizes (3.16) and at the same time (if possible) satisfies (3.17).

Residual evaluation design

The residual evaluation problem of deterministic systems has been intensively studied. One important evaluation strategy is the so-called norm based residual evaluation [18] as shown in the last section. The residual evaluation function can be chosen as (3.7) and the corresponding threshold can be selected as (3.8), such that false fault alarms can be prevented ($FAR = 0$) and meanwhile missing detection of faults can be reduced as much as possible.

The residual signals of an MJLS are stochastic variables. Their statistical properties are associated with a Markov chain and determined by (3.15). It is possible to compute γ, such that

$$\gamma > \sup_{d \in l_2} \frac{\|r(k)\|_E}{\|d(k)\|_2} \tag{3.19}$$

in a similar way as stated in [95], and to set $J_{th} = \min \gamma \|d(k)\|_2$ subject to (3.19) as given in literature. In this case only the expectation of the l_2-norm of $r(k)$ is considered for the computation of the threshold. Due to the variance of $r(k)$, there could be false alarms and the FAR is not known. It is difficult to determine how reliable the rising fault alarm is. Therefore the following residual evaluation problem is formulated:

Problem REFD (Residual evaluation for fault detection): Given system (3.12) and the residual generator (3.14), determine proper residual evaluation functions $\|r(k)\|_e$ and the corresponding threshold J_{th} under assumptions (A3.3)-(A3.5), such that FAR is not larger than a given constant and the missing detections of faults are reduced.

3.2.2 FD of stationary MJLSs

In this section the FD system design approach of a stationary MJLS is given.

Residual generation

For the design of residual generator (3.14), the dynamics of $r(k) - r_{ref}(k)$ is described at first. Then the existing bounded real lemma for MJLSs is reviewed and a new bounded real lemma is derived for the stationary MJLSs. Based on those lemmas, the solution to **RGFD** is presented.

In this section, denote $p_i(k) = p_i$ for all k. According to (3.14) and (3.18), the dynamics of $r(k) - r_{ref}(k)$ can be written as

$$\begin{aligned} x_o(k+1) &= A_o(\theta_k)x_o(k) + E_o(\theta_k)\tilde{d}(k) \\ r(k) - r_{ref}(k) &= C_o(\theta_k)x_o(k) + F_o(\theta_k)\tilde{d}(k) \end{aligned} \tag{3.20}$$

where

$$x_o = \begin{bmatrix} e \\ e_{ref} \end{bmatrix}, \tilde{d} = \begin{bmatrix} d \\ f \end{bmatrix}.$$

For convenience, denote the matrices associated with $\theta_k = i \in \psi$ by

$$A_{o,i} = \begin{bmatrix} A_i - L_iC_i & 0 \\ 0 & A_{ref} - L_oC_{ref} \end{bmatrix}, C_{o,i} = \begin{bmatrix} W_iC_i & -W_oC_{ref} \end{bmatrix},$$

$$E_{o,i} = \begin{bmatrix} E_{d,i} - L_iF_{d,i} & E_{f,i} - L_iF_{f,i} \\ E_{d,ref} - L_oF_{d,ref} & E_{f,ref} - L_oF_{f,ref} \end{bmatrix}, F_{o,i} = \begin{bmatrix} (W_iF_{d,i} - W_oF_{d,ref})^T \\ (W_iF_{f,i} - W_oF_{d,ref})^T \end{bmatrix}^T.$$

Before giving the solution, the following useful lemmas are introduced. The first one is the bounded real lemma for MJLSs which is slightly different from the standard one given by [95].

Lemma 3.6 *Consider the system*

$$\begin{aligned} x(k+1) &= A(\theta_k)x(k) + B(\theta_k)d(k) \\ y(k) &= C(\theta_k)x(k) + D(\theta_k)d(k) \end{aligned} \tag{3.21}$$

for $k = 0, 1, \cdots$, *where* $x(k)$, $y(k)$, $A(\theta_k)$, $B(\theta_k)$, $C(\theta_k)$, $D(\theta_k)$ *and* θ_k *are defined as in (3.12),* $d(k) \in \mathbb{R}^{n_d}$ *is the* l_2*-norm bounded input sequence. Given a constant* $\gamma > 0$, $x(0) = 0$ *and any possible initial mode distribution* $P(0)$, *then*

$$\sup_{d \in l_2} \frac{\|y\|_E}{\|d\|_2} < \gamma \tag{3.22}$$

if there exist $Q_i > 0$, $i \in \psi$ *satisfying the following LMI:*

$$\begin{bmatrix} A_i & B_i \\ C_i & D_i \end{bmatrix}^T \begin{bmatrix} \bar{Q}_i & 0 \\ 0 & I \end{bmatrix} \begin{bmatrix} A_i & B_i \\ C_i & D_i \end{bmatrix} - \begin{bmatrix} Q_i & 0 \\ 0 & \gamma^2 I \end{bmatrix} < 0, \bar{Q}_i = \sum_{j=1}^{N} \lambda_{ij} Q_j. \tag{3.23}$$

Proof Here a short proof is given. Define the Lyapunov function

$$V(i,k) = x(k)^T Q_i x(k)$$

for some $Q_i > 0, i \in \psi$. Given $x(0) = 0$, $V(\theta_0, 0) = 0$, it turns out

$$\sum_{k=0}^{\infty} E[V(\theta_{k+1}, k+1) - V(\theta_k, k)] = E\left[V(\theta_\infty, \infty)\right].$$

Then

$$\begin{aligned} E[\|y(k)\|_E^2] - \gamma^2 \|d(k)\|_2^2 &\leq E \sum_{k=0}^{\infty} y(k)^T y(k) - \gamma^2 d(k)^T d(k) + V(\theta_{k+1}, k+1) - V(\theta_k, k) \\ &= \sum_{k=0}^{\infty} E\left[\begin{bmatrix} x(k) \\ d(k) \end{bmatrix}^T R(\theta_k) \begin{bmatrix} x(k) \\ d(k) \end{bmatrix}\right] \end{aligned} \tag{3.24}$$

where

$$R(\theta_k) = \begin{bmatrix} A(\theta_k) & B(\theta_k) \\ C(\theta_k) & D(\theta_k) \end{bmatrix}^T \begin{bmatrix} E[Q_{\theta_{k+1}}] & 0 \\ 0 & I \end{bmatrix} \begin{bmatrix} A(\theta_k) & B(\theta_k) \\ C(\theta_k) & D(\theta_k) \end{bmatrix} - \begin{bmatrix} E[Q_{\theta_k}] & 0 \\ 0 & \gamma^2 I \end{bmatrix}.$$

With $R(\theta_k) < 0$, for $d(k) \in l_2$, it turns out $\|y\|_E < \gamma \|d\|_2$.

Notice θ_k can be any possible mode in ψ with different probability. It is clear that, no matter what $P(0)$ we have, (3.23) implies $R(\theta_k) < 0$ for each k. Thus the lemma is proved. ■

Remark 3.2 The standard bounded real lemma in [95] assumed that θ_0 is deterministic. In Lemma 3.6, θ_0 is assumed to be a stochastic value and the distribution of θ_0 is considered as the initial condition. The deterministic θ_0 is a special case with a specific $P(0)$, for example $P(0) = \begin{bmatrix} 0 & 1 & 0 & \cdots & 0 \end{bmatrix}^T$ means $\theta_0 = 2$.

The second lemma gives an equivalent expression of (3.23).

Lemma 3.7 *Consider the system (3.21). Given a constant $\gamma > 0$, $x(0) = 0$ and any possible initial mode distribution $P(0)$, then (3.23) with $Q_i > 0, i \in \psi$ are feasible, if and only if there exist matrices $Q_i > 0$ and $G_i > 0$ such that the following LMI*

$$\begin{bmatrix} \bar{Q}_i - (G_i + G_i^T) & G_i^T A_i & G_i^T B_i & 0 \\ * & -Q_i & 0 & C_i^T \\ * & * & -\gamma^2 I & D_i^T \\ * & * & * & -I \end{bmatrix} < 0$$

hold for $i \in \psi$.

Proof Following the similar procedure in [85], the lemma can be proved. ■

By observing that, θ_k is independent of θ_{k-1} in a stationary MJLS, the following bounded real lemma can be obtained:

Lemma 3.8 *Assume (3.21) is a stationary MJLS, where* $x(k)$, $y(k)$, $A(\theta_k)$, $B(\theta_k)$, $C(\theta_k)$, $D(\theta_k)$ *and* θ_k *are defined as in (3.12),* $d(k) \in \mathbb{R}^{n_d}$ *is the* l_2*-norm bounded input sequence. Given a constant* $\gamma > 0$, $x(0) = 0$, *then (3.22) is satisfied, if there exists* $S > 0$ *satisfying the following LMI:*

$$\begin{bmatrix} -\frac{1}{p_1}S & & & & & SA_1 & SB_1 \\ & -\frac{1}{p_1}I & & & & C_1 & D_1 \\ & & \ddots & & & \vdots & \vdots \\ & & & -\frac{1}{p_N}S & & SA_N & SB_N \\ & & & & -\frac{1}{p_N}I & C_N & D_N \\ * & * & * & * & * & -S & 0 \\ * & * & * & * & * & * & -\gamma^2 I \end{bmatrix} < 0 \tag{3.25}$$

Proof In a stationary MJLS, the expectation terms of $R(\theta_k)$ in (3.24) are

$$E[Q_{\theta_{k+1}}] = E[Q_{\theta_k}] = \sum_{i=1}^{N} p_i Q_i.$$

Hence $R(\theta_k)$ in (3.24) can be written as

$$R = \sum_{i=1}^{N} p_i \begin{bmatrix} A_i & B_i \\ C_i & D_i \end{bmatrix}^T \begin{bmatrix} S & 0 \\ 0 & I \end{bmatrix} \begin{bmatrix} A_i & B_i \\ C_i & D_i \end{bmatrix} - \begin{bmatrix} S & 0 \\ 0 & \gamma^2 I \end{bmatrix}.$$

with $S = \sum_{i=1}^{N} p_i Q_i$.

If $R < 0$, then for $d(k) \in l_2$, $\|y\|_E < \gamma \|d\|_2$. Applying Shur-complement and congruence transformation with $diag\{S, I, \cdots, S, I, I, I\}$, $R < 0$ can be formulated as (3.25). ■

Remark 3.3 When the number of modes of $\{\theta_k\}$ is 1, Lemma 3.6 and Lemma 3.8 reduce to the standard bounded real lemma for deterministic systems [94]. It is clear that, inequality (3.23) in Lemma 3.6 implies (3.25). But Lemma 3.8 not only requires less computational efforts but also provides less conservative results as shown in the following example.

Example Given $\psi = \{1, 2\}$, $\lambda_{11} = \lambda_{21} = 0.2$, $\lambda_{12} = \lambda_{22} = 0.8$ and

$$A_1 = \begin{bmatrix} 0.2 & 1 \\ 0 & 0.1 \end{bmatrix}, A_2 = \begin{bmatrix} 0.8 & 1 \\ 0 & 0.5 \end{bmatrix}, B_1 = \begin{bmatrix} 1 & 0 \\ 0 & 1 \end{bmatrix}, B_2 = \begin{bmatrix} 0.5 & 0 \\ 0 & 0.1 \end{bmatrix},$$

$$C_1 = C_2 = \begin{bmatrix} 1 & 0 \\ 0 & 1 \end{bmatrix}, D_1 = D_2 = \begin{bmatrix} 0 & 0 \\ 0 & 0 \end{bmatrix},$$

we have $p_1(\infty) = 0.2$, $p_2(\infty) = 0.8$. Let $P(0) = P(\infty)$, then $\min_{Q_i > 0} \gamma^2 = 12.88$ according to Lemma 3.6 and $\min_{S>0} \gamma^2 = 6.17$ according to Lemma 3.8.

The fourth lemma is given to compute the bound of summation of variances over time for a stationary MJLS.

Lemma 3.9 *Assume (3.21) is a stationary MJLS , where* $x(k)$, $y(k)$, $A(\theta_k)$, $B(\theta_k)$, $C(\theta_k)$, $D(\theta_k)$ *and* θ_k *are defined as in (3.12),* $d(k) \in \mathbb{R}^{n_d}$ *is the* l_2*-norm bounded input sequence. Given* $x(0) = 0$ *and a constant* $\alpha > 0$, *then*

$$\sum_{j=0}^{\infty} E\left[(y(j) - \bar{y}(j))^T (y(j) - \bar{y}(j))\right] < \alpha^2 \|d(k)\|_2^2$$

if there exists $S > 0$ satisfying the following LMI:

$$\begin{bmatrix} -\frac{1}{p_1}S & & & & & SA_{\sigma,1} & SB_{\sigma,1} \\ & -\frac{1}{p_1}I & & & & C_{\sigma,1} & D_{\sigma,1} \\ & & \ddots & & & \vdots & \vdots \\ & & & -\frac{1}{p_N}S & & SA_{\sigma,N} & SB_{\sigma,N} \\ & & & & -\frac{1}{p_N}I & C_{\sigma,N} & D_{\sigma,N} \\ * & * & * & * & * & -S & 0 \\ * & * & * & * & * & * & -\alpha^2 I \end{bmatrix} < 0$$

for $i \in \psi$, with

$$A_{\sigma,i} = \begin{bmatrix} A_i & 0 \\ 0 & \sum_{l=1}^{N} p_l A_l \end{bmatrix}, B_{\sigma,i} = \begin{bmatrix} B_i \\ \sum_{l=1}^{N} p_l B_l \end{bmatrix},$$

$$C_{\sigma,i} = \begin{bmatrix} C_i & -\sum_{l=1}^{N} p_l C_l \end{bmatrix}, D_{\sigma,i} = D_i - \sum_{l=1}^{N} p_l D_l.$$

Proof The expected behavior of a stationary (3.21) is described by

$$\begin{aligned} \bar{x}(k+1) &= (\sum_{l=1}^{N} p_l A_l)\bar{x}(k) + (\sum_{l=1}^{N} p_l B_l)d(k) \\ \bar{y}(k) &= (\sum_{l=1}^{N} p_l C_l)\bar{x}(k) + (\sum_{l=1}^{N} p_l D_l)d(k) \end{aligned}$$

Then the dynamics of $y(k) - \bar{y}(k)$ can be written as

$$\begin{bmatrix} x(k+1) \\ \bar{x}(k+1) \end{bmatrix} = A_\sigma(\theta_k) \begin{bmatrix} x(k) \\ \bar{x}(k) \end{bmatrix} + B_\sigma(\theta_k)d(k),$$
$$y(k) - \bar{y}(k) = C_\sigma(\theta_k) \begin{bmatrix} x(k) \\ \bar{x}(k) \end{bmatrix} + D_\sigma(\theta_k)d(k).$$

Following the similar procedure in Lemma 3.8, the result can be obtained. ■

Now it is the position to give the theorem for solving **RGFD** of a stationary MJLS.

Theorem 3.10 *Assume (3.12) is a stationary MJLS. Given a constant $\alpha > 0$ and under assumptions (A3.1)-(A3.5), the optimal $L(\theta_k)$ and $W(\theta_k)$ of the residual generator (3.14) in the sense of minimizing (3.16) and satisfying (3.17) can be obtained by solving the following optimization problem*

$$\min_{Y_i, W_i, S_1 > 0, S_2 > 0} \gamma^2$$

subject to

$$\begin{bmatrix} \ddots & & & \vdots & \vdots \\ & \Pi_{ii} & & \Pi_{i(N+1)} & \Pi_{i(N+2)} \\ & & \ddots & \vdots & \vdots \\ * & * & * & \Pi_{(N+1)(N+1)} & 0 \\ * & * & * & * & -\gamma^2 I \end{bmatrix} < 0$$

$$\begin{bmatrix} \ddots & & & \vdots & \vdots \\ & \Gamma_{ii} & & \Gamma_{i(N+1)} & \Gamma_{i(N+2)} \\ & & \ddots & \vdots & \vdots \\ * & * & * & \Gamma_{(N+1)(N+1)} & 0 \\ * & * & * & * & -\alpha^2 I \end{bmatrix} < 0$$

where

$$\Pi_{ii} = \begin{bmatrix} -\frac{1}{p_i} S_1 & 0 & 0 \\ 0 & -\frac{1}{p_i} S_2 & 0 \\ 0 & 0 & -\frac{1}{p_i} I \end{bmatrix},$$

$$\Pi_{i(N+1)} = \begin{bmatrix} S_1 A_i - Y_i C_i & 0 \\ 0 & S_2(A_{ref} - L_o C_{ref}) \\ W_i C_i & -W_o C_{ref} \end{bmatrix},$$

$$\Pi_{i(N+2)} = \begin{bmatrix} S_1 E_{d,i} - Y_i F_{d,i} & S_1 E_{f,i} - Y_i F_{f,i} \\ S_2(E_{d,ref} - L_o F_{d,ref}) & S_2(E_{f,ref} - L_o F_{f,ref}) \\ W_i F_{d,i} - W_o F_{d,ref} & W_i F_{f,i} - W_o F_{f,ref} \end{bmatrix},$$

$$\Gamma_{ii} = \begin{bmatrix} -\frac{1}{p_i} S_1 & 0 & 0 \\ 0 & -\frac{1}{p_i} S_1 & 0 \\ 0 & 0 & -\frac{1}{p_i} I \end{bmatrix},$$

$$\Gamma_{i(N+1)} = \begin{bmatrix} S_1 A_i - Y_i C_i & 0 \\ 0 & S_1 \sum_{l=1}^{N} p_l A_l - \sum_{l=1}^{N} p_l Y_l C_l \\ W_i C_i & -\sum_{l=1}^{N} p_l W_l C_l \end{bmatrix},$$

$$\Gamma_{i(N+2)} = \begin{bmatrix} S_1 E_{d,i} - Y_i F_{d,i} & S_1 E_{f,i} - Y_i F_{f,i} \\ \sum_{l=1}^{N} p_l (S_1 E_{d,l} - Y_l F_{d,l}) & \sum_{l=1}^{N} p_l (S_1 E_{f,l} - Y_l F_{f,l}) \\ W_i F_{d,i} - \sum_{l=1}^{N} p_l W_l F_{d,l} & W_i F_{f,i} - \sum_{l=1}^{N} p_l W_l F_{f,l} \end{bmatrix}$$

for $i \in \psi$ *and*

$$\Pi_{(N+1)(N+1)} = \begin{bmatrix} -S_1 & 0 \\ 0 & -S_2 \end{bmatrix},$$

$$\Gamma_{(N+1)(N+1)} = \begin{bmatrix} -S_1 & 0 \\ 0 & -S_1 \end{bmatrix}.$$

The optimal L_i *is then given by* $S_1^{-1} Y_i$.

Proof With Lemma 3.8 and Lemma 3.9, the proof is straightforward and thus omitted. ■

Residual evaluation

In this section, a new residual evaluation approach for the stationary MJLS is proposed in order to solve the **REFD** problem. Define a set of residual evaluation functions as follows

$$\|r_j(k)\|_e = |r_j(k)| \tag{3.26}$$

where $j = 1, \cdots, m$ and $r_j(k)$ is the j-th residual signal. That means the absolute value of each residual signal is selected as the evaluation function. For the evaluation function (3.26), the following threshold is suggested:

$$J_{j,th} = \sup_k(|\bar{r}_j(k)|) + \beta \sup_k(\sigma_j(r(k)))$$

where $|\bar{r}_j(k)|$ is the absolute value of the mean of $r_j(k)$ and

$$\sigma_j^2(k) = E[(r_j(k) - \bar{r}_j(k))^2]$$

is its variance, and $\beta > 0$ is some constant. The bounds of the mean and the variance of (3.26) are first computed by using the *peak*-norm and the generalized H_2-norm of the MJLS in fault-free cases. Then the threshold is determined and the upper bound of the guaranteed FAR is obtained.

The following lemma gives the computation of $|\bar{r}_j(k)|$ in terms of the *peak*-norm.

Lemma 3.11 *Assume (3.15) is a stationary MJLS. Given a constant $\gamma_{j,1} > 0$ and assumption (A3.3)-(A3.5), $j = 1, \cdots, m$, then in fault-free cases*

$$|\bar{r}_j(k)| < \gamma_{j,1}\|d(k)\|_{peak}$$

if there exist $S > 0$, $\mu > 0$ and $0 < \kappa < 1$ such that

$$\begin{bmatrix} -S & S\sum_{i=1}^N p_i(A_i - L_iC_i) & S\sum_{i=1}^N p_i(E_{d,i} - L_iF_{d,i}) \\ * & (\kappa - 1)S & 0 \\ * & * & -\mu I \end{bmatrix} < 0, \tag{3.27}$$

$$\begin{bmatrix} -\gamma_{j,1}I & \sum_{i=1}^N p_i[W_iC_i]_j & \sum_{i=1}^N p_i[W_iF_{d,i}]_j \\ * & -\kappa S & 0 \\ * & * & (\mu - \gamma_{j,1})I \end{bmatrix} < 0. \tag{3.28}$$

Proof The expected behavior of a stationary (3.15) in fault-free cases is just described by

$$\begin{aligned} \bar{e}(k+1) &= \bar{A}\bar{e}(k) + \bar{E}d(k) \\ \bar{r}(k) &= \bar{C}\bar{e}(k) + \bar{F}d(k) \end{aligned} \tag{3.29}$$

with

$$\bar{A} = \sum_{i=1}^N p_i(A_i - L_iC_i), \bar{E} = \sum_{i=1}^N p_i(E_{d,i} - L_iF_{d,i}), \bar{C} = \sum_{i=1}^N p_iW_iC_i, \bar{F} = \sum_{i=1}^N p_iW_iF_{d,i}.$$

The expected residual dynamics is governed by (3.29), which is a time-invariant system. The results can be easily obtained by following the idea in [94]. Thus the rest of the proof is omitted. ■

The variance of $r_j(k)$ can be computed in terms of the *peak*-norm by using the following lemma.

Lemma 3.12 *Assume (3.15) is a stationary MJLS. Given a constant $\gamma_{j,2}$, and assumption (A3.3)-(A3.5), $j = 1, \cdots, m$, then in fault-free cases*

$$\sigma_j(k) < \gamma_{j,2}\|d(k)\|_{peak}$$

if there exist $S > 0$, $\mu > 0$ and $\kappa > 0$ such that:

$$\begin{bmatrix} -\frac{1}{p_1}S & & & SA_{\sigma,1} & SE_{\sigma,1} \\ & \ddots & & \vdots & \vdots \\ & & -\frac{1}{p_N}S & SA_{\sigma,N} & SE_{\sigma,N} \\ * & * & * & (\kappa-1)S & 0 \\ * & * & * & * & -\mu I \end{bmatrix} < 0, \tag{3.30}$$

$$\begin{bmatrix} -\frac{\gamma_{j,2}}{p_1}I & & & [C_{\sigma,1}]_j & [D_{\sigma,1}]_j \\ & \ddots & & \vdots & \vdots \\ & & -\frac{\gamma_{j,2}}{p_N}I & [C_{\sigma,N}]_j & [D_{\sigma,N}]_j \\ * & * & * & -\kappa S & 0 \\ * & * & * & * & (\mu-\gamma_{j,2})I \end{bmatrix} < 0. \tag{3.31}$$

for $i \in \psi$ with

$$A_{\sigma,i} = \begin{bmatrix} A_i - L_iC_i & 0 \\ 0 & \sum_{l=1}^N p_l A_{L,l} \end{bmatrix}, E_{\sigma,i} = \begin{bmatrix} E_{d,i} - L_iF_{d,i} \\ \sum_{l=1}^N p_l(E_{d,l} - L_lF_{d,l}) \end{bmatrix},$$
$$C_{\sigma,i} = \begin{bmatrix} W_iC_i & -\sum_{l=1}^N p_lW_lC_l \end{bmatrix}, D_{\sigma,i} = W_iF_{d,i} - \sum_{l=1}^N p_lW_lF_{d,l}. \tag{3.32}$$

Proof From (3.15) and (3.29), it turns out

$$\begin{bmatrix} e(k+1) \\ \bar{e}(k+1) \end{bmatrix} = A_\sigma(\theta_k)\begin{bmatrix} e(k) \\ \bar{e}(k) \end{bmatrix} + E_\sigma(\theta_k)d(k)$$
$$r(k) - \bar{r}(k) = C_\sigma(\theta_k)\begin{bmatrix} e(k) \\ \bar{e}(k) \end{bmatrix} + D_\sigma(\theta_k)d(k) \tag{3.33}$$

with matrices defined in (3.32). Define

$$\chi(k) = \begin{bmatrix} e(k) \\ \bar{e}(k) \end{bmatrix}, V(\chi, i) = \chi^TQ_i\chi$$

for some $Q_i > 0, i \in \psi$, and assume that

$$E[V(\chi(k), \theta_k)] < \frac{\mu_{\theta_k}}{\kappa} \tag{3.34}$$

for $0 < \kappa < 1$ and $\mu_{\theta_k} > 0$. Note that $E[V(\chi(k), \theta_k)]$ satisfying

$$E[V(\chi(k+1), \theta_{k+1}) - (\kappa-1)V(\chi(k), \theta_k)] < \mu_{\theta_k} \tag{3.35}$$

and $V(\chi(0),\theta_0)=0$, is bounded by (3.34). The inequality

$$E\left[\begin{bmatrix}\chi(k)\\ d(k)\end{bmatrix}^T R_1 \begin{bmatrix}\chi(k)\\ d(k)\end{bmatrix}\right] < 0 \tag{3.36}$$

with

$$R_1=\sum_{i=1}^{N} p_i \begin{bmatrix} A_{\sigma,i}^T \\ E_{\sigma,i}^T\end{bmatrix} S \begin{bmatrix} A_{\sigma,i} & E_{\sigma,i}\end{bmatrix} - \begin{bmatrix}(1-\kappa)S & 0\\ 0 & \mu I\end{bmatrix}, S=\sum_{i=1}^{N} p_i Q_i, \mu=\sum_{i=1}^{N} p_i\mu_i,$$

ensures (3.35) and thus (3.34). Noticing that

$$\sigma_j^2(k)=E\left[\begin{bmatrix}\chi(k+1)\\ d(k+1)\end{bmatrix}^T R_2 \begin{bmatrix}\chi(k+1)\\ d(k+1)\end{bmatrix}\right]$$

with

$$R_2=\sum_{l=1}^{N} p_l \begin{bmatrix}[C_{\sigma,l}]_j^T\\ [D_{\sigma,l}]_j^T\end{bmatrix}\begin{bmatrix}[C_{\sigma,l}]_j & [D_{\sigma,l}]_j\end{bmatrix}$$

and $E[V(\chi(k),\theta_k)]=E\left[\chi(k)^T S\chi(k)\right]$, then the inequality

$$\gamma_{j,2}^{-1}R_2<\begin{bmatrix}\kappa S & 0\\ 0 & (\gamma_{j,2}-\mu)I\end{bmatrix} \tag{3.37}$$

can be obtained which implies

$$\sigma_j^2(k)<\gamma_{j,2}(\gamma_{j,2}d(k)^Td(k)+\kappa E[V(\chi(k+1),\theta_{k+1})]-\mu)<\gamma_{j,2}^2\|d(k)\|_{peak}^2.$$

Applying Shur-complement and congruence transformation, (3.36) and (3.37) can be reformulated as (3.30) and (3.31), respectively. ■

Remark 3.4 The matrix inequalities in Lemma 3.11 and Lemma 3.12 can be solved via iterative LMI techniques.

The methods for computing the mean and the variance of $r(k)$ based on the generalized H_2-norm of the MJLS in fault-free cases are also proposed. The following lemma gives the computation of $|\bar{r}_j(k)|$.

Lemma 3.13 *Assume (3.15) is a stationary MJLS. Given $\gamma_{j,1}>0$, $\gamma_{j,2}>0$ and under assumption (A3.3)-(A3.5), $j=1,\cdots,m$, then in fault-free cases*

$$|\bar{r}_j(k)|<\sqrt{\gamma_{j,1}^2\sum_{i=0}^{k-1}d(i)^Td(i)}+\sqrt{\gamma_{j,2}^2 d(k)^Td(k)},$$

if there exists $S>0$ satisfying the following LMIs:

$$\begin{bmatrix}-S & S\sum_{i=1}^{N}p_i(A_i-L_iC_i) & S\sum_{i=1}^{N}p_i(E_{d,i}-L_iF_{d,i})\\ * & -S & 0\\ * & * & -\gamma_{j,1}^2 I\end{bmatrix}<0, \tag{3.38}$$

$$\begin{bmatrix} -I & \sum_{i=1}^{N} p_i [W_i C_i]_j \\ * & -S \end{bmatrix} < 0, \tag{3.39}$$

$$\begin{bmatrix} -I & \sum_{i=1}^{N} p_i [W_i F_{d,i}]_j \\ * & -\gamma_{j,2}^2 I \end{bmatrix} < 0. \tag{3.40}$$

Proof The proof is similar to that of Lemma 3.11. ∎

The computation of $\sigma_j(k)$ based on the generalized H_2-norm is given in the following lemma.

Lemma 3.14 *Assume (3.15) is a stationary MJLS. Given $\gamma_{j,3} > 0$, $\gamma_{j,4} > 0$ and assumption (A3.3)-(A3.5), $j = 1, \cdots, m$, then in fault-free cases*

$$\sigma_j(k) < \sqrt{\gamma_{j,3}^2 \sum_{i=0}^{k-1} d(i)^T d(i)} + \sqrt{\gamma_{j,4}^2 d(k)^T d(k)}, \tag{3.41}$$

if there exists $S > 0$, $i \in \psi$ satisfying the following LMIs:

$$\begin{bmatrix} -\frac{1}{p_1} S & & & A_{\sigma,1} & E_{\sigma,1} \\ & \ddots & & \vdots & \vdots \\ & & -\frac{1}{p_N} S & A_{\sigma,N} & E_{\sigma,N} \\ * & * & * & -S & 0 \\ * & * & * & * & -\gamma_{j,3}^2 I \end{bmatrix} < 0. \tag{3.42}$$

$$\begin{bmatrix} -\frac{1}{p_1} I & & & [C_{\sigma,1}]_j \\ & \ddots & & \vdots \\ & & -\frac{1}{p_N} I & [C_{\sigma,N}]_j \\ * & * & * & -S \end{bmatrix} < 0. \tag{3.43}$$

$$\begin{bmatrix} -\frac{1}{p_1} I & & & [D_{\sigma,1}]_j \\ & \ddots & & \vdots \\ & & -\frac{1}{p_N} I & [D_{\sigma,N}]_j \\ * & * & * & -\gamma_{j,4}^2 I \end{bmatrix} < 0. \tag{3.44}$$

with $A_{\sigma,i}$,$E_{\sigma,i}$,$C_{\sigma,i}$,$D_{\sigma,i}$ defined in (3.32).

Proof In fault-free cases, the dynamics of $r_j(k) - \bar{r}_j(k)$ is governed by (3.33). Define

$$\chi(k) = \begin{bmatrix} e(k) \\ \bar{e}(k) \end{bmatrix}, V(\chi) = \chi^T Q_i \chi$$

for some $Q_i > 0$, $i \in \psi$. Consider that

$$E[V(\chi(k+1), \theta_{k+1}) - V(\chi(k), \theta_k)] < \gamma_{j,3}^2 d(k)^T d(k) \tag{3.45}$$

implies

$$E\left[V(\chi(k), \theta_k)\right] = E\left[\chi^T \sum_{i=1}^{N} p_i Q_i \chi\right] < \gamma_{j,3}^2 \sum_{i=0}^{k-1} d(i)^T d(i).$$

The inequality (3.45) is equivalent with

$$E\left[\left[\begin{array}{c} e(k) \\ d(k) \end{array}\right]^T R \left[\begin{array}{c} e(k) \\ d(k) \end{array}\right]\right] < 0 \tag{3.46}$$

where

$$R = \sum_{i=1}^{N} p_i \left[\begin{array}{c} A_{\sigma,i}^T \\ E_{\sigma,i}^T \end{array}\right] S \left[\begin{array}{cc} A_{\sigma,i} & E_{\sigma,i}^T \end{array}\right] - \left[\begin{array}{cc} S & 0 \\ 0 & \gamma_{j,3}^2 I \end{array}\right], S = \sum_{i=1}^{N} p_i Q_i.$$

Then (3.41) is guaranteed, if

$$\sum_{i=1}^{N} p_i [C_{\sigma,i}]_j^T [C_{\sigma,i}]_j < S \tag{3.47}$$

and

$$\sum_{i=1}^{N} p_i [D_{\sigma,i}]_j^T [D_{\sigma,i}]_j < \gamma_{j,4}^2 I. \tag{3.48}$$

Applying Shur-complement and congruence transformation, (3.46)-(3.48) can be reformulated as (3.42)-(3.44), respectively. ■

Based on above results, the following theorem gives the solution to **REFD** for a stationary MJLS.

Theorem 3.15 *Assume (3.15) is a stationary MJLS. Given a constant $\beta > 0$, assumption (A3.3)-(A3.5) and the residual evaluation function (3.26),*

- *and $\|d\|_{peak} < \delta_{d,\infty}$, then the threshold can be set as*

$$J_{j,th} = (\tilde{\gamma}_{j,1} + \beta\tilde{\gamma}_{j,2})\delta_{d,\infty} \tag{3.49}$$

where $\tilde{\gamma}_{j,1}$, $\tilde{\gamma}_{j,2}$ are the optimum of the constrained optimization problem:

$$\min \gamma_{j,1} \text{ subject to } (3.27) - (3.28),$$
$$\min \gamma_{j,2} \text{ subject to } (3.30) - (3.31).$$

- *and $\|d\|_2 < \delta_{d,2}$, $\|d\|_{peak} < \delta_{d,\infty}$, then the threshold can be set as*

$$J_{j,th} = (\tilde{\gamma}_{j,1} + \beta\tilde{\gamma}_{j,3})\delta_{d,2} + (\tilde{\gamma}_{j,2} + \beta\tilde{\gamma}_{j,4})\delta_{d,\infty} \tag{3.50}$$

where $\tilde{\gamma}_{j,1}$, $\tilde{\gamma}_{j,2}$, $\tilde{\gamma}_{j,3}$ and $\tilde{\gamma}_{j,4}$ are the optimum of the constrained optimization problem:

$$\min \gamma_{j,1}, \gamma_{j,2} \text{ subject to } (3.38) - (3.40),$$
$$\min \gamma_{j,3}, \gamma_{j,4} \text{ subject to } (3.42) - (3.44).$$

The false alarm rate is upper bounded as

$$FAR \leq \frac{1}{\beta^2}. \tag{3.51}$$

Before proving the lemma, the following lemma on Tchebycheff Inequality is given at first.

Lemma 3.16 *[86] Given a random number* $\mathbf{x}$ *with mean* η *and variance* σ^2*. For any* $0 < \varepsilon$*,*

$$\Pr\{|\mathbf{x} - \eta| \geq \varepsilon\} \leq \frac{\boldsymbol{\sigma^2}}{\boldsymbol{\varepsilon^2}}.$$

Proof of Theorem 3.15 The computation of the threshold based on the generalized H_2-norm is taken as an example. With Lemma 3.13 - 3.14,

$$\sup_k(|r_j(k)|) < \tilde{\gamma}_{j,1}\delta_{d,2} + \tilde{\gamma}_{j,2}\delta_{d,\infty}, \sup_k(\sigma_j(k)) < \tilde{\gamma}_{j,3}\delta_{d,2} + \tilde{\gamma}_{j,4}\delta_{d,\infty}$$

in fault-free cases. Hence it is reasonable to set the threshold as in (3.50), such that

$$J_{j,th} \geq \sqrt{\tilde{\gamma}_{j,1}^2 \sum_{i=0}^{k-1} d(i)^T d(i)} + \sqrt{\tilde{\gamma}_{j,2}^2 d(k)^T d(k)} + \beta \left(\sqrt{\tilde{\gamma}_{j,3}^2 \sum_{i=0}^{k-1} d(i)^T d(i)} + \sqrt{\tilde{\gamma}_{j,4}^2 d(k)^T d(k)} \right)$$

for all k. According to the Tchebycheff Inequality,

$$\Pr\{|r_j(k) - \bar{r}_j(k)| \geq \epsilon\} \leq \frac{\sigma_j^2(k)}{\epsilon^2}, \epsilon > 0$$

which yields

$$\Pr\{r_j(k) \geq \bar{r}_j(k) + \beta \sup_k(\sigma_j(k))\} \leq \frac{\sigma_j^2(k)}{\beta^2 \sup_k(\sigma_j^2(k))} \leq \frac{\sigma_j^2(k)}{\beta^2 \sigma_j^2(k)} = \frac{1}{\beta^2}.$$

Hence

$$\Pr\{|r_j(k)| \geq J_{j,th}\} \leq \frac{1}{\beta^2}$$

which means the FAR is upper bounded with $\frac{1}{\beta^2}$.

The proofs for the other case is similar. ■

Now the threshold for each evaluated residual signal is obtained. The fault can be detected if one of the evaluated residual signals exceeds its threshold, e.g.

$$\begin{aligned} |r_j(k)| &\leq J_{j,th} \Rightarrow \text{ fault-free}, \\ |r_j(k)| &> J_{j,th} \Rightarrow \text{ fault alarm}. \end{aligned}$$

A false alarm occurs when there is no fault but $|r_j(k)| > J_{j,th}$. Its probability is upper bounded by (3.51).

Remark 3.5 If the number of Markov mode is 1, then the computed $\sigma_j^2(r(k))$ will be zero. The proposed approaches reduce to the standard norm-based residual evaluation methods.

The evaluated residual $|r_j(k)|$ is a stochastic variable. By using the mean and the variance of $r_j(k)$ for the computation of the threshold, an upper bound of FAR is obtained. Such a bound is very useful in practice, as it can provide reliability information of a rising fault alarm. Without considering the variance in the residual evaluation, the FAR can be very high and no bounds of FAR can be established. Since there are disturbances in the system, only the upper bounds of the mean and the variance can be derived. Its higher order moments are difficult to obtain, which are lacking physical means.

3.2.3 FD of non-stationary MJLSs

When the MJLS is in its non-stationary state, i.e. $P(k) \neq P(\infty)$, the distribution of θ_k is time varying. In this case the mean value of $r(k)$ is difficult to obtain, and thus (3.17) can not be established. Moreover the residual evaluation approach presented in last section can not be applied. Hence in this subsection, an observer-based FD system is proposed for the non-stationary MJLS. At first the residual generator is designed to minimize (3.16) and the solution to **RGFD** is given in the following theorem.

Theorem 3.17 *Given the system (3.12) under assumptions (A3.1)-(A3.5), the optimal $L(\theta_k)$ and $W(\theta_k)$ of the residual generator (3.14) in the sense of minimizing (3.16) can be obtained by solving the following optimization problem for all $i \in \psi$:*

$$\min_{Y_i, W_i, G_i, Q_i > 0} \gamma^2$$

subject to

$$[N^i_{pq}]_{7\times 7} = [N^i_{pq}]^T_{7\times 7} < 0 \tag{3.52}$$

where the nonzero elements of N_{pq} are

$$\begin{aligned}
&N^i_{11} = \bar{Q}_{i11} - G_{i11} - G^T_{i11}, N^i_{12} = \bar{Q}_{i12}, N^i_{13} = G^T_{i11}A_i - Y_iC_i, N^i_{15} = G^T_{i11}E_{d,i} - Y_iF_{d,i},\\
&N^i_{16} = G^T_{i11}E_{f,i} - Y_iF_{f,i}, N^i_{22} = \bar{Q}_{i22} - G_{i22} - G^T_{i22}, N^i_{24} = G^T_{i22}(A_{ref} - L_oC_{ref}),\\
&N^i_{25} = G^T_{i22}(E_{d,ref} - L_oF_{d,ref}), N^i_{26} = G^T_{i22}(E_{f,ref} - L_oF_{f,ref}), N^i_{33} = -Q_{i11},\\
&N^i_{34} = -Q_{i12}, N^i_{37} = C^T_iW^T_i, N^i_{44} = -Q_{i22}, N^i_{47} = C^T_{ref}W^T_o, N^i_{55} = -\gamma^2 I_{n\times n},\\
&N^i_{57} = F^T_{d,i}W^T_i - F^T_{d,ref}W^T_o, N^i_{66} = -\gamma^2 I_{n\times n}, N^i_{67} = F^T_{f,i}W^T_i - F^T_{f,ref}W^T_o, N^i_{77} = -I_{n\times n},
\end{aligned}$$

where

$$Q_i = \begin{bmatrix} Q_{i11} & Q_{i12} \\ Q^T_{i12} & Q_{i22} \end{bmatrix} > 0, \bar{Q}_i = \begin{bmatrix} \bar{Q}_{i11} & \bar{Q}_{i12} \\ \bar{Q}^T_{i12} & \bar{Q}_{i22} \end{bmatrix} > 0,$$

and

$$\bar{Q}_i = \sum_{j=1}^{N} \lambda_{ij} Q_j, G_i = \begin{bmatrix} G_{i11} & 0 \\ 0 & G_{i22} \end{bmatrix}.$$

The optimal L_i is then given by $(G^T_{i11})^{-1}Y_i$.

Proof By applying Lemma 3.6 and 3.7 and setting $Y_i = G^T_{i11}L_i$, the LMI (3.52) can be easily obtained for system (3.20). Notice that

$$\bar{Q}_{i11} - G_{i11} - G^T_{i11} < 0$$

implies that G_{i11} is non-singular. Therefore the feasibility of (3.52) always ensures the existence of optimal L_i and W_i. ■

Then (3.7) is selected as the evaluation function and the corresponding threshold is suggested as

$$J_{th} = \beta \sup_{d \in l_2} \|r(k)\|_E, \beta > 0, \tag{3.53}$$

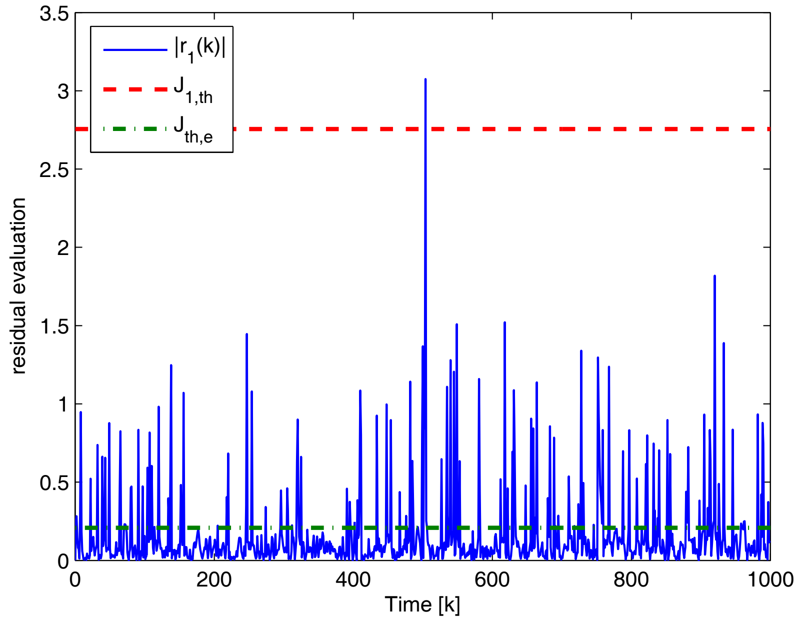

Figure 3.2: FD of a stationary MJLS based on $peak$-norm: $\tilde{\gamma}_{1,1} = 0.16$, $\tilde{\gamma}_{1,2} = 0.98$, the fault f is an impulse function with amplitude 25 at the 500th time step.

where $\sup_{d \in l_2} \|r(k)\|_E$ can be easily obtained based on the H_∞-norm of (3.15) by applying Lemma 3.6. According to the Markov Inequality [86],

$$\Pr\{\|r(k)\|_2^2 \geq \epsilon^2\} \leq \frac{\|r(k)\|_E^2}{\epsilon^2}, \epsilon > 0.$$

which yields

$$\Pr\{\|r(k)\|_e \geq \beta \sup_{d \in l_2} \|r(k)\|_E\} \leq \frac{\|r(k)\|_E^2}{\beta^2 \sup_{d \in l_2} \|r(k)\|_E^2} \leq \frac{1}{\beta^2}.$$

Hence the FAR is bounded by $\frac{1}{\beta^2}$ with the threshold (3.53). The solution to **REFD** of the non-stationary MJLS is summarized as the following theorem.

Theorem 3.18 *Given the system (3.12) under assumptions (A3.3)-(A3.5), the residual generator (3.14) and the evaluation function (3.7), the threshold can be set as (3.53) and the FAR is then upper bounded by $\frac{1}{\beta^2}$.*

Remark 3.6 The evaluation method suggested in Theorem 3.18 can also be used for the stationary MJLS. The variance of $\|r(k)\|_E$, which is difficult to obtain, is not directly involved in the computation of the threshold. But its influence is implicitly considered. When the variance of $\|r(k)\|_E$ is very small, this evaluation method can be fairly conservative.

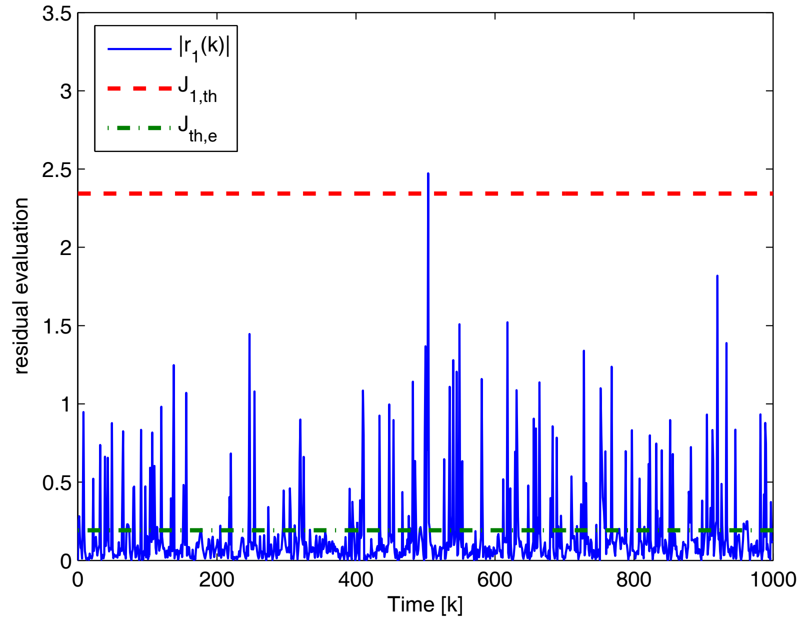

Figure 3.3: FD of a stationary MJLS based on the generalized H_2-norm: $\tilde{\gamma}_{1,1} = 0.0459$, $\tilde{\gamma}_{1,2} = 0.0738$, $\tilde{\gamma}_{1,3} = 0.3606$, $\tilde{\gamma}_{1,4} = 0.2449$, the fault f is an impulse function with amplitude 25 at the 500th time step.

3.2.4 A numerical example

To illustrate the proposed methods, the following two-mode discrete-time MJLS is considered:

$$A_1 = \begin{bmatrix} 0.6 & -0.9 \\ 0 & 0.7 \end{bmatrix}, A_2 = \begin{bmatrix} 0.1 & 0.3 \\ 0 & 0.1 \end{bmatrix}, E_{d,1} = \begin{bmatrix} 0.03 & 0.02 \\ 0.01 & 0.03 \end{bmatrix}, E_{d,2} = \begin{bmatrix} 0.01 & 0.01 \\ 0.02 & 0.01 \end{bmatrix},$$
$$E_{f,1} = E_{f,2} = \begin{bmatrix} 0.01 \\ 0.01 \end{bmatrix}, B_1 = B_2 = 0, C_1 = C_2 = \begin{bmatrix} 1 & 0 \\ 0 & 1 \end{bmatrix}, F_{f,1} = F_{f,2} = 0,$$
$$F_{d,1} = \begin{bmatrix} 0 & 0.1 \\ 0 & 0.1 \end{bmatrix}, F_{d,2} = \begin{bmatrix} 0 & 0.2 \\ 0 & 0.2 \end{bmatrix}.$$

The transition probability matrix and the corresponding $P(\infty)$ are

$$\Phi = \begin{bmatrix} 0.2 & 0.8 \\ 0.2 & 0.8 \end{bmatrix}, P(\infty) = \begin{bmatrix} 0.2 & 0.8 \end{bmatrix}^T.$$

Its reference residual model has

$$A_{ref} = \begin{bmatrix} 0.2 & 0.06 \\ 0 & 0.22 \end{bmatrix}, E_{d,ref} = \begin{bmatrix} 0.014 & 0.012 \\ 0.018 & 0.014 \end{bmatrix}, E_{f,ref} = \begin{bmatrix} 0.01 \\ 0.01 \end{bmatrix},$$
$$C_{ref} = \begin{bmatrix} 1 & 0 \\ 0 & 1 \end{bmatrix}, F_{d,ref} = \begin{bmatrix} 0 & 0.012 \\ 0 & 0.012 \end{bmatrix}, F_{f,ref} = \begin{bmatrix} 0 \\ 0 \end{bmatrix}$$

and

$$L_o = \begin{bmatrix} 3.53 & -2.53 \\ 4.26 & -3.09 \end{bmatrix}, W_o = \begin{bmatrix} -22.84 & -26.83 \\ -450.11 & 383.21 \end{bmatrix}.$$

For a stationary MJLS with $P(0) = P(\infty)$ and $\alpha = 1$, apply Theorem 3.10 and then obtain:

$$L_1 = \begin{bmatrix} 0.639 & -0.845 \\ 0.134 & 0.547 \end{bmatrix}, L_2 = \begin{bmatrix} -0.3835 & 0.070 \\ -0.509 & -0.189 \end{bmatrix},$$
$$W_1 = \begin{bmatrix} -27.088 & -1.173 \\ -18.476 & -1.405 \end{bmatrix}, W_2 = \begin{bmatrix} 5.038 & -0.136 \\ 1.815 & -0.1665 \end{bmatrix}.$$

For a non-stationary MJLS with $P(0) \neq P(\infty)$, apply Theorem 3.17 and then obtain:

$$L_1 = \begin{bmatrix} 0.593 & -0.959 \\ -0.007 & 0.651 \end{bmatrix}, L_2 = \begin{bmatrix} 0.1 & 0.282 \\ 0.001 & 0.071 \end{bmatrix},$$
$$W_1 = \begin{bmatrix} -1.401 & -7.599 \\ -1.447 & -4.650 \end{bmatrix}, W_2 = \begin{bmatrix} 0.8172 & 1.954 \\ -0.233 & 0.353 \end{bmatrix}.$$

During the simulation, assume that the disturbances are discrete-time random numbers uniformly distributed between $[-1, 1]$. Two kinds of faults are generated: a small fault as a step function and a large fault as an impulse function. These faults appear at the 500th discrete time step.

For the stationary case, the residual signals are evaluated as in (3.26) and the thresholds are computed based on the *peak*-norm and the generalized H_2-norm. The first residual signal of the system is taken as an example to show the results. The thresholds $J_{1,th}$ are computed according to Theorem 3.15 with $\beta = 2$, i.e. $FAR \leq 25\%$. The simulation results are given in the Fig. 3.2 and Fig. 3.3, where $J_{th,e}$ is the threshold calculated only based on the mean value of residual signal, i.e. $J_{th,e} = \tilde{\gamma}_{1,1}\delta_{d,\infty}$ in Fig. 3.2 and $J_{th,e} = \tilde{\gamma}_{1,1}\delta_{d,2} + \tilde{\gamma}_{1,2}\delta_{d,\infty}$ in Fig. 3.3. Figures show that, many false alarms arise with $J_{th,e}$, while the number of false alarms is significantly reduced by using $J_{1,th}$ and the fault is detected.

For the non-stationary case, the residual signals are evaluated as in (3.7) and the thresholds are computed based on the H_∞-norm. The threshold J_{th} is computed according to Theorem 3.18 with $\beta = 3$. The simulation results are given in the Fig. 3.4, where $J_{th,e}$ is the threshold calculated according to (3.19) and $J_{th,s}$ is the threshold calculated with the switched system theory [16]. With $J_{th,s}$, theoretically there is no false fault alarm. Figure shows that, with J_{th}, which is much smaller than $J_{th,s}$, the fault can be detected with the guaranteed FAR, i.e. $FAR \leq 11.1\%$. In this case $J_{th,e}$ is shown to be too small such that it results in too high FAR and can not effectively detect the faults, and $J_{th,s}$ is too conservative to detect the fault.

3.3 Conclusion

In this chapter, background of observer-based FD has been given and the design approaches for FD system of the stationary and non-stationary MJLSs have been proposed. The major focus of the work devoted on dealing with the stochastic properties of MJLSs. The main contributions include: (1) the residual generator has been designed to stochastically match an optimal reference residual model in order to achieve an optimal trade-off between robustness against disturbances and sensitivity to faults, where a way to choose the proper reference residual model has also been given; (2) novel residual evaluation methods based

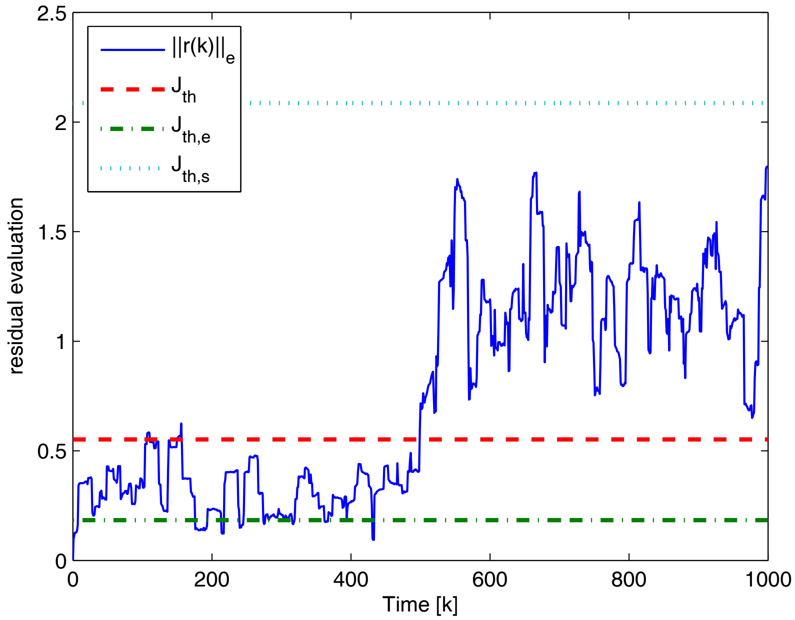

Figure 3.4: FD of a non-stationary MJLS based on H_∞-norm: $\tilde{\gamma} = 0.0409$, the fault f is a step function with amplitude 5 since the 500th time step and $T = 20$.

on the *peak*-norm, the generalized H_2-norm as well as H_∞-norm have been proposed for MJLSs, which can guarantee an expected FAR and meanwhile reduce missing detections of faults. In these evaluation methods, not only the mean values of evaluated residuals but also their variances have been taken into account for the computation of thresholds. The proposed FD system can reduce false fault alarms and provide reliability information of the rising fault alarms, which allows a practical application in real physical systems. This chapter provides also a basis for the later design of FD over networks. Especially, the developed FD system of MJLSs is ready for applications in NCSs with packet dropouts.

4 Remote FD System

The major objective of this chapter is to design observer-based FD systems as shown in Fig. 1.3, where the measured outputs of technical systems are transmitted via communication channels and the channels could be either constant or time-varying. In such scenarios, the transmission delay plays a small role. There is no feedback from the FD system to the technical systems, so that the dynamics of the technical system is not influenced by the transmission delay. By applying the error control strategy in communications, the main focus of this chapter is to deal with bit errors and quantization errors in the design procedure. For this purpose, the characteristics of communication channels are first studied and the relation between bit errors, quantization errors and transmission errors is derived. The residual generators are then designed to achieve an optimal trade-off between the robustness against transmission errors and the sensitivity to faults. The way to integrate the statistics of the generated residual signals into the residual evaluation and the threshold computation is also proposed. The remote FD systems with centralized transmission and decentralized transmission are designed separately. Finally, the achieved results are illustrated by numerical examples. Parts of this chapter are based on [69] and [65].

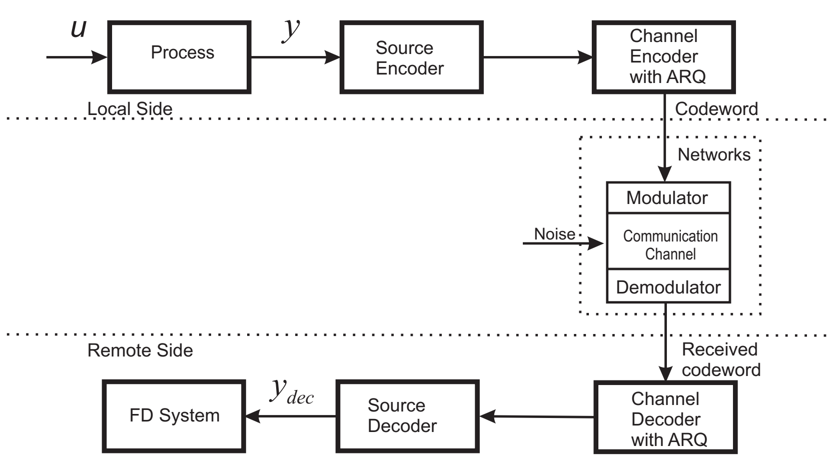

Figure 4.1: The detailed structure of remote FD system.

4.1 Problem formulation

The detailed scheme of the remote FD system is depicted in Fig. 4.1, where the FD system is located at a remote site. Consider the following discrete-time LTI process:

$$\begin{aligned} x_p(k+1) &= A_p x_p(k) + B_p u(k) + E_{p,d} d(k) + E_{p,f} f(k) \\ y(k) &= C_p x_p(k) + D_p u(k) + F_{p,d} d(k) + F_{p,f} f(k) \\ u(z) &= K(z) y(z) \end{aligned} \tag{4.1}$$

where $x_p \in \mathbb{R}^n$ denotes the state vector, $u \in \mathbb{R}^p$ denotes the control inputs, $y \in \mathbb{R}^m$ denotes the measured output vector, $d \in \mathbb{R}^{n_d}$ denotes the unknown inputs and $f \in \mathbb{R}^{n_f}$ are the faults to be detected. A_p, B_p, C_p, D_p, $E_{p,d}$, $E_{p,f}$ $F_{p,d}$ and $F_{p,f}$ are known real matrices of compatible dimensions. $K(z)$ stands for the output feedback controller applied in the process, i.e.

$$K(z) = \begin{bmatrix} A_c & B_c \\ C_c & D_c \end{bmatrix} \tag{4.2}$$

which is located at the process side and can be a static one or a dynamic one.

In this remote FD system only the process measurements are transmitted over channels, and thus u is not directly available for the FD system. However it is reasonable to assume that, the control law $K(z)$ is known to the FD system. Denote

$$x(k) = \begin{bmatrix} x_p(k) \\ x_c(k) \end{bmatrix}$$

where $x_c(k)$ is the state of the output feedback controller $K(z)$. With (4.2), the close-loop system of (4.1) can be written as

$$\begin{aligned} x(k+1) &= Ax(k) + E_d d(k) + E_f f(k) \\ y(k) &= Cx(k) + F_d d(k) + F_f f(k) \end{aligned} \tag{4.3}$$

with

$$A = \begin{bmatrix} A_p + B_p D_c C_p & B_p C_c \\ B_c C_p & A_c \end{bmatrix}, E_d = \begin{bmatrix} E_{p,d} + B_p D_c F_{p,d} \\ B_c F_{p,d} \end{bmatrix}, E_f = \begin{bmatrix} E_{p,f} + B_p D_c F_{p,f} \\ B_c F_{p,f} \end{bmatrix},$$
$$C = \begin{bmatrix} C_p + D_p D_c C_p & D_p C_c \end{bmatrix}, F_d = \begin{bmatrix} F_{p,d} + D_p D_c F_{p,d} \end{bmatrix}, F_f = \begin{bmatrix} F_{p,f} + D_p D_c F_{p,f} \end{bmatrix}.$$

Then the following residual generator is proposed for the purpose of fault detection:

$$\begin{aligned} \hat{x}(k+1) &= A\hat{x}(k) + L_k(y_{dec}(k) - \hat{y}(k)) \\ \hat{y}(k) &= C\hat{x}(k), \\ r(k) &= W_k\left(y_{dec}(k) - \hat{y}(k)\right) \end{aligned} \tag{4.4}$$

where $\hat{x}$ and $\hat{y}$ are estimated state vector and output vector, respectively; $r(k) \in \mathbb{R}^m$ is the vector of residual signals; y_{dec} is the decoded outputs received by the FD system; L_k and W_k are free parameters and should be designed properly, such that $r(k)$ is robust against network-induced effects as well as disturbances $d(k)$ and simultaneously sensitive to faults $f(k)$. Notice that, L_k and W_k could be time varying.

In the residual evaluator, the residual signals are evaluated as in (3.7) over a time window T, and then a threshold J_{th} should be selected such that the occurrence of fault can be tested according to the logic rule (3.11).

In the rest of this chapter, the design of L_k and W_k in (4.4) and the selection of J_{th} for the evaluation function (3.7) will be studied.

4.2 Communication over noisy channels

The communication part of the networked FD system consists of the source encoder/decoder, the channel encoder/decoder and the communication channel as shown in Fig. 2.1. This section investigates the characteristics of transmission errors induced by networks.

4.2.1 Coding and decoding

The source encoder is usually an A/D converter. The quantized value Y_i, $i = 1, \cdots, 2^{k_c}$, is used to represent the range of one process measurement from $(Y_i - 0.5l)$ to $(Y_i + 0.5l]$, where l is the length of the quantization cells.

In communication theory, two kinds of error control strategies based on the channel coding/decoding can be applied to improve the communication reliability. One is the forward error correction (FEC) which employs the error-correcting codes that automatically correct errors detected at the receiver. The other one is the automatic repeated request (ARQ). In an ARQ system, when errors are detected at the receiver, a request is sent to the transmitter to repeat the codeword until there is no detected bit error in the received codeword [72]. For the remote FD system, applying the ARQ is preferred, which can minimize the probability of decoding errors. When the channel quality is relatively good, the k_c-bit information sequence can also be directly transmitted and an acceptable FD performance can still be guaranteed with low transmission load and low computation effort for decoding. In this case, $n_c = k_c$.

Remark 4.1 If the ARQ strategy is applied, the codeword may be retransmitted for several times. Here it is assumed that, the codeword can be received with a bounded delay which is smaller than the sampling period of the process.

4.2.2 Transmission errors

The i-th decoded measurement can be written as

$$y_{i,dec} = y_i + \Delta_i,$$

$$y_{dec}(k) = \begin{bmatrix} y_{1,dec}(k) & \cdots & y_{m,dec}(k) \end{bmatrix}^T$$

where Δ_i stands for the transmission error of the i-th measurement.

In coding, a unique codeword is assigned to each quantized value. This procedure is usually called the binary labeling in communication theory. Here a definition on binary labeling is given as follows.

Definition A binary labeling $\mathbb{L}(n_c, k_c)$ is a set of pairs

$$\mathbb{L}(n_c, k_c) = \{(C_i, Y_i)\}, C_i \in \{0,1\}^{n_c}, i = 1, \cdots, 2^{k_c}, C_i \neq C_j, i \neq j,$$

where C_i is the codeword belonging to an (n_c, k_c)-code and Y_i is the quantized physical value represented by C_i.

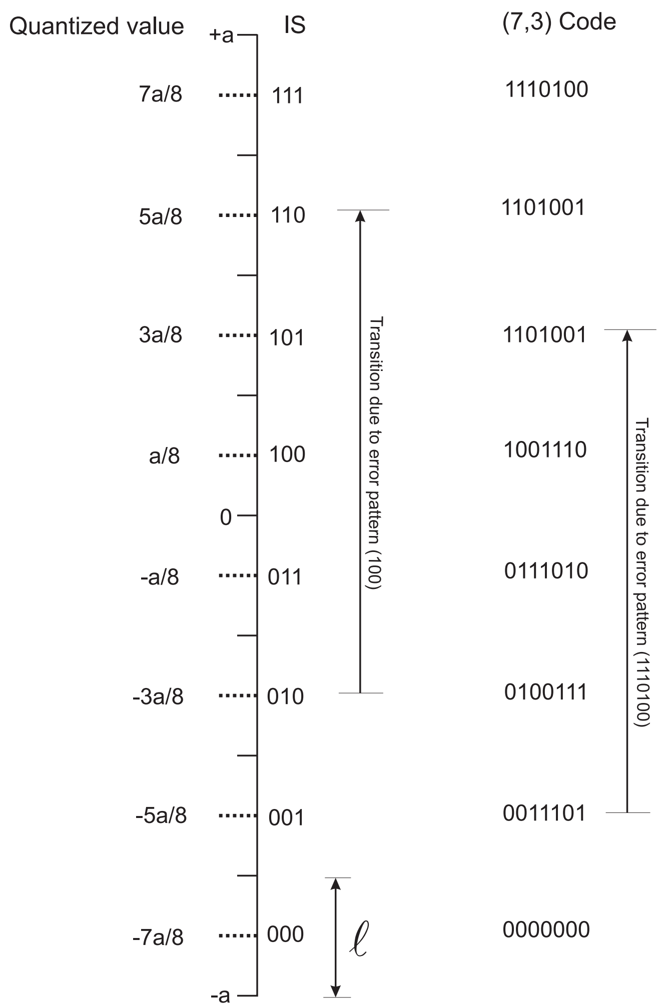

Figure 4.2: Uniform quantizer with 3 bits information sequence binary labeling and 7 bits codeword binary labeling. The (7,3)-code is a cyclic code.

Fig. 4.2 shows the $(3,3)$ binary labeling and the $(7,3)$ cyclic codeword binary labeling. Before going further, the following assumptions and notations for the system are made in this chapter:

- (A4.1) The ARQ error control strategy is applied in the communication system, where the data transmission is repeated until an n_c-bit codeword belonging to the (n_c, k_c)-code is received. With the ARQ, the reliability of communication channels can be significantly improved.

- (A4.2) Each measurement of the process is assumed to be quantized with a uniform quantizer individually, and each quantization cell is represented by an (n_c, k_c)-codeword. Denote $C_i^t(k)$ and $C_i^r(k), i = 1, \cdots, m$, as the transmitted and received codeword representing the i-th measurement at the k-th time step, respectively. Hence for each time step, there is a set of codewords, i.e. $(C_1^t(k), \cdots, C_m^t(k))$, should be transmitted. Define a decoding operator ϕ, which transfers the codeword to its represented physical value, then

$$y_i(k) = \phi(C_i^t(k)) + \Delta_q(k), y_{i,dec}(k) = \phi(C_i^r(k)) \tag{4.5}$$

where $\Delta_q(k)$ is the quantization error.

- (A4.3) The communication channel is assumed to be a BSC. The different measurements of the process could be transmitted via different channels. Then the probabilities of bit errors at the k-th time step can be denoted as

$$p_b(k) = \begin{bmatrix} p_{1,b}(k) & \cdots & p_{m,b}(k) \end{bmatrix}^T,$$

$$p_{i,b}(k) \in [0,1], i = 1, \cdots, m$$

which is called the BER vector. $p_{i,b}(k)$ represents BER of the i-th measurement at the k-th time step. Denote the upper bound of $p_{i,b}(k)$ as $\bar{p}_{i,b}$.

Remark 4.2 With assumption (A4.1), packet dropouts in networks can be prevented by the ARQ strategy. It is worth to mention that, the proposed approaches in this chapter do not depend on the employed error control strategies. With slight modifications, they can also be applied with FEC.

The influence of bit errors is to be analyzed in terms of error patterns. If the weight of the error pattern is zero, then the correct codeword is received; if the weight of the error pattern is not zero, the received codeword is the wrong one. For instance, if the codeword 0011101 in Fig. 4.2 is transmitted, then the received one can possibly be 1101001 due to the error pattern 1110100, or 0111101 due to the error pattern 0100000. In the first case, the received codeword is a valid one and no bit error is detected. That means if the error pattern is one of the valid codewords, it can not be detected [72] and there exists a transition between codewords due to the error pattern. In the second case, the received message is not a codeword and thus bit errors are detected. With ARQ, the codeword will be retransmitted until a valid one is received. The transitions between codewords are illustrated by Fig. 4.3. With assumption (A4.1)-(A4.3), the transition probability from $C_i^t(k)$ to $C_i^r(k)$ can be calculated according to (2.8) as follows:

$$P_{C_i^r(k),C_i^t(k)} = p_{i,b}(k)^{h(C_i^r(k),C_i^t(k))}(1 - p_{i,b}(k))^{n_c - h(C_i^r(k),C_i^t(k))} \tag{4.6}$$

where $h(.)$ stands for the hamming distance between two codewords. The BER actually indicates the reliability of the communication channels.

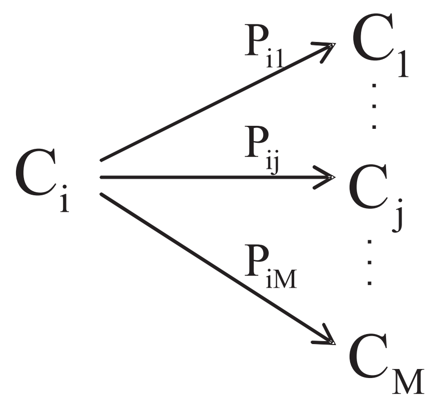

Figure 4.3: Transitions between codewords due to different error patterns, $M = 2^{k_c}$

According to (4.5), the difference between the i-th decoded and original measurement, i.e. the transmission error of the i-th measurement, can be written as

$$\Delta_i(k) = y_{i,dec}(k) - y_i(k), i = 1, \cdots, m.$$

Apparently, $\Delta_i(k)$ is also a stochastic variable. The conditional expectation of $\Delta_i(k)$ is

$$\eta_i(k) = E[\Delta_i(k)|C_i^t(k)] = \sum_{j=1}^{2^{k_c}} P_{C_j,C_i^t(k)}(\phi(C_j) - \phi(C_i^t(k))) + \Delta_q(k) \tag{4.7}$$

and its second moment is

$$\sigma_{i,2}(k) = E[\Delta_i(k)^2|C_i^t(k)] = \sum_{j=1}^{2^{k_c}} P_{C_j,C_i^t(k)}(\phi(C_j) - \phi(C_i^t(k)) - \Delta_q(k))^2. \tag{4.8}$$

Besides, its forth moment is also of interest, i.e.

$$\sigma_{i,4}(k) = E[\Delta_i(k)^4|C_i^t(k)] = \sum_{j=1}^{2^{k_c}} P_{C_j,C_i^t(k)}(\phi(C_j) - \phi(C_i^t(k)) - \Delta_q(k))^4. \tag{4.9}$$

Now the remote FD system applies the ARQ error control strategy and the resulting transmission error is characterized by (4.7)-(4.9).

4.3 Remote FD systems over constant communication channels

In this section, the remote FD system is designed when the measurements are transmitted over a constant communication channel, i.e. $p_{1,b}(k) = \cdots = p_{m,b}(k) = p_b$, where p_b is a constant value.

4.3.1 Residual generation

Since the BER are constant, L_k, W_k in (4.4) are also constant. As

$$y_{i,dec}(k) - \hat{y}_i(k) = y_i(k) - \hat{y}_i(k) + y_{i,dec}(k) - y_i(k),$$

the residual generator (4.4) can be rewritten into

$$\begin{aligned} \hat{x}(k+1) &= A\hat{x}(k) + L(y(k) - \hat{y}(k) + \Delta_t(k)) \\ \hat{y}(k) &= C\hat{x}(k) \\ r(k) &= W\left(y(k) - \hat{y}(k) + \Delta_t(k)\right). \end{aligned} \tag{4.10}$$

where

$$\Delta_t(k) = \begin{bmatrix} \Delta_1(k) & \cdots & \Delta_m(k) \end{bmatrix}^T$$

denotes the transmission error. Define $e(k) = x(k) - \hat{x}(k)$ and

$$\tilde{d}(k) = \begin{bmatrix} d(k) \\ \Delta_t(k) \end{bmatrix},$$

then the dynamics of the residual generator (4.4) can be written as

$$\begin{aligned} e(k+1) &= (A-LC)e(k) + (\tilde{E}_d - L\tilde{F}_d)\tilde{d}(k) + (E_f - LF_f)f(k) \\ r(k) &= W(Ce(k) + \tilde{F}_d\tilde{d}(k) + F_f f(k)) \end{aligned} \tag{4.11}$$

where

$$\tilde{E}_d = \left[\begin{array}{cc} E_d & 0 \end{array}\right], \tilde{F}_d = \left[\begin{array}{cc} F_d & I \end{array}\right].$$

In the frequency domain, it can be written as

$$\begin{aligned} G_{r\tilde{d}}(z) &= W\tilde{F}_d + WC(Iz - A + LC)(\tilde{E}_d - L\tilde{F}_d), \\ G_{rf}(z) &= WF_f + WC(Iz - A + LC)(E_f - LF_f). \end{aligned}$$

By selecting L and W the performance of the FD system (4.10) can be optimized with the Theorem 3.3.

4.3.2 Residual evaluation

It is evident that the residual $r(k)$ is corrupted by the unknown disturbance $d(k)$ and the transmission error $\Delta_t(k)$. In order to reduce false alarms caused by $d(k), \Delta(k)$ and simultaneously ensure a high fault detectability, the residual evaluation function (3.7) is applied. According to (4.11), the threshold can be set as

$$J_{th} = \|G_{r\tilde{d}}\|_\infty \sup \|\tilde{d}(k)\|_T \tag{4.12}$$

where $\|G_{r\tilde{d}}\|_\infty$ denotes the $\mathcal{H}_\infty$-norm of the transfer matrix $G_{r\tilde{d}}(z)$. Then the computation of J_{th} is given in two steps. First, consider the bound of $\|\tilde{d}(k)\|_T$. Note that

$$\|\tilde{d}(k)\|_T^2 = \|d(k)\|_T^2 + \|\Delta_t(k)\|_T^2 \tag{4.13}$$

with

$$\|\Delta_t(k)\|_T^2 = \sum_{j=k-T+1}^{k} \Delta_t(j)^T \Delta_t(j), \|d(k)\|_T^2 = \sum_{j=k-T+1}^{k} d(j)^T d(j).$$

Recall that $\Delta_t(k)$ is a stochastic variable. An estimate of the upper bound of $\|\Delta_t(k)\|_T^2$ can be

$$E\left[\|\Delta_t(k)\|_T^2\right] + \beta\sqrt{E[(\|\Delta_t(k)\|_T^2 - E[\|\Delta_t(k)\|_T^2])^2]}$$

where $\beta > 0$ is a factor indicating the confidence interval of the estimate. The larger β is, the more confident the estimate becomes. The following lemma gives a relationship between the estimate of the upper bound of $\|\Delta(k)\|_T^2$ and the confidence interval.

Lemma 4.1 *Given a binary labeling $\mathbb{L}(n_c, k_c)$ and a BSC channel with the BER vector $p_b(k)$. The expectation of $\|\Delta_i(k)\|_T^2, i = 1, \cdots, m$, is*

$$\eta_{i,T}(k) = \sum_{j=k-T+1}^{k} \sigma_{i,2}(j)$$

and its variance is

$$\sigma_{i,T}^2(k) = \sum_{j=k-T+1}^{k} \sigma_{i,4}(j) - \sum_{j=k-T+1}^{k} \sigma_{i,2}^2(j).$$

Then

$$\|\Delta_i(k)\|_T^2 < \eta_{i,T}(k) + \beta\sigma_{i,T}(k) \tag{4.14}$$

and

$$\|\Delta_t(k)\|_T^2 < \eta_T(k) + \beta\sigma_T(k)$$

with the probability larger than $1 - \frac{1}{\beta^2}$*, where*

$$\eta_T(k) = \sum_{i=1}^{m} \eta_{i,T}(k), \sigma_T(k) = \sum_{i=1}^{m} \sigma_{i,T}(k).$$

Proof With the given binary labeling, it turns out

$$\begin{aligned}
\eta_{i,T}(k) &= E[\|\Delta_i(k)\|_T^2] \\
&= E[\sum_{j=k-T+1}^{k} \Delta_i(j)^2] \\
&= \sum_{j=k-T+1}^{k} E[\Delta_i(j)^2] \\
&= \sum_{j=k-T+1}^{k} \sigma_{i,2}(j).
\end{aligned}$$

Since error patterns occurred at different time steps are independent, it yields

$$\begin{aligned}
\sigma_{i,T}^2(k) &= E[(\|\Delta_i(k)\|_T^2 - \eta_{i,T}(k))^2] \\
&= E[(\|\Delta_i(k)\|_T^2)^2] - \eta_{i,T}^2(k) \\
&= \sum_{j=k-T+1}^{k} E[\Delta_i(j)^4] \\
&+ \sum_{m,n=k-T,..,k}^{m\neq n} 2\sigma_{i,2}\sigma_{i,2} \\
&- \sum_{j=k-T+1}^{k} (E[\Delta_i(j)^2])^2 \\
&- \sum_{m,n=k-T,..,k}^{m\neq n} 2\sigma_{i,2}\sigma_{i,2} \\
&= \sum_{j=k-T+1}^{k} \sigma_{i,4}(j) - \sum_{j=k-T+1}^{k} \sigma_{i,2}^2(j).
\end{aligned}$$

With Lemma 3.16 and by setting

$$\varepsilon = \beta\sigma_T(k),$$

it turns out

$$\Pr\{\eta_T(k) + \beta\sigma_T(k) > \|\Delta_t(k)\|_T^2\} \geq 1 - \frac{1}{\beta^2}. \tag{4.15}$$

■

Lemma 4.1 provides us with an estimate of the upper bound on $\|\Delta(k)\|_T^2$ under a given confidence probability $1 - \frac{1}{\beta^2}$. Unfortunately the received codeword may be different from the transmitted one due to bit errors. Since Lemma 4.1 is based on the transmitted codeword, it can not be directly used at the receiver side. Hence, only the worst case can be considered by the FD system. Let

$$\begin{aligned}
\sigma_{i,2,\max} &= \max_{C_i^t} \sigma_{i,2}, \\
\sigma_{i,2,\min} &= \min_{C_i^t} \sigma_{i,2}, \\
\sigma_{i,4,\max} &= \max_{C_i^t} \sigma_{i,4}, i = 1, \cdots, m
\end{aligned} \tag{4.16}$$

and

$$\eta_{i,T,\max} = T\sigma_{i,2,\max} \geq \eta_{i,T}(k),$$
$$\sigma_{i,T,\max}^2 = T(\sigma_{i,4,\max} - \sigma_{i,2,\min}^2) \geq \sigma_{i,T}^2(k).$$

Finally

$$\|\Delta_t(k)\|_T^2 \leq \eta_{T,\max} + \beta\sigma_{T,\max}, \eta_{T,\max} = \sum_{i=1}^{m} \eta_{i,T,\max}, \sigma_{T,\max} = \sum_{i=1}^{m} \sigma_{i,T,\max} \tag{4.17}$$

with probability larger than $1 - \frac{1}{\beta^2}$. With (4.7), (4.8) and (4.9), $\sigma_{i,2}$ and $\sigma_{i,4}$ can be off-line calculated with the given BER and the binary labeling $\mathbb{L}(n_c, k_c)$. Therefore (4.16) can be off-line determined and $\|\Delta_t(k)\|_T^2$ can be obtained from (4.17) for the worst case.

It is interesting to note that, according to (4.15) and (4.17) following inequality holds

$$\Pr\{\|\Delta(k)\|_T^2 > \eta_{T,\max} + \beta\sigma_{T,\max}\} \leq \frac{1}{\beta^2}$$

which provides an upper bound of FAR, if the threshold is set to be

$$J_{th} = \|G_{r\tilde{d}}\|_\infty \sqrt{\delta_{d,2}^2 + \eta_{T,\max} + \beta\sigma_{T,\max}}.$$

As a result, the following theorem for the threshold computation can be obtained.

Theorem 4.2 *Given the system (4.3), residual generator (4.10), BER p_b, the binary labeling $\mathbb{L}(n_c, k_c)$, $\|d\|_2 < \delta_{d,2}$ and $FAR \leq \frac{1}{\beta^2}$. Under the residual evaluation function (3.7), the threshold J_{th} can be set as*

$$J_{th} = \check{\gamma}\sqrt{\delta_{d,2}^2 + \eta_{T,\max} + \beta\sigma_{T,\max}} \tag{4.18}$$

where $\check{\gamma}$ is the optimum of constrained optimization problem:

$$min\ \gamma$$

with following LMI admitting a solution $S > 0$*:*

$$\begin{bmatrix} -S & \Pi_{12} & \Pi_{13} & 0 \\ * & -S & 0 & C^TW^T \\ * & * & -\gamma I & \tilde{F}_d^TW^T \\ * & * & * & -\gamma I \end{bmatrix} < 0 \tag{4.19}$$

with

$$\Pi_{12} = SA - SLC,$$
$$\Pi_{13} = S(\tilde{E}_d - L\tilde{F}_d).$$

Proof According to the bounded real lemma [123], the feasibility of (4.19) is equivalent to

$$\|G_{r\tilde{d}}(z)\|_\infty < \gamma.$$

Thus the threshold can be computed based on an iterative procedure of checking the feasibility of (4.19) till the minimum γ is found. Then according to Lemma 4.1, (4.13) and (4.17), the threshold can be calculated with (4.18). ■

4.3.3 A numerical example

In this section, the above derived results are illustrated by following LTI process:

$$A = \begin{bmatrix} 1.1 & 0.3 \\ 0 & 0.65 \end{bmatrix}, B = \begin{bmatrix} 1 \\ 1 \end{bmatrix}, C = \begin{bmatrix} 1 & 0.8 \end{bmatrix},$$
$$E_d = \begin{bmatrix} 0.1 \\ 0 \end{bmatrix}, F_d = 0.5, E_f = \begin{bmatrix} 1 \\ 1 \end{bmatrix}, F_f = 0, K = -0.3.$$

The sampling time of the system is $1s$. An 8-bit linear A/D converter is applied and the range of the valid measurement y is assumed to be $(-1, 1)$. The unknown disturbance d is simulated as a uniform random number in the range of $[-0.1, 0.1]$. The measurement is decoded according to (4.5) and L, W are designed as

$$L = \begin{bmatrix} -0.01 \\ -0.06 \end{bmatrix}, W = 0.883$$

by solving the optimization problem according to Theorem 3.3.

The time window is selected as $T = 5$s and the simulation time is 10000s. A bias actuator fault is generated at $t = 5000$s with $f = 0.2$. Fig. 4.4 shows the original measurement y of the process.

First, the 8-bit information sequence is directly transmitted without channel coding. The decoded measurements under different BERs are shown in Fig. 4.5 and 4.7. It is clear that the transmission error can be really large due to the bit errors. The influence of such transmission errors in residual evaluation can be observed in Fig. 4.6 and 4.8. With the given FAR, J_{th} is calculated according to (4.18) for different BERs. For a lower BER, a smaller threshold can be obtained with an acceptable FAR.

With ARQ applying $(15, 8)$-cyclic code, most of the bit errors are detected and the transmission errors are reduced as shown in Fig. 4.9 and 4.11. In the case of $p_b = 0.01$, even no transmission error is observed from the simulation results. From Fig. 4.10 and 4.12, it can observed that, a smaller J_{th} is obtained from (4.18) in this case with a desired FAR. The above results demonstrate the relation between BER and FAR, and the efficiency of the proposed approach for threshold computation.

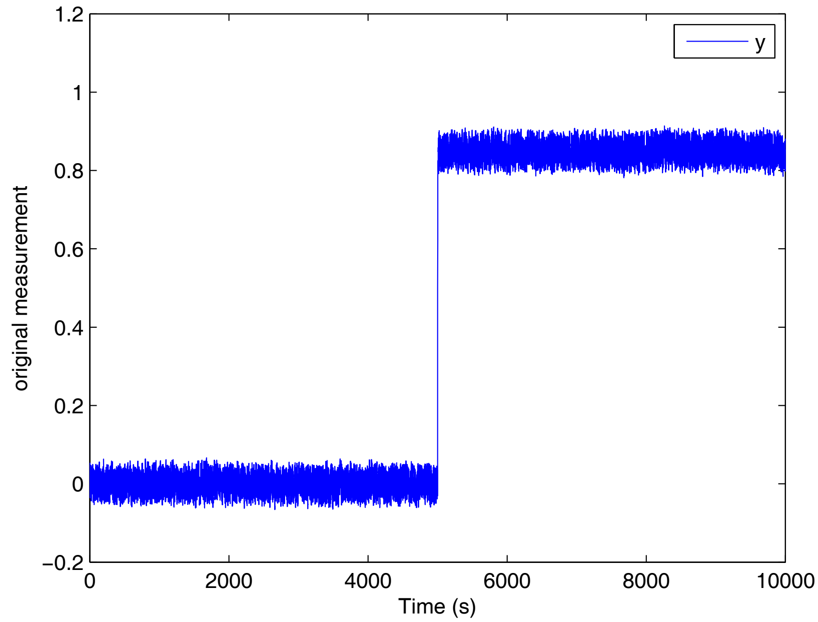

Figure 4.4: Original measurement from the process

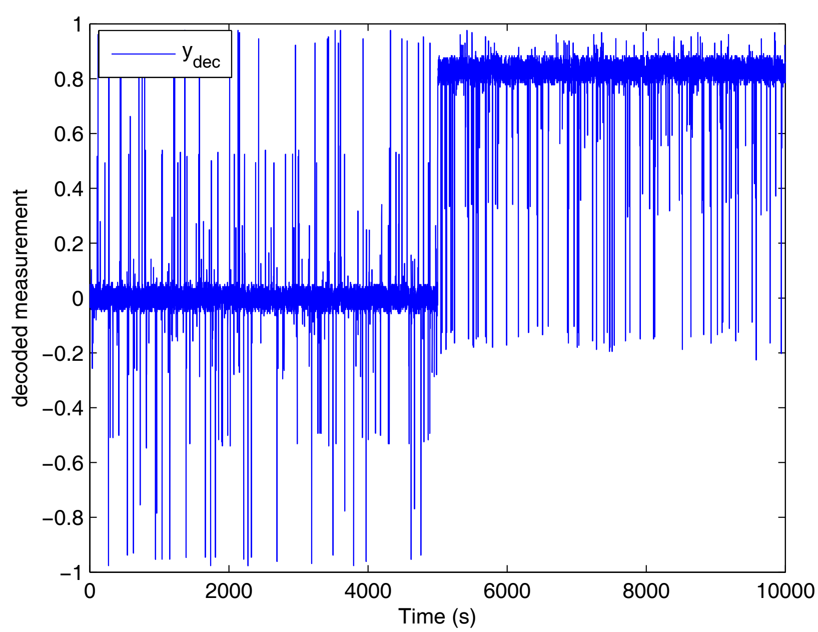

Figure 4.5: Decoded measurement without channel coding. BER is 0.01.

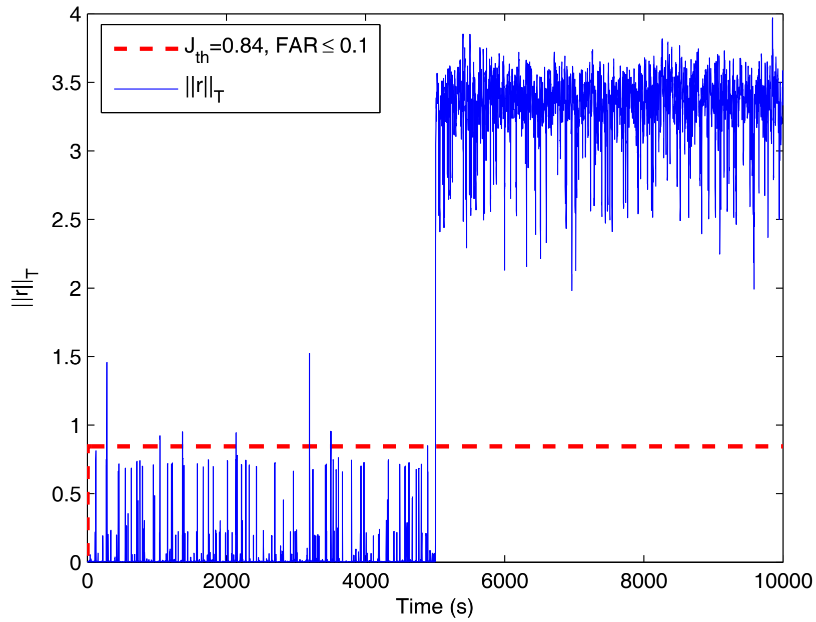

Figure 4.6: $\|r(k)\|_T$ without channel coding. BER is 0.01.

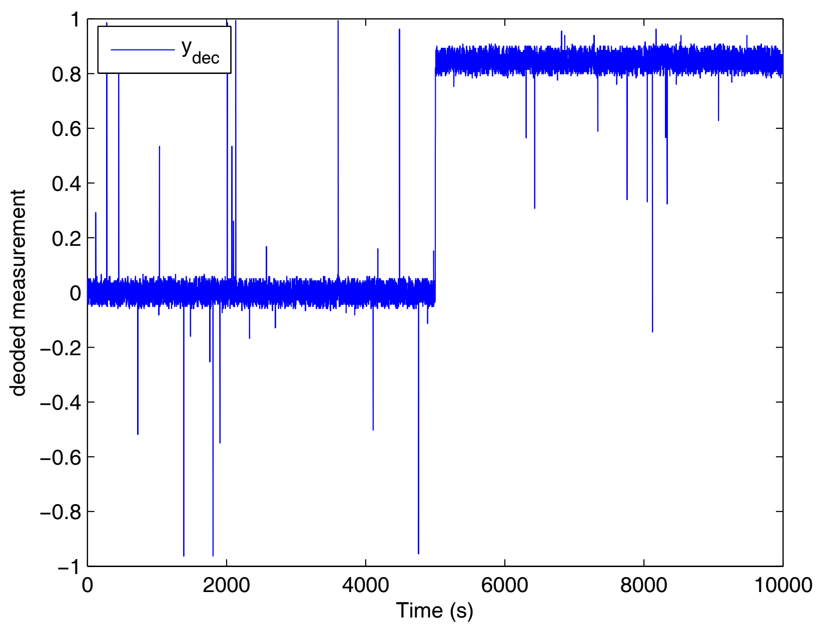

Figure 4.7: Decoded measurement without channel coding. BER is 0.001.

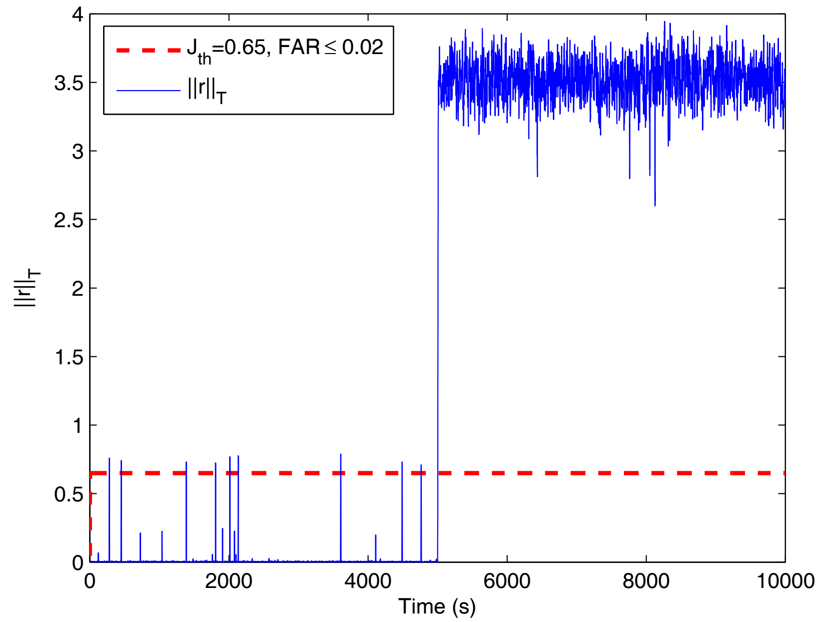

Figure 4.8: $\|r(k)\|_T$ without channel coding. BER is 0.001.

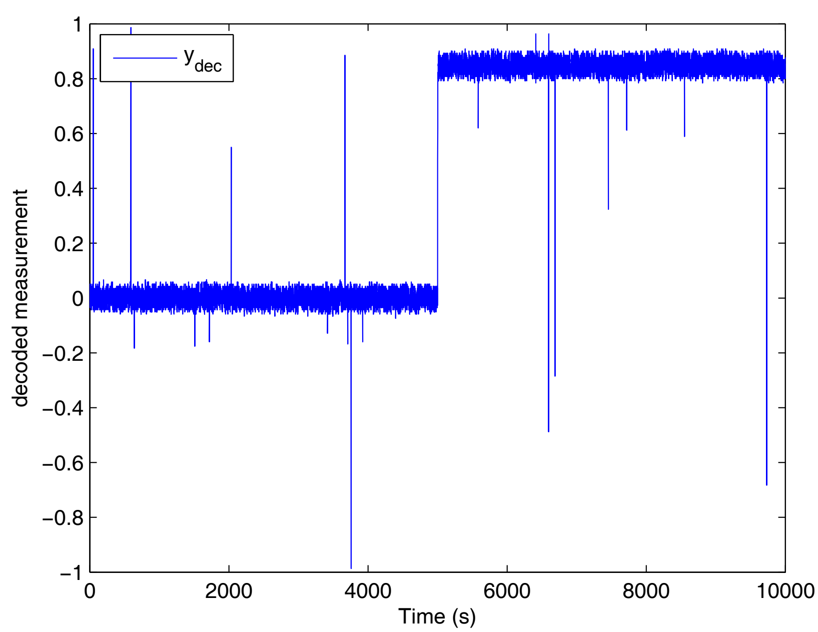

Figure 4.9: Decoded measurement with $(15, 8)$ cyclic code. BER is 0.1.

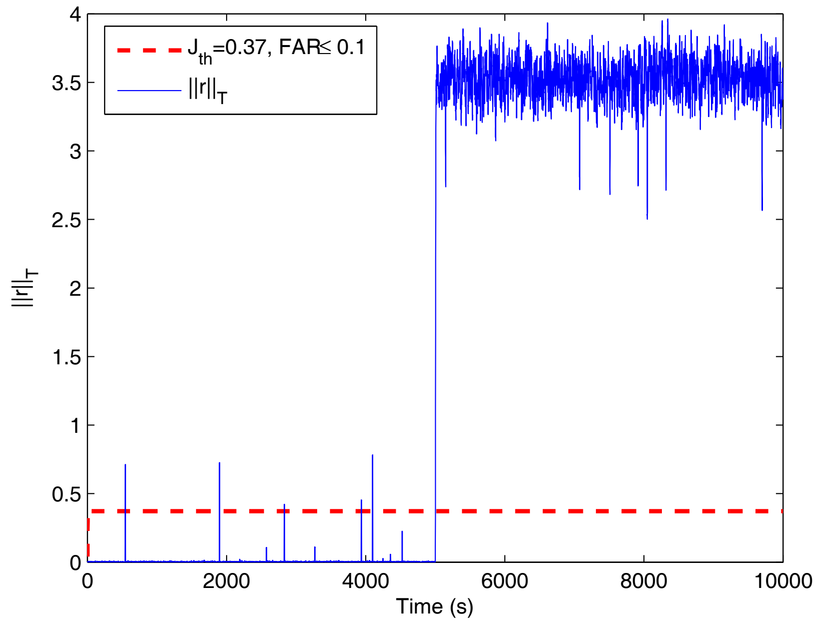

Figure 4.10: $\|r\|_T$ with $(15, 8)$-cyclic code. BER is 0.1.

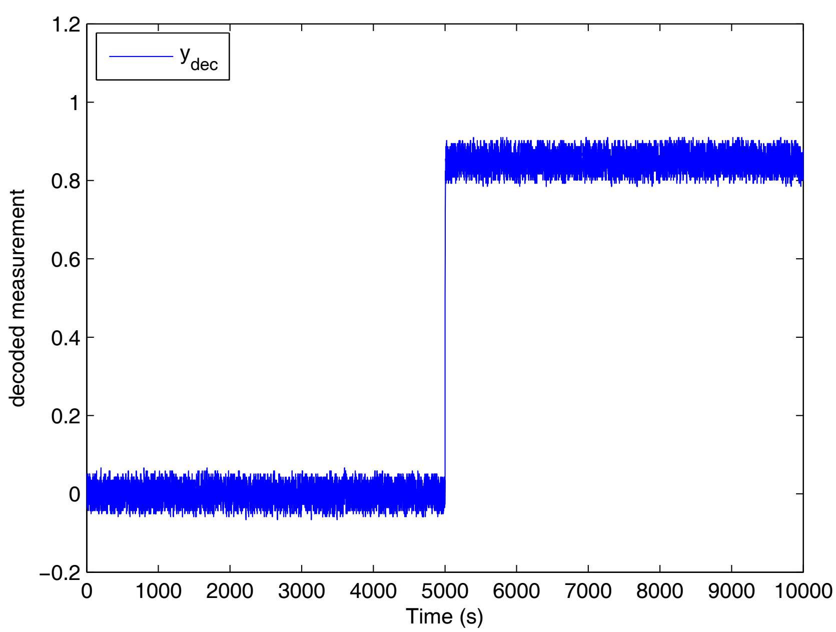

Figure 4.11: Decoded measurement with $(15, 8)$-cyclic code. BER is 0.01.

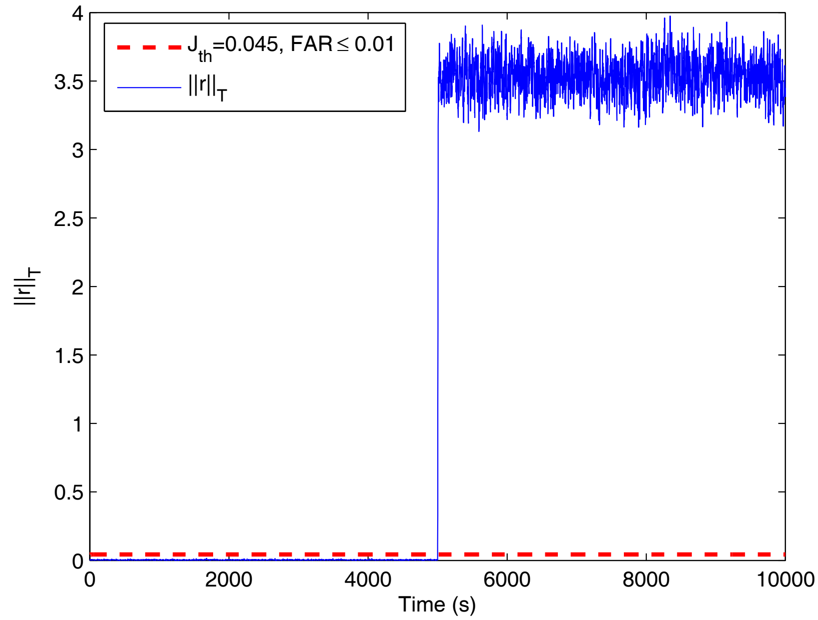

Figure 4.12: $\|r\|_T$ with $(15,8)$-cyclic code. BER is 0.01.

4.4 Remote FD over time-varying communication channels

Until now communication channels are assumed to be constant, i.e. BERs are time-invariant. But in real communication systems, the quality of transmissions may be always changing, as communication is influenced by disturbances or interferences from the environment, especially when wireless networks are applied. Hence suitable remote FD system over such time-varying communication channels is desired.

Over time-varying communication channels, the dynamics of (4.4) is still described by (4.10), while $\|\Delta_t(k)\|_T^2$ apparently depends on the time varying BER. Its expectation $\eta_{i,T}(k)$ and variance $\sigma_{i,T}(k)$ could be time-varying. As shown with (2.9), BER can be calculated for given channels according to the current quality of signals, which means that the reliability information about channels can be provided by communication systems and online available. Hence in this section, a design procedure of remote FD system is proposed by using the knowledge of BER, such that the FD system can adapt to the channels. Without loss of generality, divide $(0, \bar{p}_{i,b}]$ into l equivalent intervals, e.g.

$$(0, p_{i,b,1}], (p_{i,b,1}, p_{i,b,2}], \cdots, (p_{i,b,l-1}, \bar{p}_{i,b}], 0 = p_{i,0} < p_{i,b,1} < p_{i,b,2} < \cdots < p_{i,b,l-1} < p_{i,b,l} = \bar{p}_{i,b}. \tag{4.20}$$

When $p_{i,b}(k)$ belongs to $(p_{i,b,s(k)-1}, p_{i,b,s(k)}], s(k) = 1, \cdots, l$, the communication channel is said to be in the $s(k)$-th reliability class at the k-th time step. With the online reliability information, $s(k)$ of each measurement is known to the remote FD system. It is clear that, for the $s(k)$-th reliability class the upper bound of the transition probability from one codeword to another codeword, $P_{C_i^r, C_i^t}$, can be computed according to (4.6). Consequently the expectation of the peak norm of $\Delta_i(k)$ in the $s(k)$-th reliability class can be computed according to (4.8). For convenience, denote $\theta_{i,s(k)} = \sigma_{i,2}(k)$.

Define

$$\tilde{d}(k) = \begin{bmatrix} d(k) \\ \bar{\Delta}_t(k) \end{bmatrix}$$

where

$$\bar{\Delta}_i(k) = \Delta_i(k)\frac{\delta_{d,\infty}}{\sqrt{m\theta_{i,s(k)}}}, \|d(k)\|_{peak} = \sup_k \sqrt{d(k)^T d(k)} < \delta_{d,\infty}. \tag{4.21}$$

Then the dynamics of (4.4) can be written as

$$\begin{aligned} e(k+1) &= (A - L_k C)e(k) + (\tilde{E}_{d,k} - L_k \tilde{F}_{d,k})\tilde{d}(k) + (E_f - L_k F_f)f(k) \\ r(k) &= W_k(Ce(k) + \tilde{F}_{d,k}\tilde{d}(k) + F_f f(k)) \end{aligned} \tag{4.22}$$

with

$$\tilde{E}_{d,k} = \begin{bmatrix} E_d & 0 \end{bmatrix}, \tilde{F}_{d,k} = \begin{bmatrix} F_d & N_k \end{bmatrix}$$

and

$$N_k = \begin{bmatrix} N_{1,k} & 0 & \cdots & 0 \\ 0 & N_{2,k} & \cdots & 0 \\ 0 & 0 & \ddots & 0 \\ 0 & 0 & 0 & N_{m,k} \end{bmatrix}, N_{i,k} = \frac{\sqrt{m\theta_{i,s(k)}}}{\delta_{d,\infty}}, i = 1, \cdots, m.$$

The expectation of $\Delta_t(k)$ is normalized and

$$E\left[\|\bar{\Delta}_t(k)\|^2\right] \leq \delta_{d,\infty}^2.$$

In this way, with (4.6), (4.8) and (4.21) the online reliability information is represented by a time-varying matrix N_k and a stochastic vector, which is a part of the system dynamics (4.22). It is obvious that,

$$\theta_{i,1} < \theta_{i,2} < \cdots < \theta_{i,l}, i = 1, \cdots, m.$$

Now the question is: how to design L_k, W_k according to the reliability information. The objective of the design is to generate the residual signals which are robust against disturbances and sensitive to faults. Although for linear time-invariant systems with additive unknown inputs, the optimal residual generator has been obtained as mentioned in chapter 3, as to time-varying systems, it is still an open problem. Following the idea in FD system design of MJLSs, a reference residual model is proposed and then the dynamics of the residual generator (4.22) is designed to match the reference model. In this approach the matrices L_k and W_k are selected such that

$$\sup_{f,d \in l_2} \frac{\|r_{ref} - r\|_2}{\left\| \begin{bmatrix} \tilde{d} \\ f \end{bmatrix} \right\|_2} \tag{4.23}$$

is minimized, where r_{ref} denotes the residual signals generated by the reference residual model. As pointed out in [18], the reference model should be realistic and achieve an optimal trade-off between system robustness and fault sensitivity. Hence the reference residual model is suggested as

$$\begin{aligned} e_{ref}(k+1) &= (A_{ref} - L_o C_{ref})e_{ref}(k) + (E_{d,ref} - L_o F_{d,ref})d(k) + (E_{f,ref} - L_o F_{f,ref})f(k) \\ r_{ref}(k) &= W_o C_{ref} e_{ref}(k) + W_o F_{d,ref} d(k) + W_o F_{f,ref} f(k) \end{aligned} \tag{4.24}$$

The matrices are selected as

$$A_{ref} = A, E_{d,ref} = \begin{bmatrix} E_d & 0 \end{bmatrix}, E_{f,ref} = E_f, C_{ref} = C, F_{d,ref} = \begin{bmatrix} F_d & 0 \end{bmatrix}, F_{f,ref} = F_f,$$

which means the nominal dynamics of (4.22) without transmission errors are considered as the reference residual model. L_o and W_o can be chosen in a similar way as the ones in (4.11), such that an optimal fault detection performance for the nominal system can be guaranteed.

It is clear that, the dynamics of $r(k) - r_{ref}(k)$ is governed by

$$\begin{aligned} x_o(k+1) &= A_o(k)x_o(k) + E_o(k)\begin{bmatrix} \tilde{d}(k) \\ f(k) \end{bmatrix} \\ r(k) - r_{ref}(k) &= C_o(k)x_o(k) + F_o(k)\begin{bmatrix} \tilde{d}(k) \\ f(k) \end{bmatrix} \end{aligned} \tag{4.25}$$

where

$$x_o = \begin{bmatrix} e \\ e_{ref} \end{bmatrix}$$

and

$$\begin{aligned} A_o(k) &= \begin{bmatrix} A - L_kC & 0 \\ 0 & A_{ref} - L_oC_{ref} \end{bmatrix}, \\ C_o(k) &= \begin{bmatrix} W_kC & -W_oC_{ref} \end{bmatrix}, \\ E_o(k) &= \begin{bmatrix} \tilde{E}_{d,k} - L_k\tilde{F}_{d,k} & E_f - L_kF_f \\ E_{d,ref} - L_oF_{d,ref} & E_{f,ref} - L_oF_{f,ref} \end{bmatrix}, \\ F_o(k) &= \begin{bmatrix} \left(W_k\tilde{F}_{d,k} - W_oF_{d,ref}\right)^T \\ \left(W_kF_f - W_oF_{d,ref}\right)^T \end{bmatrix}^T. \end{aligned}$$

According to different application scenarios, the transmission manners of process measurements can be different. In the following, the residual generators and evaluators with centralized and decentralized transmissions will be designed separately.

4.4.1 When all measurements are transmitted via the same channel

In case of centralized transmission, all the measurements are transmitted via the same channel. Therefore the BERs of different measurements are the same, i.e.

$$p_{1,b}(k) = p_{2,b}(k) = \cdots = p_{m,b}(k).$$

Then the system can be modeled as a switched system, where the switching signal is the variation of the channel reliability class and it can take its values in the finite set $\psi = \{1, \cdots, l\}$ with l being the number of reliability classes. That means each reliability class is corresponding to a switching value. Denote

$$L_i = L_k, W_i = W_k, \tilde{E}_{d,i} = \tilde{E}_{d,k}, \tilde{F}_{d,i} = \tilde{F}_{d,k}$$

and

$$A_{o,i} = A_o(k), C_{o,i} = C_o(k), E_{o,i} = E_o(k), F_{o,i} = F_o(k),$$

when $s(k) = i, i \in \psi$.

Before giving the solution for minimizing (4.23), the following useful lemma is introduced.

Lemma 4.3 *(Zhang, Shi, Wang and Gao [115]) Consider the system (4.25). Given a constant $\gamma > 0$, $x_o(0) = 0$, if there exist matrices $X_i > 0$ and $G_i > 0$ such that the following LMI*

$$\begin{bmatrix} X_j - (G_i + G_i^T) & G_i^T A_{o,i} & G_i^T E_{o,i} & 0 \\ * & -X_i & 0 & C_{o,i}^T \\ * & * & -\gamma^2 I & F_{o,i}^T \\ * & * & * & -I \end{bmatrix} < 0$$

holds for all $i, j \in \psi$, then

$$\frac{\|r - r_{ref}\|_2}{\left\| \begin{bmatrix} \tilde{d} \\ f \end{bmatrix} \right\|_2} < \gamma.$$

The following theorem gives the solution to (4.23).

Theorem 4.4 *Consider the remote FD system with the centralized transmission. Given the system (4.25), $x_o(0) = 0$, the $\mathbb{L}(n_c, k_c)$, the reliability classes (4.20) and a constant $\gamma > 0$, the optimal L_i and W_i of the residual generator (4.4) in the sense of minimizing (4.23) can be obtained by solving the following optimization problem*

$$\min_{X_j > 0, Y_i, W_i, Q_i} \gamma^2$$

subject to

$$[\Pi_{gh}]_{7\times 7} = [\Pi_{gh}]_{7\times 7}^T < 0$$

for all $i, j \in \psi$, with

$$\begin{bmatrix} \Pi_{11} & \Pi_{12} \\ * & \Pi_{22} \end{bmatrix} = \begin{bmatrix} X_{j,11} - Q_{i,11} - Q_{i,11}^T & X_{j,12} \\ * & X_{j,22} - Q_{i,22} - Q_{i,22}^T \end{bmatrix}$$

and other nonzero terms

$$\begin{aligned}
&\Pi_{14} = Q_{i,11}A - Y_iC, \Pi_{16} = Q_{i,11}E_d - Y_i\tilde{F}_{d,i}, \Pi_{17} = Q_{i,11}E_f - Y_iF_f, \\
&\Pi_{25} = Q_{i,22}(A - L_oC), \Pi_{26} = Q_{i,22}(E_d - L_oF_d), \Pi_{27} = Q_{i,22}(E_f - L_oF_f), \\
&\Pi_{33} = -I, \Pi_{34} = W_iC, \Pi_{35} = -W_oC, \\
&\Pi_{36} = W_i\tilde{F}_{d,i} - W_oF_{d,ref}, \Pi_{37} = W_iF_f - W_oF_{d,ref}, \\
&\Pi_{44} = -X_{j,11}, \Pi_{45} = -X_{j,12}, \Pi_{55} = -X_{j,22}, \\
&\Pi_{66} = -\gamma^2 I_{n\times n}, \Pi_{77} = -\gamma^2 I_{n\times n},
\end{aligned}$$

where

$$X_j = \begin{bmatrix} X_{j,11} & X_{j,12} \\ * & X_{j,22} \end{bmatrix}, Q_i = \begin{bmatrix} Q_{i,11} & 0 \\ 0 & Q_{i,22} \end{bmatrix},$$

then the optimal $L_i = Q_{i,11}^{-1} Y_i$.

Proof With Lemma 4.3, the proof is straightforward with $Y_i = Q_{i,11}L_i$. ∎

The following algorithm gives a way to set the threshold in case of the centralized transmission.

Algorithm
- Step 1: Given the system (4.3), the residual generator (4.4) and a constant $\gamma > 0$, solve the following constrained optimization problem

$$\min_{X_j>0} \gamma^2$$

subject to

$$\begin{bmatrix} -X_j & X_j(A-L_iC) & X_j(\tilde{E}_{d,i}-L_i\tilde{F}_{d,i}) & 0 \\ * & -X_i & 0 & (W_iC)^T \\ * & * & -\gamma^2 I & (W_i\tilde{F}_{d,i})^T \\ * & * & * & -I \end{bmatrix} < 0.$$

for all $i, j \in \psi$. Denote $\breve{\gamma}$ as the solution to the above optimization problem.

- Step 2: according to Lemma 4.1, the threshold can be set as

$$J_{th}(k) = \breve{\gamma}\sqrt{\delta_{d,2}^2 + \bar{\eta}_{T,max}(k) + \beta\bar{\sigma}_{T,max}(k)} \tag{4.26}$$

where

$$\bar{\eta}_{T,max}(k) = \sum_{i=1}^{m}\sum_{j=k-T+1}^{k}\max_{C_i^t}\frac{\delta_{d,\infty}^2}{m\theta_{i,s(j)}}\sigma_{i,2}(j)$$

and

$$\bar{\sigma}_{T,max}^2(k) = \sum_{i=1}^{m}\sum_{j=k-T+1}^{k}\max_{C_i^t}\frac{\delta_{d,peak}^4}{m^2\theta_{i,s(j)}^2}\left(\sigma_{i,4}(j) - \sigma_{i,2}^2(j)\right).$$

The worst-case $\bar{\eta}_{T,max}(k)$ and $\bar{\sigma}_{T,max}$ are employed in (4.26), as $C_i^t(k)$ is unknown to the remote FD system. The FAR is upper bounded by $\frac{1}{\beta^2}$.

4.4.2 When measurements are transmitted via different channels

In case of the decentralized transmission, different sensor signals are transmitted via different channels, i.e. the BERs of different measurements are different. Then the system is no longer proper to be modeled as a switched system, as the the set of switching values may be too large, which is l^m. It is clear that, N_k is a polytopic type time-varying matrix, i.e. N_k can be written as

$$N_k = \sum_{i=1}^{2^m} a_i(k)V_i, \sum_{i=1}^{2^m} a_i(k) = 1, a_i(k) \geq 0$$

where V_i is the i-th vertex and

$$V_i = \begin{bmatrix} v_1 & 0 & \cdots & 0 \\ 0 & v_2 & \cdots & 0 \\ \vdots & \ddots & \ddots & \vdots \\ 0 & 0 & \cdots & v_m \end{bmatrix}, v_j \in \{\frac{\sqrt{m\theta_{j,1}}}{\delta_{d,\infty}}, \frac{\sqrt{m\theta_{j,l}}}{\delta_{d,\infty}}\}, j = 1, \cdots, m,$$

$$V_1 \neq V_2 \neq \cdots \neq V_{2^m}.$$

Then it turns out

$$\tilde{F}_{d,k} = \begin{bmatrix} F_d & 0 \end{bmatrix} + \begin{bmatrix} 0 & \sum_{i=0}^{2^m} a_i(k) V_i \end{bmatrix}.$$

Denote

$$\tilde{F}_{d,i} = \begin{bmatrix} F_d & 0 \end{bmatrix} + \begin{bmatrix} 0 & V_i \end{bmatrix}, i = 1, 2, \cdots, 2^m.$$

With the reliability information provided by the communication systems, $a_i(k)$ is known to the remote FD system. The following theorem gives the solution to (4.23).

Theorem 4.5 *Consider the remote FD system with the decentralized transmission. Given the system (4.25), $x_o(0) = 0$, the $\mathbb{L}(n_c, k_c)$, the reliability classes (4.20) and a constant $\gamma > 0$, the optimal L_k and W_k of the residual generator (4.4) in the sense of minimizing (4.23) can be obtained by solving the following optimization problem*

$$\min_{X_1>0, X_2>0, Y_i, W_i} \gamma^2$$

subject to

$$\left[\begin{array}{cccccccc} -X_1 & 0 & X_1 A - \frac{1}{2}(Y_i + Y_j)C & 0 & X_1 E_d - \frac{1}{2}(Y_i + Y_j)F_d & -\frac{1}{2}(Y_i V_j + Y_j V_i) & X_1 E_f - \frac{1}{2}(Y_i + Y_j)F_f & 0 \\ * & -X_2 & 0 & X_2(A - L_o C) & X_2(E_d - L_o F_d) & 0 & X_2(E_f - L_o F_f) & 0 \\ * & * & -X_1 & 0 & 0 & 0 & 0 & \frac{1}{2}(W_i C + W_j C)^T \\ * & * & * & -X_2 & 0 & 0 & 0 & (-W_o C)^T \\ * & * & * & * & -\gamma^2 I & 0 & 0 & (\frac{1}{2}(W_i + W_j)F_d - W_o F_d)^T \\ * & * & * & * & * & -\gamma^2 I & 0 & \frac{1}{2}(W_i V_j + W_j V_i)^T \\ * & * & * & * & * & * & -\gamma^2 I & (\frac{1}{2}(W_i + W_j)F_f - W_o F_f)^T \\ * & * & * & * & * & * & * & -I \end{array}\right] < 0 \tag{4.27}$$

for $i, j = 1, \cdots, 2^m$. Then the optimal L_k and W_k can be chosen as

$$L_k = \sum_{i=1}^{2^m} a_i(k) L_i, W_k = \sum_{i=1}^{2^m} a_i(k) W_i,$$

where $L_i = X_1^{-1} Y_i$.

Proof Rewrite (4.25) as

$$\begin{aligned} x_o(k+1) &= \sum_{i=1}^{2^m} \sum_{j=1}^{2^m} \mu_i \mu_j \left\{ \frac{1}{2}(A_{o,i} + A_{o,j}) x_o(k) + \frac{1}{2}(E_{o,i} + E_{o,j}) \begin{bmatrix} \tilde{d}(k) \\ f(k) \end{bmatrix} \right\} \\ r(k) - r_{ref}(k) &= \sum_{i=1}^{2^m} \sum_{j=1}^{2^m} \mu_i \mu_j \left\{ \frac{1}{2}(C_{o,i} + C_{o,j}) x_o(k) + \frac{1}{2}(F_{o,i} + F_{o,j}) \begin{bmatrix} \tilde{d}(k) \\ f(k) \end{bmatrix} \right\} \end{aligned}$$

where

$$\begin{aligned}
A_{o,i} &= \begin{bmatrix} A - L_i C & 0 \\ 0 & A_{ref} - L_o C_{ref} \end{bmatrix}, A_{o,j} = \begin{bmatrix} A - L_j C & 0 \\ 0 & A_{ref} - L_o C_{ref} \end{bmatrix}, \\
C_{o,i} &= \begin{bmatrix} W_i C & -W_o C_{ref} \end{bmatrix}, C_{o,j} = \begin{bmatrix} W_j C & -W_o C_{ref} \end{bmatrix}, \\
F_{o,i} &= \begin{bmatrix} \left(W_i \tilde{F}_{d,j} - W_o F_{d,ref}\right)^T \\ \left(W_i F_f - W_o F_{d,ref}\right)^T \end{bmatrix}^T, F_{o,j} = \begin{bmatrix} \left(W_j \tilde{F}_{d,i} - W_o F_{d,ref}\right)^T \\ \left(W_j F_f - W_o F_{d,ref}\right)^T \end{bmatrix}^T, \\
E_{o,i} &= \begin{bmatrix} \tilde{E}_{d,i} - L_i \tilde{F}_{d,j} & E_f - L_i F_f \\ E_{d,ref} - L_o F_{d,ref} & E_{f,ref} - L_o F_{f,ref} \end{bmatrix}, \\
E_{o,j} &= \begin{bmatrix} \tilde{E}_{d,j} - L_j \tilde{F}_{d,i} & E_f - L_j F_f \\ E_{d,ref} - L_o F_{d,ref} & E_{f,ref} - L_o F_{f,ref} \end{bmatrix}, \\
&\sum_{i=1}^{2^m} \mu_i = 1, \sum_{j=1}^{2^m} \mu_j = 1, \mu_i \geq 0, \mu_j \geq 0.
\end{aligned}$$

Define a Lyapunov function $V(k) = x_o(k)^T X x_o(k)$, where

$$X = \begin{bmatrix} X_1 & 0 \\ 0 & X_2 \end{bmatrix} > 0.$$

With $x_o(0) = 0$, it turns out

$$\sum_{k=0}^{\infty} V(k+1) - V(k) = V(\infty) \geq 0.$$

Then

$$\begin{aligned}
&\|r(k) - r_{ref}(k)\|_2^2 - \gamma^2 \| \begin{bmatrix} \tilde{d}(k) \\ f(k) \end{bmatrix} \|_2^2 \\
&\leq \sum_{k=1}^{\infty} (r(k) - r_{ref}(k))^T (r(k) - r_{ref}(k)) - \gamma^2 \begin{bmatrix} \tilde{d}(k) \\ f(k) \end{bmatrix}^T \begin{bmatrix} \tilde{d}(k) \\ f(k) \end{bmatrix} + V(k+1) - V(k) \\
&\leq \begin{bmatrix} x_o(k) \\ \tilde{d}(k) \\ f(k) \end{bmatrix}^T R_{ij} \begin{bmatrix} x_o(k) \\ \tilde{d}(k) \\ f(k) \end{bmatrix}
\end{aligned}$$

where

$$\begin{aligned}
R_{ij} = &\left(\frac{1}{2} \sum_{i=1}^{N} \sum_{j=1}^{N} \mu_i \mu_j \begin{bmatrix} A_{o,i} + A_{o,j} & E_{o,i} + E_{o,j} \\ C_{o,i} + C_{o,j} & F_{o,i} + F_{o,j} \end{bmatrix}^T \right) \begin{bmatrix} X & 0 \\ 0 & I \end{bmatrix} \times \\
&\left(\frac{1}{2} \sum_{i=1}^{N} \sum_{j=1}^{N} \mu_i \mu_j \begin{bmatrix} A_{o,i} + A_{o,j} & E_{o,i} + E_{o,j} \\ C_{o,i} + C_{o,j} & F_{o,i} + F_{o,j} \end{bmatrix} \right) - \begin{bmatrix} X & 0 \\ 0 & -\gamma^2 I \end{bmatrix}.
\end{aligned}$$

If $R_{ij} < 0$ for any $i, j = 1, 2, \cdots, 2^m$, then for any $\begin{bmatrix} \tilde{d}(k) \\ f(k) \end{bmatrix} \in l_2$ it turns out

$$\frac{\|r_{ref} - r\|_2}{\| \begin{bmatrix} \tilde{d} \\ f \end{bmatrix} \|_2} < \gamma.$$

Obviously,

$$\begin{bmatrix} \frac{1}{2}(A_{o,i}+A_{o,j}) & \frac{1}{2}(E_{o,i}+E_{o,j}) \\ \frac{1}{2}(C_{o,i}+C_{o,j}) & \frac{1}{2}(F_{o,i}+F_{o,j}) \end{bmatrix}^T \begin{bmatrix} X & 0 \\ 0 & I \end{bmatrix} \begin{bmatrix} \frac{1}{2}(A_{o,i}+A_{o,j}) & \frac{1}{2}(E_{o,i}+E_{o,j}) \\ \frac{1}{2}(C_{o,i}+C_{o,j}) & \frac{1}{2}(F_{o,i}+F_{o,j}) \end{bmatrix} - \begin{bmatrix} X & 0 \\ 0 & \gamma^2 I \end{bmatrix} < 0 \tag{4.28}$$

implies $R_{ij} < 0$. By defining $Y_i = X_1 L_i$ and applying Schur-complement as well as congruency transformation, (4.28) can be rewritten as in (4.27). ■

The following algorithm gives a way to set the threshold in case of the decentralized transmission.

Algorithm

- Step 1: Given the system (4.3), the residual generator (4.4) and a constant $\gamma > 0$, solve the following constrained optimization problem

$$\min_{X>0} \gamma^2$$

subject to

$$\begin{bmatrix} -X & XA - \frac{1}{2}X(L_iC + L_jC) & XE_{d,i} - \frac{1}{2}X(L_i\tilde{F}_{d,j} + L_j\tilde{F}_{d,i}) & 0 \\ * & -X & 0 & \frac{1}{2}((W_i+W_j)C)^T \\ * & * & -\gamma^2 I & \frac{1}{2}(W_i\tilde{F}_{d,j} + W_j\tilde{F}_{d,i})^T \\ * & * & * & -I \end{bmatrix} < 0$$

for all $i, j \in \psi$. Denote $\breve{\gamma}$ as the solution to the above optimization problem.

- Step 2: the threshold can be set as in (4.26).

The FAR is upper bounded by $\frac{1}{\beta^2}$. It is worth to notice that with given maximum BERs, the observer gain can be designed for all possible $N(k)$ within the polytopic space.

4.4.3 A numerical example

In this section, a numerical example is given to illustrate the effectiveness of the proposed methods. Consider the following closed-loop system:

$$A = \begin{bmatrix} 0.1 & 0.2 & 0.3 \\ 0 & 0.65 & 0.3 \\ 0 & 0 & 0.3 \end{bmatrix}, E_d = \begin{bmatrix} 0.2 & 0 \\ 0.1 & 0 \\ 0.4 & 0.2 \end{bmatrix}, E_f = \begin{bmatrix} 0.2 \\ 0 \\ 0.1 \end{bmatrix},$$
$$C = \begin{bmatrix} 1 & 0 & 1 \\ 0 & 0 & 1 \end{bmatrix}, F_d = \begin{bmatrix} 0.1 & 0.4 \\ 0.2 & 0.3 \end{bmatrix}, F_f = 0.$$

The sampling time of the system is 1s. The 8-bit uniform quantizer is applied for both measurements in the source encoder and the range of the each valid measurement is assumed to be $(0, 4)$. The unknown disturbances $d(k)$ is simulated as a uniform random number in the range of $[-0.1, 0.1]$. The simulation time is 500s. A bias actuator fault is generated at $t = 250$s. The measurements are decoded according to (4.5). The upper

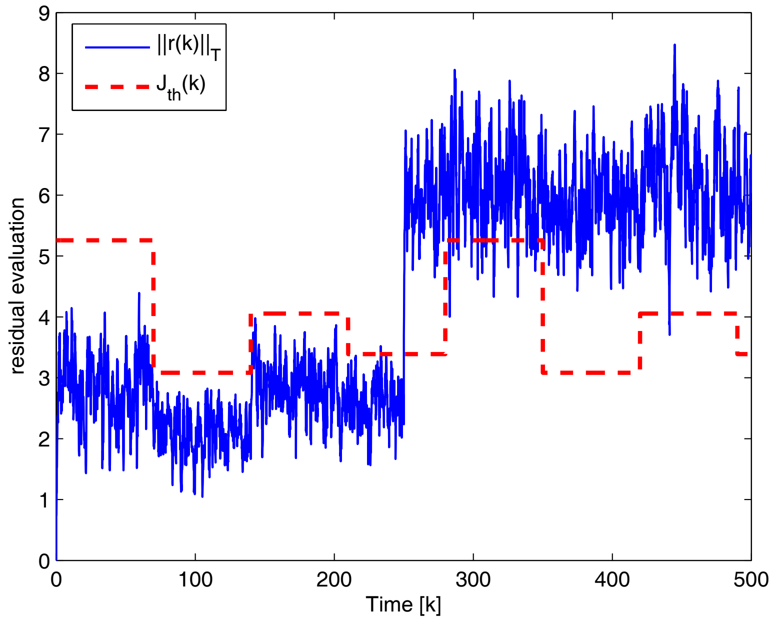

Figure 4.13: with $(15, 8)$ channel coding, $\beta = 2$, $f = 3$, centralized transmission.

Table 4.1: $\delta_{i,2}$ and $\delta_{i,4}, i = 1, 2$ with $(8, 8)$-code. [a] with the probability larger than 75%.

	(0,0.05]	(0.05,0.1]	(0.1,0.15]	(0.15,0.2]
$\delta_{i,2}$	< 0.0733	< 0.1597	< 0.2593	< 0.3721
$\delta_{i,4}$	< 0.0716	< 0.1831	< 0.3396	< 0.5360
$\Vert\Delta_i(k)\Vert_T$ [a]	< 2.36	< 4.1	< 5.89	< 7.7

bound of $p_b(k)$ is assumed to be $\begin{bmatrix} 0.2 & 0.2 \end{bmatrix}^T$ and four reliability classes are considered, i.e.

$$(0, 0.05], (0.05, 0.1], (0.1, 0.15], (0.15, 0.2].$$

Two kinds of codes are applied to illustrate the results. The first is an $(8, 8)$-code. That means the 8-bit binary sequence after quantization is directly transmitted without further channel coding. By selecting $\beta = 2$ and $T = 10$, then according to (4.14) the expectation of the energy level of $\Delta_t(k)$ is approximated. In Table 4.1, the important statistical properties of the code are given. The second code is a $(15, 8)$-cyclic code, in which the 8-bit binary sequence after quantization is encoded by the channel encoder with the $(15, 8)$-cyclic code and then transmitted over communication channels. With $\beta = 2$ and $T = 10$, its statistical properties can be found in Table 4.2.

When all the measurements are transmitted over the same channels, i.e. centralized transmission, according to Theorem 4.4, the optimal residual generator for channels applying $(8, 8)$-code are with

$$L_1 = \begin{bmatrix} 0.2194 & 0.0785 \\ 0.1474 & 0.0536 \\ 0.1212 & 0.0594 \end{bmatrix}, L_2 = \begin{bmatrix} 0.2274 & 0.0814 \\ 0.1432 & 0.0522 \\ 0.1282 & 0.0557 \end{bmatrix},$$

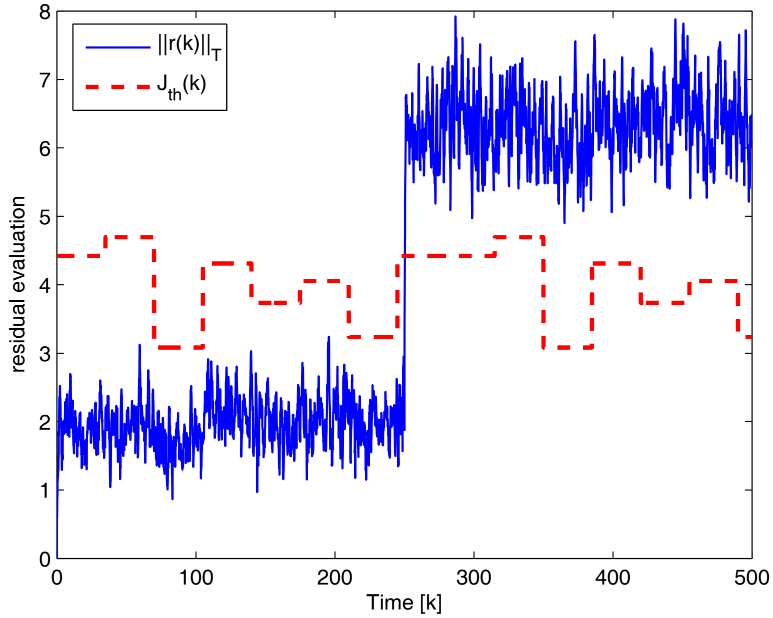

Figure 4.14: with $(15, 8)$ channel coding, $\beta = 2$, $f = 3$, decentralized transmission.

Table 4.2: $\delta_{i,2}$ and $\delta_{i,4}, i = 1, 2$ with $(15, 8)$-code. [a] with the probability larger than 75%.

	(0,0.05]	(0.05,0.1]	(0.1,0.15]	(0.15,0.2]
$\delta_{i,2}$	$< 0.6524 \cdot 10^{-4}$	< 0.0014	< 0.0103	< 0.0504
$\delta_{i,4}$	$< 0.999 \cdot 10^{-4}$	< 0.0022	< 0.0172	< 0.0869
$\lVert\Delta_i(k)\rVert_T$ [a]	< 0.063	< 0.31	< 0.93	< 2.33

$$L_3 = \begin{bmatrix} 0.2178 & 0.0784 \\ 0.1336 & 0.0489 \\ 0.1245 & 0.0520 \end{bmatrix}, L_4 = \begin{bmatrix} 0.2002 & 0.0725 \\ 0.1219 & 0.0448 \\ 0.1156 & 0.0475 \end{bmatrix},$$

$$W_1 = \begin{bmatrix} 0.0090 & -0.0252 \\ -0.0012 & 0.0223 \end{bmatrix}, W_2 = \begin{bmatrix} 0.0053 & -0.0154 \\ 0.0034 & 0.0150 \end{bmatrix},$$

$$W_3 = \begin{bmatrix} 0.0027 & -0.0117 \\ 0.0063 & 0.0123 \end{bmatrix}, W_4 = \begin{bmatrix} 0.0007 & -0.0098 \\ 0.0078 & 0.0108 \end{bmatrix}$$

and for channel applying $(15, 8)$-code are with

$$L_1 = \begin{bmatrix} 0.1807 & 0.0984 \\ 0.1448 & 0.0723 \\ 0.0051 & 0.3253 \end{bmatrix}, L_2 = \begin{bmatrix} 0.2081 & 0.0809 \\ 0.1518 & 0.0604 \\ 0.0900 & 0.1256 \end{bmatrix},$$

$$L_3 = \begin{bmatrix} 0.2508 & 0.0887 \\ 0.1581 & 0.0589 \\ 0.1326 & 0.0807 \end{bmatrix}, L_4 = \begin{bmatrix} 0.3192 & 0.1108 \\ 0.1624 & 0.0593 \\ 0.1803 & 0.0772 \end{bmatrix},$$

$$W_1 = \begin{bmatrix} 0.1783 & -0.4882 \\ -0.1413 & 0.3942 \end{bmatrix}, W_2 = \begin{bmatrix} 0.0530 & -0.1440 \\ -0.0400 & 0.1169 \end{bmatrix},$$

$$W_3 = \begin{bmatrix} 0.0204 & -0.0542 \\ -0.0130 & 0.0448 \end{bmatrix}, W_4 = \begin{bmatrix} 0.0087 & -0.0236 \\ 0.0013 & 0.0217 \end{bmatrix}.$$

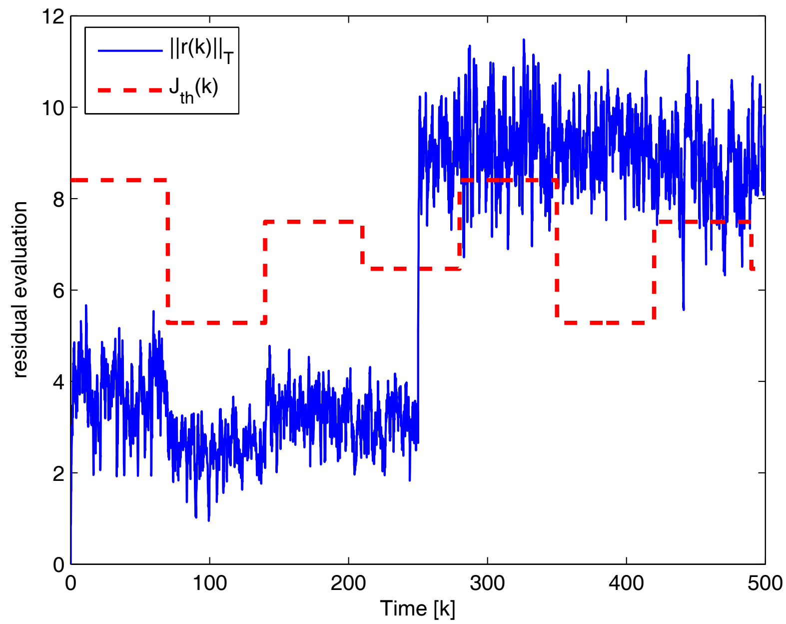

Figure 4.15: with $(8,8)$ coding, $\beta = 2$, $f = 5$, centralized transmission.

When different measurements are transmitted over different channels, i.e. decentralized transmission, according to Theorem 4.5, the optimal residual generator for channels applying $(8,8)$-code are with

$$L_1 = \begin{bmatrix} 0.2445 & 0.0873 \\ 0.1539 & 0.0574 \\ 0.1364 & 0.0606 \end{bmatrix}, L_2 = \begin{bmatrix} 0.2043 & 0.1370 \\ 0.1264 & 0.0846 \\ 0.1155 & 0.0887 \end{bmatrix},$$

$$L_3 = \begin{bmatrix} 0.2590 & 0.0463 \\ 0.1619 & 0.0312 \\ 0.1466 & 0.0325 \end{bmatrix}, L_4 = \begin{bmatrix} 0.2117 & 0.0820 \\ 0.1319 & 0.0508 \\ 0.1215 & 0.0534 \end{bmatrix},$$

$$W_1 = \begin{bmatrix} 0.0079 & -0.0181 \\ -0.0001 & 0.0166 \end{bmatrix}, W_2 = \begin{bmatrix} 0.0046 & -0.0167 \\ 0.0028 & 0.0176 \end{bmatrix},$$

$$W_3 = \begin{bmatrix} 0.0050 & -0.0104 \\ 0.0031 & 0.0095 \end{bmatrix}, W_4 = \begin{bmatrix} 0.0016 & -0.0105 \\ 0.0060 & 0.0112 \end{bmatrix}$$

and for channel applying $(15,8)$-code are

$$L_1 = \begin{bmatrix} 0.2577 & 0.0755 \\ 0.1610 & 0.0610 \\ 0.1282 & 0.0924 \end{bmatrix}, L_2 = \begin{bmatrix} 0.3051 & 0.2485 \\ 0.1476 & 0.1350 \\ 0.1620 & 0.1767 \end{bmatrix},$$

$$L_3 = \begin{bmatrix} 0.2966 & 0.0145 \\ 0.1792 & 0.0183 \\ 0.1607 & 0.0291 \end{bmatrix}, L_4 = \begin{bmatrix} 0.3487 & 0.1256 \\ 0.1665 & 0.0672 \\ 0.1955 & 0.0887 \end{bmatrix},$$

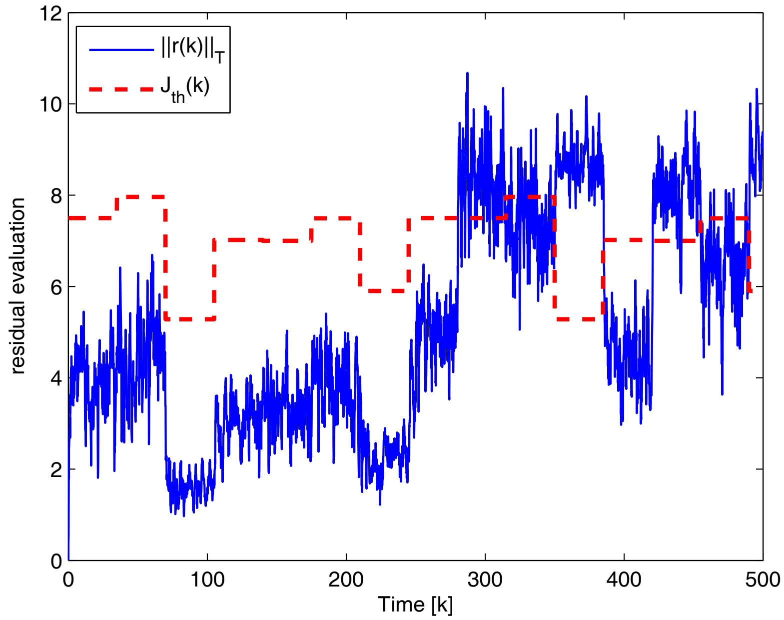

Figure 4.16: with $(8,8)$ coding, $\beta = 2$, $f = 5$, decentralized transmission.

$$W_1 = \begin{bmatrix} 0.0336 & -0.0887 \\ -0.0242 & 0.0723 \end{bmatrix}, W_2 = \begin{bmatrix} 0.0232 & -0.0617 \\ -0.0136 & 0.0536 \end{bmatrix},$$

$$W_3 = \begin{bmatrix} 0.0154 & -0.0375 \\ -0.0088 & 0.0302 \end{bmatrix}, W_4 = \begin{bmatrix} 0.0089 & -0.0298 \\ 0.0002 & 0.0263 \end{bmatrix}.$$

Fig. 4.13-4.16 shows the results. It can be seen that, the obtained thresholds are adaptive to BERs. In Fig. 4.13 and Fig. 4.15 the transmissions are over the same channel, while in Fig. 4.14 and Fig. 4.16 the transmissions of the two measurements are over different channels. In Fig. 4.13 and Fig. 4.14, the $(15,8)$-cyclic code is applied and $f = 3$. In Fig. 4.15 and Fig. 4.16, no channel coding is applied and $f = 5$. By comparing the results, it can be concluded that, the influence of bit errors is significantly reduced with channel coding and thus the fault of smaller size can be detected. The FAR is upper bounded by 25%.

4.5 Conclusions

In this chapter an observer-based remote FD system with channel reliability information has been designed. With the knowledge of the encoder/decoder in communication systems, the statistical properties of bit errors have been investigated, and based on that, the influence of bit errors and quantization errors are described through stochastic unknown inputs with constant or time-varying polytopic type distribution matrices. The reference residual model has been suggested in order to design an optimal residual generator for time-varying systems, and then thresholds have been selected by considering the stochastic behavior introduced by bit errors. The design procedures for centralized transmission and decentralized transmission have been given separately. The later one is much meaningful for practical applications in industry.

5 FD of Networked Control Systems

In this chapter, the design scheme of the FD system for NCSs considering time varying transmission delays, packet dropouts and quantization errors, is proposed. The design of the residual generator is formulated in the H_∞ framework, where the transmission delays are described as polytopic uncertainties, quantization errors are modeled as norm bounded uncertainties and packet dropouts are described as a binary Bernoulli process. The dynamics of residual generator is shown to be governed by an MJLS with both polytopic and norm bounded uncertainties. Based on the results obtained in chapter 3, the residual generator is designed to match a reference model such that it is sensitive to system faults and robust against network-induced effects and system disturbances. Then the absolute value of each residual signal is selected as the evaluation function and the computation of its mean value and variance is given in terms of LMIs. The corresponding threshold is calculated based on the mean value and variance, which can on one side ensure the upper bound of the FAR and on the other side reduce the miss detections of faults. Parts of this chapter are based on [64].

5.1 NCS model and problem formulation

In this chapter the NCS with the structure shown in Fig. 1.4 is considered, where sensors, actuators and controller are connected with networks and the FD system is located together with the controller. Consider the continuous-time process

$$
\begin{aligned}
\dot{x}(t) &= A_c x(t) + B_c u(t) + E_{c,d} d(t) + E_{c,f} f(t) \\
y(t) &= C_c x(t) + F_{c,d} d(t) + F_{c,f} f(t)
\end{aligned}
\tag{5.1}
$$

where $x \in \mathbb{R}^n$ denotes the state vector, $u \in \mathbb{R}^p$ denotes the control inputs applied in the plant, $y \in \mathbb{R}^m$ denotes the measured output vector, $d \in \mathbb{R}^{n_d}$ denotes the unknown inputs and $f \in \mathbb{R}^{n_f}$ are the faults to be detected. $A_c, B_c, C_c, E_{c,d}, E_{c,f}, F_{c,d}, F_{c,f}$ are known matrices of appropriate dimensions.

It is assumed that, the sensors are clock driven and their sampling period is T_s, while the actuators are event driven and immediately apply the new control inputs when they arrive. The sum of the transmission delays from sensors to controller/FD and from controller/FD to actuators is denoted as τ_k. Suppose that, τ_k is bounded by $\mu_1 T_s \le \tau_k < \mu_2 T_s$, where μ_1 and μ_2 are known nonnegative constant integers and the packets arrive in the right order as in [37]. Then there will be at most $\mu + 1$ ($\mu = \mu_2 - \mu_1$) control inputs applied at the actuator during $[kT_s, (k+1)T_s)$, and in this case $h = \tau_{-1}^k \ge \tau_0^k \ge \tau_1^k \ge \cdots \ge \tau_\mu^k = 0$ where $kT + \tau_i^k$ ($i = 0, \cdots, \mu$) denotes the time instant at which $u(k - \mu_1 - i)$ applied. When $u(k - \mu_1 - i)$ arrives before kT_s, set $\tau_i^k = \tau_{i+1}^k = \cdots = \tau_\mu^k = 0$. Now the process (5.1) can be rewritten as a discrete-time system as follows

$$\begin{aligned} x(k+1) &= A_d x(k) + \sum_{i=0}^{\mu} \Gamma_i^k u(k-\mu_1-i) + E_{d,d} d(k) + E_{d,f} f(k) \\ y(k) &= C_d x(k) + F_{d,d} d(k) + F_{d,f} f(k) \end{aligned}$$

where $\Gamma_i^k = \int_{\tau_i^k}^{\tau_{i-1}^k} e^{A_c(\tau_{i-1}^k - t)} B_c dt$ and

$$A_d = e^{A_c T_s}, C_d = C_c, F_{d,d} = F_{c,d}, F_{d,f} = F_{c,f},$$

$$E_{d,d} = \int_0^{T_s} e^{A_c(T_s - t)} E_{c,d} dt, E_{d,f} = \int_0^{T_s} e^{A_c(T_s - t)} E_{c,f} dt.$$

As shown in [40] and [106], Γ_i^k belongs to a convex hull $co\{U_{i,1}, \cdots, U_{i,2n}\}$. Hence the above system can be reformulated as the following augmented system

$$\begin{aligned} \xi(k+1) &= A(k)\xi(k) + B(k)u(k-\mu_1) + E_d d(k) + E_f f(k) \\ y(k) &= C\xi(k) + F_d d(k) + F_f f(k) \end{aligned} \tag{5.2}$$

where

$$\begin{aligned} \xi(k) &= \begin{bmatrix} x(k)^T & u(k-\mu_1-1)^T & \cdots & u(k-\mu_2)^T \end{bmatrix}^T, \\ E_d &= \begin{bmatrix} E_{d,d}^T & 0 & \cdots & 0 \end{bmatrix}^T, E_f = \begin{bmatrix} E_{d,f}^T & 0 & \cdots & 0 \end{bmatrix}^T, \\ C &= \begin{bmatrix} C_d & 0 & 0 & \cdots & 0 \end{bmatrix}, F_d = F_{d,d}, F_f = F_{d,f}, \end{aligned}$$

and

$$A(k) = \left(A_0 + \sum_{i=1}^{(2n)^\mu} \alpha_i^k A_{V_i} \right), B(k) = \left(B_0 + \sum_{i=1}^{(2n)^\mu} \alpha_i^k B_{V_i} \right)$$

with

$$A_0 = \begin{bmatrix} A_d & 0 & 0 & \cdots & 0 \\ 0 & 0 & 0 & \cdots & 0 \\ 0 & I & 0 & \cdots & 0 \\ \vdots & \ddots & \ddots & \vdots & \\ 0 & 0 & \cdots & I & 0 \end{bmatrix}, B_{V_i} = \begin{bmatrix} -\sum_{j=1}^{\mu} U_{j,i_j} \\ I \\ 0 \\ \vdots \\ 0 \end{bmatrix},$$

$$A_{V_i} = \begin{bmatrix} 0 & U_{1,i_1} & U_{2,i_2} & \cdots & U_{\mu,i_\mu} \\ 0 & 0 & 0 & \cdots & 0 \\ 0 & 0 & 0 & \cdots & 0 \\ \vdots & \ddots & \ddots & \vdots & \\ 0 & 0 & \cdots & 0 & 0 \end{bmatrix}, B_0 = \begin{bmatrix} \sum_{i=0}^{\mu} \Gamma_i^k \\ I \\ 0 \\ \vdots \\ 0 \end{bmatrix}$$

where V_i represents a possible set of $\{i_j\}, i_j \in \{1, 2, \cdots, 2n\}$ and U_{j,i_j} are known matrices and $\sum_{i=1}^{(2n)^\mu} \alpha_i^k = 1$ at each time step k. Please refer to [106] for the details about U_{j,i_j}. Here it is assumed that, the sampled measurements $y(k)$ are first quantized via the logarithmic quantizer (2.7) before transmissions and the quantized measurements are denoted as $y_q(k)$.

For the augmented uncertain system (5.2), the following residual generator is proposed:

$$\begin{aligned}\hat{\xi}(k+1) &= A_0\hat{\xi}(k) + B_0 u_r(k-\mu_1) + L(\theta_k)(y_r(k) - \hat{y}(k)) \\ \hat{y}(k) &= C\hat{\xi}(k) \\ r(k) &= W(\theta_k)(y_r(k) - \hat{y}(k))\end{aligned} \tag{5.3}$$

where $u_r(k)$ is the vector of control inputs computed by the controller, $y_r(k)$ the vector of quantized measurements received by the residual generator, $r(k)$ the vector of residual signals, $\hat{\xi}(k)$ the estimate of $\xi(k)$ and $\hat{y}(k)$ the estimated measurements. When $y_q(k)$ arrives at the FD system, the residual generator compute the new residual $r(k)$. Hence the transmission delay of $y_q(k)$ does not influence the dynamics of (5.3). Due to disturbances in the network, there can be packet dropouts during the transmissions of $u_r(k)$ and $y_q(k)$. Here it is assumed that the following rule adapted in the actuators:

$$\begin{aligned}u(k) &= u(k-1), \text{ if packet dropout of } u_r(k), \\ u(k) &= u_r(k), \text{ otherwise}\end{aligned}$$

and the estimated measurements are used instead of $y_q(k)$ if packet dropout of the measurement occurs, i.e.

$$\begin{aligned}y_r(k) &= \hat{y}(k) \text{ if packet dropout of } y_q(k), \\ y_r(k) &= y_q(k) \text{ otherwise.}\end{aligned} \tag{5.4}$$

The matrices $L(\theta_k)$ and $W(\theta_k)$ are design parameters of the residual generator (5.3). They can be time varying and selected according to the occurrences of packet dropouts of $u_r(k)$ and $y_q(k)$, which are assumed to be two independent binary Bernoulli processes with probabilities α_u and α_y, respectively. Hence (5.3) is associated with a Bernoulli process $\{\theta_k\}$, where θ_k takes values in a four state space $\psi = \{1, 2, 3, 4\}$ with probabilities $\Phi = [\lambda_i]_{i\in\psi}$, and λ_i is defined as

$$\lambda_i = \Pr\{\theta_k = i\}$$

which is subject to the restriction $\lambda_i \geq 0$ and $\sum_{i=1}^{N} \lambda_i = 1$. Clearly, (5.3) is a special kind of stationary MJLSs.

For the convenience, denote the matrices associated with $\theta_k = i \in \psi$ by

$$\Omega^i = \Omega(\theta_k)$$

where Ω can be L, W, etc., and $\Omega^{1,2,\cdots}$ represents the enumeration of Ω^1, Ω^2, $\cdots$.

In the NCS, $i = 1$ represents no packet dropouts, $i = 2$ represents packet dropout of $u_r(k)$, $i = 3$ represents packet dropout of $y_q(k)$ and $i = 4$ represents packet dropouts of $u_r(k)$ and $y_q(k)$. Obviously λ_i can be calculated as follows

$$\begin{aligned}\lambda_1 &= (1-\alpha_u)(1-\alpha_y), \\ \lambda_2 &= \alpha_u(1-\alpha_y), \\ \lambda_3 &= (1-\alpha_u)\alpha_y, \\ \lambda_4 &= \alpha_u\alpha_y.\end{aligned}$$

A negative acknowledgement will be sent back from actuators, if there is no new control inputs received within an expected time delay. Since the residual generator has the knowledge of dropouts of $y_q(k)$, therefore the state of θ_k is fully observable. With (5.4), a trivial solution for $L^{3,4}$ and $W^{3,4}$ can be

$$L^{3,4} = 0, W^{3,4} = 0.$$

Since $r(k)$ is a stochastic vector, its statistical properties should be taken into consideration in selecting the evaluation function and computing the threshold.

5.2 Residual generation

In order to find the best trade-off between the robustness against disturbances and the sensitivity to faults, the proposed residual generator is designed to match a reference model by following the idea introduced in chapter 3. Since the probability of packet dropouts is usually a small value, $\theta_k = 1$ can be regarded as the dominant mode of the Bernoulli process. Hence the optimal residual generator for (5.2) without considering the network-induced effects is taken as the reference residual model, which is given as

$$\begin{aligned} e_{ref}(k+1) &= A_r e_{ref}(k) + E_{d,r} d(k) + E_{f,r} f(k) \\ r_{ref}(k) &= C_r e_{ref}(k) + F_{d,r} d(k) + F_{f,r} f(k)) \end{aligned}$$

with

$$A_r = A_0 - L_{ref}C, E_{d,r} = E_d - L_{ref}F_d,$$

$$E_{f,r} = E_f - L_{ref}F_f, C_r = W_{ref}C, F_{d,r} = W_{ref}F_d, F_{f,r} = W_{ref}F_f.$$

Here L_{ref} and W_{ref} are selected according to Theorem 3.3.

Define $e(k) = \xi(k) - \hat{\xi}(k)$. The dynamics of the matching error $r_e(k)$ and the residual signal $r(k)$ is governed by

$$\begin{aligned} \zeta(k+1) &= \tilde{A}(\theta_k)\zeta(k) + \tilde{B}(\theta_k)\omega(k) \\ r(k) &= \tilde{C}(\theta_k)\zeta(k) + \tilde{D}(\theta_k)\omega(k) \\ r_e(k) &= \tilde{C}_e(\theta_k)\zeta(k) + \tilde{D}_e(\theta_k)\omega(k) \end{aligned} \tag{5.5}$$

where $r_e(k) = r_{ref}(k) - r(k)$ and

$$\zeta(k) = \begin{bmatrix} e_{ref}(k) \\ \xi(k) \\ e(k) \end{bmatrix}, \omega(k) = \begin{bmatrix} u(k-\mu_1) \\ u_r(k-\mu_1) - u(k-\mu_1) \\ d(k) \\ f(k) \end{bmatrix}.$$

By denoting $\theta_k = i \in \psi$,

$$\begin{aligned} &\tilde{C}^i = \tilde{C}^i_{00} + \Delta C^i, \tilde{D}^i = \tilde{D}^i_{00} + \Delta D^i, \\ &\tilde{C}^i_e = \tilde{C}^i_{e,00} + \Delta C^i_e, \tilde{D}^i_e = \tilde{D}^i_{e,00} + \Delta D^i_e, \end{aligned}$$

$$\tilde{A}^i = \tilde{A}^i_{00} + \sum_{j=1}^{(2n)^\mu} \alpha^k_j \tilde{A}^i_j + \Delta A^i, \tilde{B}^i = \tilde{B}^i_{00} + \sum_{j=1}^{(2n)^\mu} \alpha^k_j \tilde{B}^i_j + \Delta B^i$$

with

$$\tilde{A}_{00}^{1,2} = \begin{bmatrix} A_r & 0 & 0 \\ 0 & A_0 & 0 \\ 0 & 0 & A_0 - L^{1,2}C \end{bmatrix}, \tilde{A}_{00}^{3,4} = \begin{bmatrix} A_r & 0 & 0 \\ 0 & A_0 & 0 \\ 0 & 0 & A_0 \end{bmatrix},$$

$$\tilde{B}_{00}^{1,3} = \begin{bmatrix} 0 & 0 & E_{d,r} & E_{f,r} \\ B_0 & 0 & E_d & E_f \\ 0 & 0 & E_d - L^{1,3}F_d & E_f - L^{1,3}F_f \end{bmatrix},$$

$$\tilde{B}_{00}^{2,4} = \begin{bmatrix} 0 & 0 & E_{d,r} & E_{f,r} \\ B_0 & 0 & E_d & E_f \\ 0 & B_0 & E_d - L^{2,4}F_d & E_f - L^{2,4}F_f \end{bmatrix},$$

$$\begin{aligned} \tilde{C}_{00}^{1,2} &= \begin{bmatrix} 0 & 0 & W^{1,2}C \end{bmatrix}, \tilde{C}_{00}^{3,4} = 0, \\ \tilde{D}_{00}^{1,2} &= \begin{bmatrix} 0 & 0 & W^{1,2}F_d & W^{1,2}F_f \end{bmatrix}, \tilde{D}_{00}^{3,4} = 0, \\ \tilde{C}_{e,00}^{1,2} &= \begin{bmatrix} W_{ref}C & 0 & -W^{1,2}C \end{bmatrix}, \tilde{C}_{e,00}^{3,4} = \begin{bmatrix} W_{ref}C & 0 & 0 \end{bmatrix}, \\ \tilde{D}_{e,00}^{1,2} &= \begin{bmatrix} 0 & 0 & F_{d,r} - W^{1,2}F_d & F_{f,r} - W^{1,2}F_f \end{bmatrix}, \\ \tilde{D}_{e,00}^{3,4} &= \begin{bmatrix} 0 & 0 & F_{d,r} & F_{f,r} \end{bmatrix}. \end{aligned}$$

The norm bounded uncertainties can be reformulated as

$$\begin{bmatrix} \Delta A^i & \Delta B^i \\ \Delta C^i & \Delta D^i \\ \Delta C_e^i & \Delta D_e^i \end{bmatrix} = \begin{bmatrix} E^i \\ F^i \\ F_e^i \end{bmatrix} \Delta(k) \begin{bmatrix} G^i & H^i \end{bmatrix}, \Delta^T(k)\Delta(k) \leq I$$

where

$$\begin{aligned} E^i &= \begin{bmatrix} 0 & 0 & (L^i)^T \end{bmatrix}^T, F^i = F_e^i = W^i, \\ G^i &= \begin{bmatrix} 0 & \delta_q C & 0 \end{bmatrix}, H^i = \begin{bmatrix} 0 & 0 & \delta_q F_d & \delta_q F_f \end{bmatrix} \end{aligned}$$

and the vertices of the polytopic uncertainties are

$$\tilde{A}_j^{1,3} = \begin{bmatrix} 0 & 0 & 0 \\ 0 & A_{V_j} & 0 \\ 0 & A_{V_j} & 0 \end{bmatrix}, \tilde{B}_j^{1,3} = \begin{bmatrix} 0 & 0 & 0 & 0 \\ B_{V_j} & 0 & 0 & 0 \\ B_{V_j} & 0 & 0 & 0 \end{bmatrix},$$

$$\tilde{A}_j^{2,4} = 0, \tilde{B}_j^{2,4} = 0.$$

It can be seen that, (5.5) is also a special stationary MJLS with system uncertainties, where $\lambda_{ij} = \lambda_i, i, j \in \psi$. Following the idea in the FD system design of MJLS, the model matching problem

$$\min \sup_{\omega(k) \in l_2} \frac{\|r_e(k)\|_E}{\|\omega(k)\|_2} \tag{5.6}$$

is solved by choosing $L(\theta_k)$ and $W(\theta_k)$ such that $r(k)$ is robust against the transmission delays, packet dropouts, quantization errors and disturbances and simultaneously sensitive to faults.

The following lemma is useful to deal with the norm bounded uncertainty.

Lemma 5.1 *[110] Let G, M and N be real matrices of appropriate dimensions with G symmetrical, then*

$$G + M\Delta(k)N + N^T\Delta(k)^T M^T < 0$$

where $\Delta^T(k)\Delta(k) \leq I$, if and only if there exists a scalar $\varepsilon > 0$ such that

$$G + \sqrt{\varepsilon}MM^T + \frac{1}{\sqrt{\varepsilon}}N^T N < 0. \tag{5.7}$$

In order to solve the model matching problem, the lemma concerning the H_∞-norm of the system (5.5) is introduced.

Lemma 5.2 *Consider the system (5.5). Given a constant $\gamma > 0$, $\zeta(0) = 0$ and $\theta_0 \in \psi$, then*

$$\sup_{\omega(k)\in l_2 \neq 0} \frac{\|r_e(k)\|_E}{\|\omega(k)\|_2} < \gamma \tag{5.8}$$

if there exist positive matrices $S_i > 0$ and a scalar $\epsilon > 0$ such that

$$\begin{bmatrix} -\bar{S} & \Pi_{12} & \Pi_{13} & 0 & \bar{S}E^i & 0 \\ * & -S_i & 0 & (\tilde{C}^i_{e,00})^T & 0 & (G^i)^T \\ * & * & -\epsilon\gamma^2 I & (\tilde{D}^i_{e,00})^T & 0 & (H^i)^T \\ * & * & * & -\epsilon I & \epsilon F^i_e & 0 \\ * & * & * & * & -I & 0 \\ * & * & * & * & * & -I \end{bmatrix} < 0 \tag{5.9}$$

is satisfied for all $i = 1, \cdots, 4$ and $j = 1, \cdots, (2n)^\mu$, where

$$\bar{S} = \sum_{i=1}^{4} \lambda_i S_i$$

and

$$\Pi_{12} = \bar{S}(\tilde{A}^i_{00} + \tilde{A}^i_j), \Pi_{13} = \bar{S}(\tilde{B}^i_{00} + \tilde{B}^i_j).$$

Proof Following the similar procedure in Lemma 3.6, define

$$V(\zeta, i) = \zeta^T Q_i \zeta.$$

for some $Q_i > 0, i = 1, \cdots, 4$. Given $\zeta(0) = 0$ for any initial mode $\theta(0) \in \psi$, then

$$\sum_{k=0}^{\infty} E\{V(\zeta(k+1), \theta_{k+1})\} - E\{V(\zeta(k), \theta_k)\} = E\{V(\zeta(\infty), \theta(\infty))\} \geq 0.$$

Denoting $\theta_k = i$ and

$$R^i = \begin{bmatrix} \tilde{A}^i & \tilde{B}^i \\ \tilde{C}^i_e & \tilde{D}^i_e \end{bmatrix}^T \begin{bmatrix} \bar{Q} & 0 \\ 0 & 0 \end{bmatrix} \begin{bmatrix} \tilde{A}^i & \tilde{B}^i \\ \tilde{C}^i_e & \tilde{D}^i_e \end{bmatrix} - \begin{bmatrix} Q_i & 0 \\ 0 & \gamma^2 I \end{bmatrix}$$

with

$$\bar{Q} = \sum_{i=1}^{4} \lambda_i Q_i,$$

it turns out

$$
\begin{aligned}
& \|r_e\|_E^2 - \gamma^2\|\omega\|_2^2 \\
\leq \; & \sum_{k=0}^{\infty}\big(r_e(k)^T r_e - \omega(k)^T\omega(k) - E\{V(\zeta(k),\theta_k)\}\big) \\
& + \sum_{k=0}^{\infty}(E\{V(\zeta(k+1),\theta_{k+1})\}) \\
= \; & E\{\sum_{k=0}^{\infty}\begin{bmatrix} \zeta(k) \\ \omega(k) \end{bmatrix}^T \begin{bmatrix} \tilde{A}(\theta_k) & \tilde{B}(\theta_k) \\ \tilde{C}_e(\theta_k) & \tilde{D}_e(\theta_k) \end{bmatrix}^T \\
& \times \begin{bmatrix} Q_{\theta_{k+1}} & 0 \\ 0 & 0 \end{bmatrix} \begin{bmatrix} \tilde{A}(\theta_k) & \tilde{B}(\theta_k) \\ \tilde{C}_e(\theta_k) & \tilde{D}_e(\theta_k) \end{bmatrix} \\
& - \begin{bmatrix} Q_{\theta_k} & 0 \\ 0 & \gamma^2 I \end{bmatrix} \begin{bmatrix} \zeta(k) \\ \omega(k) \end{bmatrix}\} \\
= \; & E\{\begin{bmatrix} \zeta(k) \\ \omega(k) \end{bmatrix}^T R(\theta_k) \begin{bmatrix} \zeta(k) \\ \omega(k) \end{bmatrix}\} \qquad (5.10)
\end{aligned}
$$

It is clear that, if $R^i < 0, i \in \psi$, then (5.10) < 0, i.e. $\|r_e\|_E^2 < \gamma^2\|\omega\|_2^2$, for any $\omega \in l_2$. With schur-complement and congruency transformation, the above inequality can be reformulated as

$$
\begin{bmatrix} -\bar{Q} & \bar{Q}\tilde{A}^i & \bar{Q}\tilde{B}^i & 0 \\ * & -Q_i & 0 & \tilde{C}_e^i \\ * & * & -\gamma^2 I & \tilde{D}_e^i \\ * & * & * & -I \end{bmatrix} \leq 0
$$

which is equivalent with $R_j^i < 0$ for all $i \in \psi$ and $j = 1, \cdots, (2n)^\mu$, with

$$
R_j^i = \begin{bmatrix} -\bar{Q} & \bar{Q}(\tilde{A}_{00}^i + \tilde{A}_j^i + \Delta A^i) & \bar{Q}(\tilde{B}_{00}^i + \tilde{B}_j^i + \Delta B^i) & 0 \\ * & -Q_i & 0 & (\tilde{C}_{e,00}^i + \Delta C_e^i)^T \\ * & * & -\gamma^2 I & (\tilde{D}_{e,00}^i + \Delta D_e^i)^T \\ * & * & * & -I \end{bmatrix}.
$$

Then R_j^i can be rewritten as follows

$$
\begin{aligned}
R_j^i \; = \; & \begin{bmatrix} -\bar{Q} & \bar{Q}(\tilde{A}_{00}^i + \tilde{A}_j^i) & \bar{Q}(\tilde{B}_{00}^i + \tilde{B}_j^i) & 0 \\ * & -Q_i & 0 & (\tilde{C}_{e,00}^i)^T \\ * & * & -\gamma^2 I & (\tilde{D}_{e,00}^i)^T \\ * & * & * & -I \end{bmatrix} \\
& + \begin{bmatrix} \bar{Q}E^i \\ 0 \\ 0 \\ F_e^i \end{bmatrix} \Delta(k) \begin{bmatrix} 0 & G^i & H^i & 0 \end{bmatrix} + \begin{bmatrix} 0 & G^i & H^i & 0 \end{bmatrix}^T \Delta(k) \begin{bmatrix} \bar{Q}E^i \\ 0 \\ 0 \\ F_e^i \end{bmatrix}^T
\end{aligned}
$$

By applying Lemma 5.1, congruency transformation with $diag\{\sqrt{\epsilon}, \sqrt{\epsilon}, \sqrt{\epsilon}, \sqrt{\epsilon}, I\}$ and defining $S_i = \epsilon Q_i$, then $R_j^i < 0$ if and only if (5.9) is satisfied for all $i \in \psi$ and $j = 1, \cdots, (2n)^\mu$. ■

With Lemma 5.2, it is easy to obtain the following theorem which solves (5.6).

Theorem 5.3 *For the system (5.5), if there is a solution for the optimization problem*

$$\min \gamma$$

subject to

$$M^i = (M^i)^T = [M_{\alpha\beta}]_{8\times 8} < 0 \tag{5.11}$$

admitting a solution for $S_i > 0$, W^1, W^2, Y^1, Y^2 *and*

$$P = \begin{bmatrix} P_1 & 0 \\ 0 & P_2 \end{bmatrix}$$

for all $i \in \psi$ *and* $j = 1, \cdots, (2n)^\mu$, *where*

$$\begin{bmatrix} M_{11} & M_{12} \\ M_{12}^T & M_{22} \end{bmatrix} = \bar{S} - (P + P^T), \bar{S} = \sum_{i=1}^{4} \lambda_i S_i,$$

and the other nonzero $M_{\alpha\beta}$ *are*

$$\begin{aligned}
M_{13} &= P_1^T \begin{bmatrix} A_r & 0 & 0 \\ 0 & A_0 & 0 \end{bmatrix} + P_1^T \begin{bmatrix} 0 & 0 & 0 \\ 0 & A_{V_j} & 0 \end{bmatrix}, \\
M_{23}^{1,2} &= \begin{bmatrix} 0 & 0 & P_2^T A_0 - Y^{1,2} C \end{bmatrix} + \begin{bmatrix} 0 & P_2^T A_{V_j} & 0 \end{bmatrix}, \\
M_{23}^{3,4} &= \begin{bmatrix} 0 & 0 & P_2^T A_0 \end{bmatrix}, \\
M_{14}^{1,3} &= P_1^T \begin{bmatrix} 0 & 0 \\ B_0 & 0 \end{bmatrix} + P_1^T \begin{bmatrix} 0 & 0 \\ B_{V_j} & 0 \end{bmatrix}, \\
M_{24}^{1,3} &= \begin{bmatrix} P_2^T B_{V_j} & 0 \end{bmatrix}, M_{24}^{2,4} = \begin{bmatrix} 0 & P_2^T B_0 \end{bmatrix}, \\
M_{14}^{2,4} &= P_1^T \begin{bmatrix} 0 & 0 \\ B_0 & 0 \end{bmatrix}, M_{15} = P_1^T \begin{bmatrix} E_{d,r} & E_{f,r} \\ E_d & E_f \end{bmatrix}, \\
M_{25}^{1,2} &= \begin{bmatrix} P_2^T E_d - Y^{1,2} F_d & P_2^T E_f - Y^{1,2} F_f \end{bmatrix}, \\
M_{25}^{3,4} &= \begin{bmatrix} P_2^T E_d & P_2^T E_f \end{bmatrix}, M_{27}^{1,2} = Y^{1,2}, \\
M_{33} &= -S_i, M_{36}^{1,2} = \begin{bmatrix} W_{ref} C & 0 & -W^{1,2} C \end{bmatrix}^T, \\
M_{36}^{3,4} &= \begin{bmatrix} W_{ref} C & 0 & 0 \end{bmatrix}^T, M_{38} = \begin{bmatrix} 0 & C & 0 \end{bmatrix}^T, \\
M_{44} &= -\epsilon \gamma^2 I, M_{55} = -\epsilon \gamma^2 I, \\
M_{56}^{1,2} &= \begin{bmatrix} F_{d,r} - W^{1,2} F_d & F_{f,r} -^{1,2} F_f \end{bmatrix}^T, \\
M_{58} &= \begin{bmatrix} F_d & F_f \end{bmatrix}^T, M_{66} = -I, M_{67}^{1,2} = W^{1,2}, \\
M_{77} &= -I, M_{88} = -I.
\end{aligned}$$

Then the optimal parameters for the residual generator (5.3) minimizing (5.6) can be set as

$$L_{opt}^1 = P_2^{-1} Y^1, L_{opt}^2 = P_2^{-1} Y^2, L_{opt}^{3,4} = 0, W_{opt}^{1,2} = W^{1,2}, W_{opt}^{3,4} = 0. \tag{5.12}$$

Proof From the discussion in section 5.1, it is known that $L^{3,4} = W^{3,4} = 0$.

With (5.12), it is clear that (5.11) can be reformulated as

$$\begin{bmatrix} \Pi_{11} & \Pi_{12}^i & \Pi_{13}^i & 0 & \Pi_{14}^i & 0 \\ * & -S_i & 0 & (\tilde{C}_{e,00}^i)^T & 0 & \epsilon(G^i)^T \\ * & * & -\epsilon\gamma^2 I & (\tilde{D}_{e,00}^i)^T & 0 & \epsilon(H^i)^T \\ * & * & * & -I & \epsilon F_e^i & 0 \\ * & * & * & * & -I & 0 \\ * & * & * & * & * & -I \end{bmatrix} < 0 \tag{5.13}$$

where

$$\Pi_{11} = \bar{S} - (P + P^T), \Pi_{12}^i = P^T(\tilde{A}_{00}^i + \tilde{A}_j^i)$$
$$\Pi_{13}^i = P^T(\tilde{B}_{00}^i + \tilde{B}_j^i), \Pi_{14}^i = P^T E^i.$$

Note that, $\bar{S}$ is positive definite and (5.11) implies that P (as well as P_2) is nonsingular. Therefore $(\bar{S} - P)^T \bar{S}^{-1}(\bar{S} - P) \geq 0$ which yields

$$-P^T \bar{S} P \leq \bar{S} - (P + P^T).$$

By replacing Π_{11} with $-P^T \bar{S} P$ and performing a congruence transformation to (5.13) with $diag\{\bar{S}(P^T)^{-1}, I, I, I, I, I\}$, it can be shown that (5.13) implies (5.9). Hence the feasibility of (5.11) means that, (5.8) is satisfied. Then by minimizing γ, the parameters for the residual generator (5.3) can be obtained according to (5.12). ■

Remark 5.1 The inequality (5.9) also implies (5.13), which can be seen by defining $\bar{S} = P = P^T$. The matrix P is structured in order to obtain the solution of $L^{1,2}$, which will introduce some conservatism in the computation.

5.3 Residual evaluation

The dynamics of the designed residual generator (5.3) is governed by (5.5) with the optimal parameters obtained in Theorem 5.3. Obviously the residual $r(k)$ is a stochastic vector, which is associated with a Bernoulli process. As in the FD of MJLSs, define a set of residual evaluation functions as follows

$$\begin{aligned} \|r_h(k)\|_e &= |r_h(k)| \\ &= |[\tilde{C}(\theta_k)]_h e(k) + [\tilde{D}(\theta_k)]_h \omega(k)| \end{aligned} \tag{5.14}$$

where $h = 1, \cdots, m$ and $r_h(k)$ is the h-th residual signal. Here the absolute value of each residual signal is selected as the evaluation function. The threshold for the h-th evaluated residual signal is set as

$$J_{h,th} = \sup_k(|\bar{r}_h(k)|) + \sup_k(\beta\sigma_h(r(k)))$$

where

$$|\bar{r}_h(k)| = |E[r_h(k)]|$$

is the absolute value of the mean value of $r_h(k)$ and

$$\sigma_h^2(r(k)) = E[(r_h(k) - \bar{r}_h(k))^2]$$

is its variance. $\beta > 0$ is some constant. As shown later in Theorem 5.6, the upper bound of FAR can be guaranteed.

In order to compute $\sup_k(|\bar{r}(k)|)$ and $\sup_k(\sigma_h(r(k)))$, the dynamics of $\bar{r}(k)$ is given at first. Defining

$$\bar{\zeta}(k) = E[\zeta(k)]$$

then

$$\begin{aligned} \bar{\zeta}(k+1) &= \bar{A}_0\bar{\zeta}(k) + \bar{B}_0\omega(k), \\ \bar{r}(k) &= \bar{C}_0\bar{\zeta}(k) + \bar{D}_0\omega(k) \end{aligned} \tag{5.15}$$

with

$$\bar{A}_0 = \sum_{i=1}^{4}\lambda_i(\tilde{A}_{00}^i + \Delta A^i) + \sum_{i=1}^{4}\sum_{j=1}^{(2n)^\mu}\lambda_i\alpha_j^k\tilde{A}_j^i,$$

$$\bar{B}_0 = \sum_{i=1}^{4}\lambda_i(\tilde{B}_{00}^i + \Delta B^i) + \sum_{i=1}^{4}\sum_{j=1}^{(2n)^\mu}\lambda_i\alpha_j^k\tilde{B}_j^i,$$

$$\bar{C}_0 = \sum_{i=1}^{4}\lambda_i(\tilde{C}_{00}^i + \Delta C^i), \bar{D}_0 = \sum_{i=1}^{4}\lambda_i(\tilde{D}_{00}^i + \Delta D^i).$$

For the FD of NCSs, the generalized H_2-norm is applied for the residual evaluation. The following lemma gives the computation of $|\bar{r}_h(k)|$ by extending the Lemma 3.13 to MJLSs with uncertainties.

Lemma 5.4 *Given the system (5.15), $\gamma_{h,1} > 0$ and $\gamma_{h,2} > 0$, then*

$$|\bar{r}_h(k)| < \sqrt{\gamma_{h,1}^2\sum_{i=0}^{k-1}\omega(i)^T\omega(i)} + \sqrt{\gamma_{h,2}^2\omega(k)^T\omega(k)},$$

if there exist $S > 0$ satisfying the following matrix inequalities for all $j = 1, \cdots, (2n)^\mu$:

$$\begin{bmatrix} -S & \Pi_{12} & \Pi_{13} & S\sum_{i=1}^4\lambda_iE^i & 0 \\ * & -S & 0 & 0 & \sum_{i=1}^4\lambda_i(G^i)^T \\ * & * & -\epsilon\gamma_{h,1}^2I & 0 & \sum_{i=1}^4\lambda_i(H^i)^T \\ * & * & * & -I & 0 \\ * & * & * & * & -I \end{bmatrix} < 0 \tag{5.16}$$

$$\begin{bmatrix} -\epsilon & \epsilon\sum_{i=1}^4\lambda_i[\tilde{C}_{00}^i]_h & \epsilon\sum_{i=1}^4\lambda_i[F^i]_h & 0 \\ * & -S & 0 & \sum_{i=1}^4\lambda_i[G^i]_h^T \\ * & * & -I & 0 \\ * & * & * & -I \end{bmatrix} < 0 \tag{5.17}$$

$$\begin{bmatrix} -\epsilon & \epsilon\sum_{i=1}^4\lambda_i[\tilde{D}_{00}^i]_h & \epsilon\sum_{i=1}^4\lambda_i[F^i]_h & 0 \\ * & -\epsilon\gamma_{h,2}^2I & 0 & \sum_{i=1}^4\lambda_i[H^i]_h^T \\ * & * & -I & 0 \\ * & * & * & -I \end{bmatrix} < 0 \tag{5.18}$$

with

$$\Pi_{12} = S\sum_{i=1}^{4}\lambda_i(\tilde{A}_{00}^i + \tilde{A}_j^i), \Pi_{13} = S\sum_{i=1}^{4}\lambda_i(\tilde{B}_{00}^i + \tilde{B}_j^i).$$

Proof According to Lemma 3.13 and with the similar manipulation in Lemma 5.2, the lemma can be proved. ■

In a similar way, $\sigma_h(r(k))$ can be computed. Defining

$$r_\sigma(k) = r(k) - \bar{r}(k), e_\sigma(k) = \zeta(k) - \bar{\zeta}(k),$$

then

$$\begin{aligned} \chi(k+1) &= \bar{A}(\theta_k)\chi(k) + \bar{B}(\theta_k)\omega(k) \\ r_\sigma(k) &= \bar{C}_\sigma(\theta_k)\chi(k) + \bar{D}_\sigma(\theta_k)\omega(k) \end{aligned} \tag{5.19}$$

where

$$\chi(k) = \begin{bmatrix} \bar{\zeta}(k) \\ e_\sigma(k) \end{bmatrix}$$

and

$$\begin{aligned} \bar{A}(\theta_k) &= \begin{bmatrix} \bar{A}_0 & 0 \\ \tilde{A}(\theta_k) - \bar{A}_0 & \tilde{A}(\theta_k) \end{bmatrix}, \\ \bar{B}(\theta_k) &= \begin{bmatrix} \bar{B}_0 \\ \tilde{B}(\theta_k) - \bar{B}_0 \end{bmatrix}, \\ \bar{D}_\sigma(\theta_k) &= \tilde{D}(\theta_k) - \bar{D}_0, \\ \bar{C}_\sigma(\theta_k) &= \begin{bmatrix} \tilde{C}(\theta_k) - \bar{C}_0 & \tilde{C}(\theta_k) \end{bmatrix}. \end{aligned}$$

The following lemma gives the results.

Lemma 5.5 *Given the system (5.19), $\gamma_{h,3} > 0$ and $\gamma_{h,4} > 0$, then*

$$\sigma_h(r(k)) < \sqrt{\gamma_{h,3}^2 \sum_{i=0}^{k-1} \omega(i)^T \omega(i)} + \sqrt{\gamma_{h,4}^2 \omega(k)^T \omega(k)}, \tag{5.20}$$

if there exist $S > 0$, $\epsilon > 0$ satisfying the following matrix inequalities for all $j = 1, \cdots, (2n)^\mu$:

$$\begin{bmatrix} -\frac{1}{\lambda_1}S & & & \Pi_{15,j} & \Pi_{16,j} & \Pi_{17} & 0 \\ & \ddots & & \vdots & \vdots & \vdots & \vdots \\ & & -\frac{1}{\lambda_4}S & \Pi_{45,j} & \Pi_{46,j} & \Pi_{47} & 0 \\ * & * & * & -S & 0 & 0 & \Pi_{58} \\ * & * & * & 0 & -\epsilon\gamma_{h,3}^2 I & 0 & \Pi_{68} \\ * & * & * & * & * & -I & 0 \\ * & * & * & * & * & * & -I \end{bmatrix} < 0 \tag{5.21}$$

$$\begin{bmatrix} -\epsilon I & & & \epsilon\Pi_{1C} & \epsilon\Pi_{1F} & 0 \\ & \ddots & & \vdots & \vdots & \vdots \\ & & -\epsilon I & \epsilon\Pi_{4C} & \epsilon\Pi_{4F} & 0 \\ * & * & * & -S & 0 & \Pi_H \\ * & * & * & * & -I & 0 \\ * & * & * & * & * & -I \end{bmatrix} < 0 \tag{5.22}$$

$$\begin{bmatrix} -\epsilon I & & & \epsilon\Pi_{1D} & \epsilon\Pi_{1F} & 0 \\ & \ddots & & \vdots & \vdots & \vdots \\ & & -\epsilon I & \epsilon\Pi_{4D} & \epsilon\Pi_{4F} & 0 \\ * & * & * & -\epsilon\gamma_{h,4}^2 I & 0 & \Pi_H \\ * & * & * & * & -I & 0 \\ * & * & * & * & * & -I \end{bmatrix} < 0 \tag{5.23}$$

with

$$\Pi_{i5,j} = S\sum_{l=1}^{4}\lambda_l \begin{bmatrix} \tilde{A}_{00}^l + \tilde{A}_j^l & 0 \\ \tilde{A}_{00}^i + \tilde{A}_j^i - (\tilde{A}_{00}^l + \tilde{A}_j^l) & \tilde{A}_{00}^i + \tilde{A}_j^i \end{bmatrix},$$

$$\Pi_{i6,j} = S\sum_{l=1}^{4}\lambda_l \begin{bmatrix} \tilde{B}_{00}^l + \tilde{B}_j^l \\ \tilde{B}_{00}^i + \tilde{B}_j^i - (\tilde{B}_{00}^l + \tilde{B}_j^l) \end{bmatrix},$$

$$\Pi_{i7} = S\sum_{l=1}^{4}\lambda_l \begin{bmatrix} E^l & 0 \\ -E^l & E^i \end{bmatrix}, \Pi_{58} = \sum_{l=1}^{4}\lambda_l \begin{bmatrix} G^l & 0 \\ G^i & G^i \end{bmatrix}^T,$$

$$\Pi_{68} = \sum_{l=1}^{4}\lambda_l \begin{bmatrix} H^l & H^i \end{bmatrix}^T,$$

$$\Pi_{iC} = \sum_{l=1}^{4}\lambda_l \begin{bmatrix} \tilde{C}_{00}^i + \tilde{C}_j^i - (\tilde{C}_{00}^l + \tilde{C}_j^l) & \tilde{C}_{00}^i + \tilde{C}_j^i \end{bmatrix}_h,$$

$$\Pi_{iF} = \sum_{l=1}^{4}\lambda_l \begin{bmatrix} F^l & -F^i \end{bmatrix}_h, \Pi_G = \sum_{l=1}^{4}\lambda_l \begin{bmatrix} G^l & G^i \\ 0 & G^i \end{bmatrix}^T,$$

$$\Pi_{iD} = \sum_{l=1}^{4}\lambda_l \begin{bmatrix} \tilde{C}_{00}^i + \tilde{C}_j^i - (\tilde{C}_{00}^l + \tilde{C}_j^l) \end{bmatrix}_h,$$

$$\Pi_H = \sum_{l=1}^{4}\lambda_l \begin{bmatrix} H^l & H^i \end{bmatrix}^T.$$

Proof According to Lemma 3.14 and with the similar manipulation in Lemma 5.2, the lemma can be proved. ■

Now it is the position to give the theorem for the computation of the threshold.

Theorem 5.6 *Given the system (5.1), residual generator (5.3) whose dynamics is governed by (5.5), $\|\omega(k)\|_2 < \delta_{\omega,2}$, $\|\omega(k)\|_{peak} < \delta_{\omega,\infty}$ and the residual evaluation function (5.14), then the threshold can be set as*

$$J_{h,th} = (\check{\gamma}_{h,1} + \beta\check{\gamma}_{h,3})\delta_{\omega,2} + (\check{\gamma}_{h,2} + \beta\check{\gamma}_{h,4})\delta_{\omega,\infty} \tag{5.24}$$

where $\beta > 0$, $\check{\gamma}_{h,1}$, $\check{\gamma}_{h,2}$, $\check{\gamma}_{h,3}$ and $\check{\gamma}_{h,4}$ are the optimum of the constrained optimization problem:

$$\min \gamma_{h,1}, \gamma_{h,2} \text{ subject to } (5.16) \text{ - } (5.18),$$

$$\min \gamma_{h,3}, \gamma_{h,4} \text{ subject to } (5.21) \text{ - } (5.23).$$

Then the false alarm rate is upper bounded as

$$FAR \leq \frac{1}{\beta^2} \tag{5.25}$$

Proof See Theorem 3.15. ■

Remark 5.2 It is clear that, for the fault-free system

$$\delta_{\omega,2}^2 = \|d(k)\|_2^2 + \|u(k)\|_2^2 + \|u(k) - u_r(k)\|_2^2.$$

In many practical cases, the bound of $\delta_{\omega,2}$ is not known. As in literature, the norms of unknown inputs are assumed to be upper bounded with

$$\|d(k)\|_2 \leq \delta_{d,2}, \|d(k)\|_{peak} \leq \delta_{d,\infty},$$

while $\|u(k)\|_2$, $\|u(k) - u_r(k)\|_2$ are approximated with

$$\|u(k)\|_e = \sqrt{\sum_{j=k-T+1}^{k} u(j)^T u(j)}$$

and

$$\|u(k) - u_r(k)\|_e = \sqrt{\sum_{j=k-T+1}^{k} (u(j) - u_r(j))^T (u(j) - u_r(j))},$$

respectively. Then $\delta_{\omega,2}^2$ can be estimated online. Clearly, $\|u(k)\|_\infty$ and $\|u(k) - u_r(k)\|_\infty$ can also be estimated online. Hence in practice the threshold can be set as

$$\begin{aligned} J_{h,th}(k) &= \sqrt{\check{\gamma}_{h,1}^2 \delta_{\omega,e}(k)^2} + \sqrt{\check{\gamma}_{h,2}^2 \delta_{\omega,\infty}(k)^2} \\ &\quad + \beta \left(\sqrt{\check{\gamma}_{h,3}^2 \delta_{\omega,e}(k)^2} + \sqrt{\check{\gamma}_{h,4}^2 \delta_{\omega,\infty}(k)^2} \right) \end{aligned}$$

with

$$\delta_{\omega,e}(k)^2 = \delta_{d,2}^2 + \|u(k)\|_e^2 + \|u(k) - u_r(k)\|_e^2$$

and

$$\delta_{\omega,\infty}(k)^2 = \delta_{d,\infty}^2 + \|u(k)\|_{peak}^2 + \|u(k) - u_r(k)\|_{peak}^2.$$

Hence the threshold is an adaptive one.

Remark 5.3 The assumption of the negative acknowledgement from actuators is for the purpose of simplifying the derivation of the threshold and improving the fault detection performance (reducing miss detections of faults), as $\|u(k) - u_r(k)\|_e$ can be calculated exactly. If there is no such acknowledgements, it is difficult to get the knowledge of packet dropouts of $u_r(k)$. Consequently, L^1 and L^2 should be the same by setting $Y_1 = Y_2$ in Theorem 5.3 and only the estimated upper bound of $\|u(k) - u_r(k)\|_e$ can be used in the computation of thresholds.

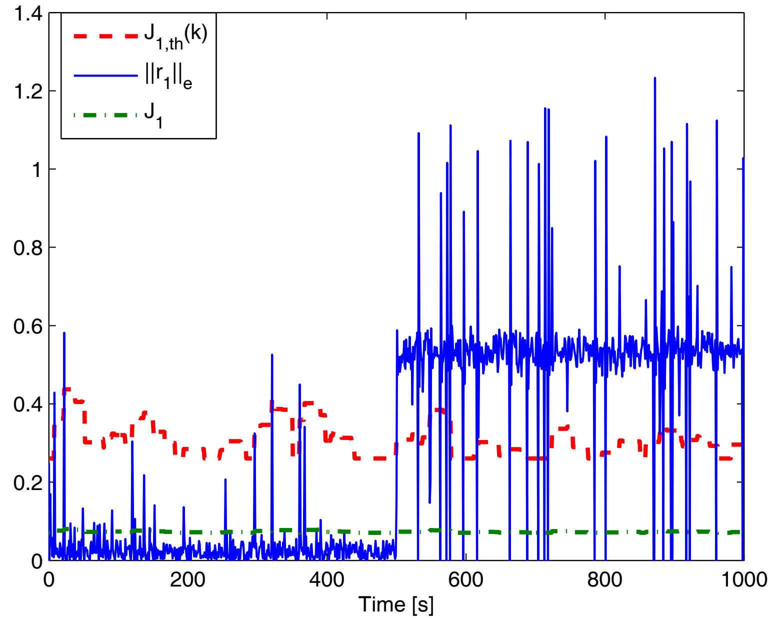

Figure 5.1: Fault detection of NCS: the first evaluated residual signal, $\beta = 5$.

5.4 A numerical example

In this section, a numerical example is given to illustrate the effectiveness of the proposed methods. Consider the following continuous-time system:

$$A_c = \begin{bmatrix} -1.609 & 6.931 \\ 0 & -2.303 \end{bmatrix}, B_c = \begin{bmatrix} 2.012 & -5.466 \\ 0 & 2.558 \end{bmatrix}$$
$$E_{c,f} = \begin{bmatrix} -1.439 & -0.8921 \\ 0.7675 & 0.5117 \end{bmatrix}, E_{c,f} = \begin{bmatrix} 1 \\ 0 \end{bmatrix},$$
$$C_c = \begin{bmatrix} 1 & 0 \\ 0 & 1 \end{bmatrix}, F_{c,d} = \begin{bmatrix} 0.1 & 0 \\ 0 & 0.1 \end{bmatrix}, F_{c,f} = 0.$$

Assume that $T_s = 1$s, the transmission time delay $\tau(k)$ is a random sequence uniformly distributed between 0 and T_s, the unknown input d is a white noise with zero mean and 0.1 variance, a step fault $f = 2$ occurs at $t = 500$s, the parameter of the logarithmic quanitzer is $\delta_q = 0.12$ and the packet dropout probability is $\alpha_u = \alpha_y = 0.05$. The reference model is set as the optimal residual generator of the system without considering the network, i.e.

$$A_r = \begin{bmatrix} 0.2000 & 0.0000 & 0 & 0 \\ -2.4000 & -0.0000 & 0 & 0 \\ 0 & 0 & 0 & 0 \\ 0 & 0 & 0 & 0 \end{bmatrix},$$
$$E_{d,r} = \begin{bmatrix} 0 & 0 \\ 0.0500 & -0.0500 \\ 0 & 0 \\ 0 & 0 \end{bmatrix}, E_{d,r} = \begin{bmatrix} 1 \\ 0 \\ 0 \\ 0 \end{bmatrix},$$

$$C_r = \begin{bmatrix} -3.2044 & -3.6298 & 0 & 0 \\ -15.4833 & 13.6684 & 0 & 0 \end{bmatrix},$$
$$F_{d,r} = \begin{bmatrix} -0.6834 & -0.6834 \\ -0.1815 & -0.1815 \end{bmatrix}.$$

By applying the method proposed in Theorem 5.3 based on MATLAB LMI Control

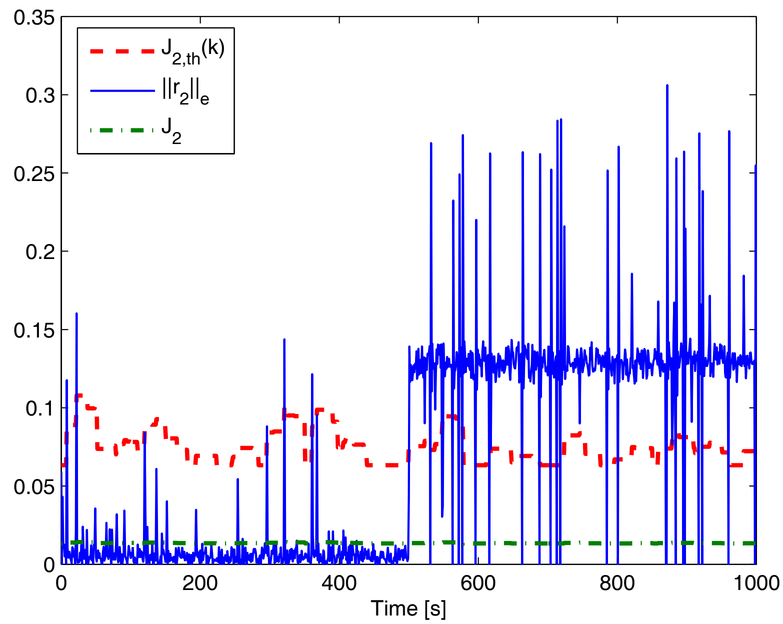

Figure 5.2: Fault detection of NCS: the second evaluated residual signal, $\beta = 5$.

Toolbox, the respective optimal L and W are

$$L^1 = \begin{bmatrix} 0.2523 & 1.0129 \\ 0.2329 & 0.1656 \\ 0.0053 & 0.0046 \\ 0.0031 & 0.0030 \end{bmatrix}, L^2 = \begin{bmatrix} 0.2570 & 1.0060 \\ 0.2371 & 0.1618 \\ 0.0086 & 0.0011 \\ 0.0051 & 0.0008 \end{bmatrix},$$
$$W^1 = \begin{bmatrix} -0.227 & -0.073 \\ -0.060 & -0.011 \end{bmatrix}, W^2 = \begin{bmatrix} -0.226 & -0.069 \\ -0.059 & -0.013 \end{bmatrix},$$
$$L^3 = L^4 = 0, W^3 = W^4 = 0$$

and $\gamma_{1,1} = 0.0141$, $\gamma_{1,2} = 0.0424$, $\gamma_{1,3} = 0.05$, $\gamma_{1,4} = 0.0001$, $\gamma_{2,1} = 0.0015$, $\gamma_{2,2} = 0.0101$,$\gamma_{2,3} = 0.013$,$\gamma_{2,4} = 0.0001$.

Setting the evaluation window $T = 30$, Fig. 5.1 and Fig. 5.2 give the simulation results. The thresholds J_1 and J_2 are computed based on only the mean values of r_1 and r_2, i.e. $J_1 = \check{\gamma_{1,1}}\delta_{\omega,2} + \check{\gamma_{1,2}}\delta_{\omega,\infty}$, $J_2 = \check{\gamma_{2,1}}\delta_{\omega,2} + \check{\gamma_{2,2}}\delta_{\omega,\infty}$, respectively. It can be observed that, there are lots of false alarms in the first 500 seconds. The thresholds $J_{1,th}(k)$ and $J_{2,th}(k)$ are computed according to Theorem 5.6 with $\beta = 5$, such that the FAR is upper bounded by 4%. As shown in the figures, the number of false alarms is significantly reduced. By selecting a proper β, the FAR can be guaranteed to be below an acceptable level and at the same time the miss detections of faults can be reduced.

5.5 Conclusion

In this chapter the FD problem of NCSs considering time varying transmission delays, packet dropouts and quantization errors was addressed. The design approaches for the residual generation and evaluation have been given. These network-induced effects have been first transformed into system uncertainties and stochastic parameters governed by a Bernoulli process. The dynamics of the residual generator was then characterized in the framework of MJLSs with both norm bounded and polytopic uncertainties. A method has been proposed for designing residual generator which can achieve the optmial trade-off between robustness against network-induced effects and sensitivity to faults. Then a new residual evaluation approach was proposed for the FD of NCSs. In this approach, the mean values and variances of the evaluated residual signals have been used to compute the thresholds, such that the FAR can be significantly reduced and upper bounded. The simulation results have also been given to illustrate the effectiveness of the proposed approaches.

6 Simulation Results - Networked Three-tank System Benchmark

6.1 Description of the three-tank system

The three-tank system has the typical characteristics of tanks, pipelines and pumps used in chemical industry, and thus it often serves as the benchmark process in laboratories for process control. The three-tank system introduced in this thesis is shown in Fig. 6.1. It consists of three cylindrical tanks with the cross section area A_c. The tanks are connected to each other through cylindrical pipes with the cross sectional area s_n. There is an outlet pipe in tank 2 for the liquid outflow. The outflow liquid goes to the reservoir. There are two pumps P_1 and P_2 which pump the liquid to tank 1 and tank 2 with flow rates of Q_1 and Q_2, respectively. The fluid levels in the three tanks, h_1, h_2, h_3, are measured. If the liquid level in tank 1 or tank 2 exceeds a maximum level H_{max}, the corresponding pump is automatically switched off. Table 6.1 shows the technical data of the three-tank system. The so-called component faults such as leakage, plugging in pipes and actuator faults as well as sensor faults are defined. The control objective is to maintain the liquid levels in tank 1 and tank 2.

6.1.1 Nonlinear model

Using the incoming and outgoing mass flows under consideration of Torricellies law the dynamics of the three-tank system is modeled by:

$$\begin{aligned}
A_c\dot{h}_1(t) &= Q_1(t) - Q_{13}(t) \\
A_c\dot{h}_2(t) &= Q_2(t) + Q_{32}(t) - Q_{20}(t) \\
A_c\dot{h}_3(t) &= Q_{13}(t) - Q_{32}(t) \\
Q_{13}(t) &= a_1 s_n \mathrm{sgn}(h_1(t) - h_3(t))\sqrt{2g|h_1(t) - h_3(t)|} \\
Q_{32}(t) &= a_3 s_n \mathrm{sgn}(h_3(t) - h_2(t))\sqrt{2g|h_3(t) - h_2(t)|} \\
Q_{20}(t) &= a_2 s_n \sqrt{2gh_2(t)}
\end{aligned} \tag{6.1}$$

where $Q_1(t)$, $Q_2(t)$ are incoming mass flows and $h_1(t)$, $h_2(t)$, $h_3(t)$ are the liquid levels in tanks and can be measured. The three circular tanks have the same cross section A_c and are interconnected via circular pipes with the cross sections s_n. The outlet pipe is also circular with the cross section s_n. a_1,a_2 and a_3 are scaling constants and g is the gravity constant.

Define

$$x = \begin{bmatrix} x_1 \\ x_2 \\ x_3 \end{bmatrix} = \begin{bmatrix} h_1 \\ h_2 \\ h_3 \end{bmatrix}, u = \begin{bmatrix} u_1 \\ u_2 \end{bmatrix} = \begin{bmatrix} Q_1 \\ Q_2 \end{bmatrix}.$$

Table 6.1: Parameters of the three-tank system

Parameters	Symbol	Value	Unit
cross section area of tanks	A_c	154	cm^2
cross section area of pipes	s_n	0.5	cm^2
max. height of tanks	H_{max}	62	cm^2
max. flow rate of pump 1	$Q_{1_{max}}$	100	cm^3/sec
max. flow rate of pump 2	$Q_{2_{max}}$	100	cm^3/sec
coeff. of flow for pipe 1	a_1	0.46	
coeff. of flow for pipe 2	a_2	0.60	
coeff. of flow for pipe 3	a_3	0.45	

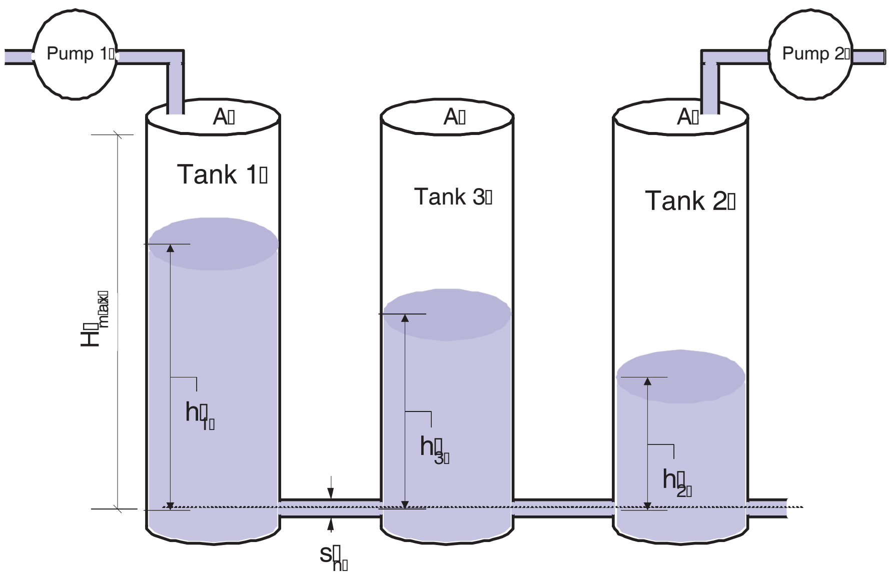

Figure 6.1: Three-tank system

Then (6.1) can be written as follows:

$$\begin{aligned} \dot{x}(t) &= f(x(t)) + g(x(t))u(t) \\ y(t) &= h(x(t)) \end{aligned} \tag{6.2}$$

where

$$f(x(t)) = \frac{1}{A_c} \begin{bmatrix} -Q_{13}(t) \\ Q_{32}(t) - Q_{20}(t) \\ Q_{13}(t) - Q_{32}(t) \end{bmatrix},$$

$$g(x(t)) = \frac{1}{A_c} \begin{bmatrix} 1 & 0 \\ 0 & 1 \\ 0 & 0 \end{bmatrix},$$

$$h(x(t)) = \begin{bmatrix} x_1(t) \\ x_2(t) \\ x_3(t) \end{bmatrix}.$$

6.1.2 Linearized model

By using the Taylor series expansion around an operating point with $x_0 = [x_{10}\ x_{20}\ x_{30}]^T$, $u_0 = [u_{10}\ u_{20}]^T$ and $y_0 = x_0$ and neglecting the higher order terms, system (6.2) is linearized as the following system:

$$\begin{aligned} \Delta\dot{x}(t) &= A\Delta x(t) + B\Delta u(t) \\ \Delta y(t) &= C\Delta x(t) \end{aligned} \tag{6.3}$$

with

$$\Delta x = x - x_0, \Delta u = u - u_0, \Delta y = y - y_0$$

and

$$\begin{aligned} A &= \frac{1}{A_c}\begin{bmatrix} -\theta_{13} & 0 & \theta_{13} \\ 0 & -(\theta_{32}+\theta_{20}) & \theta_{32} \\ \theta_{13} & \theta_{32} & -(\theta_{13}+\theta_{32}) \end{bmatrix}, \\ B &= \frac{1}{A_c}\begin{bmatrix} 1 & 0 \\ 0 & 1 \\ 0 & 0 \end{bmatrix}, \quad C = \begin{bmatrix} 1 & 0 & 0 \\ 0 & 1 & 0 \\ 0 & 0 & 1 \end{bmatrix} \end{aligned}$$

where $\theta_{13} = a_1 s_n \sqrt{\frac{g}{2|x_{10}-x_{30}|}}$, $\theta_{32} = a_3 s_n \sqrt{\frac{g}{2|x_{30}-x_{20}|}}$ and $\theta_{20} = a_2 s_n \sqrt{\frac{g}{2x_{20}}}$. In the above linearization, the only assumption is made that $x_{10} \neq x_{20} \neq x_{30}$. By taking $x_{10} = 45$, $x_{20} = 15$ and $x_{30} = 30$, $u_{10} = 43.1, u_{20} = 17.1$ as the operating point, the linearized model is given by:

$$\begin{aligned} A &= \begin{bmatrix} -0.0085 & 0 & 0.0085 \\ 0 & -0.0195 & 0.0084 \\ 0.0085 & 0.0084 & -0.0169 \end{bmatrix}, \\ B &= \begin{bmatrix} 0.0065 & 0 \\ 0 & 0.0065 \\ 0 & 0 \end{bmatrix}, \quad C = \begin{bmatrix} 1 & 0 & 0 \\ 0 & 1 & 0 \\ 0 & 0 & 1 \end{bmatrix}. \end{aligned}$$

The linearized model of the three-tank system is discretized with the sampling time being $T_s = 0.1$s. The system matrices of the discrete-time system are given as follows:

$$A_d = \begin{bmatrix} 0.992 & 0 & 0.000849 \\ 0 & 0.998 & 0.000839 \\ 0.000849 & 0.000839 & 0.9833 \end{bmatrix}, B_d = \begin{bmatrix} 0.000649 & 0 \\ 0 & 0.000649 \\ 0 & 0 \end{bmatrix},$$
$$C_d = \begin{bmatrix} 1 & 0 & 0 \\ 0 & 1 & 0 \\ 0 & 0 & 1 \end{bmatrix}, D_d = \begin{bmatrix} 0 & 0 \\ 0 & 0 \\ 0 & 0 \end{bmatrix}.$$

6.1.3 Modeling of faults and disturbances

Following types of faults are presented in the three-tank system:

- Sensor faults: scaling faults from 0% to 100% are defined in all three sensors measuring h_1, h_2, h_3, and they are denoted as f_1, f_2 and f_3, respectively.

- Actuator faults: scaling faults from 0% to 100% are defined in pump 1 and pump 2. The faults are represented by f_4 and f_5, respectively.

The measurement noises in three liquid level sensors are considered as disturbances in the system. It is possible to incorporate the faults and disturbances in the state space realization of the system as follows:

$$\begin{aligned}\Delta x(k+1) &= A_d \Delta x(k) + B_d \Delta u(k) + E_f f(k) \\ \Delta y(k) &= C_d \Delta x(k) + F_d d(k) + F_f f(k)\end{aligned}$$

$$F_d = \begin{bmatrix} 0.1 & 0 & 0 \\ 0 & 0.1 & 0 \\ 0 & 0 & 0.1 \end{bmatrix}, d(k) \in \mathbb{R}^3,$$

$$f^T = [f_1 \ f_2 \ \cdots \ f_5], \ E_f = [0 \ B_d] \in \mathbb{R}^{3\times 5}, \ F_f = [I_{3\times 3} \ 0] \in \mathbb{R}^{3\times 5}.$$

6.1.4 Control of three-tank system

In the benchmark, the control objective is to maintain the liquid levels in tank 1 and tank 2. Hence a nonlinear controller is implemented which decouples the three-tank system into two independent linear subsystems of the first order and a nonlinear system of the first order. The controller can be described as follows:

$$\begin{aligned}u_1 &= Q_1 = Q_{13} + A_c(a_{11}h_1 + v_1(w_1 - h_1)), \\ u_2 &= Q_2 = Q_{20} - Q_{32} + A_c(a_{22}h_2 + v_2(w_2 - h_2))\end{aligned}$$

where $a_{11}, a_{22} \leq 0$, v_1, v_2 represent two pre-filters and w_1, w_2 represent the reference signals of tank 1 and tank 2, respectively. Then the nominal closed loop model is:

$$\begin{bmatrix} \dot{x}_1(t) \\ \dot{x}_2(t) \\ \dot{x}_3(t) \end{bmatrix} = \begin{bmatrix} (a_{11} - v_1) \\ (a_{22} - v_2) \\ \frac{a_1 \mathrm{sgn}(x_1(t) - x_3(t))\sqrt{2g|x_1(t) - x_3(t)|} - a_3 \mathrm{sgn}(x_3(t) - x_2(t))\sqrt{2g|x_3(t) - x_2(t)|}}{A_c} \end{bmatrix} + \begin{bmatrix} v_1 & 0 \\ 0 & v_2 \\ 0 & 0 \end{bmatrix} \begin{bmatrix} w_1(t) \\ w_2(t) \end{bmatrix}.$$

The linearized closed-loop system around the operating point $x_{10} = 45$, $x_{20} = 15$, $x_{30} = 30$, $u_{10} = 43.1$, $u_{20} = 17.1$ is

$$\Delta\dot{x}(t) = \begin{bmatrix} (a_{11} - v_1) & 0 & 0 \\ 0 & (a_{22} - v_2) & 0 \\ 0.0085 & 0.0084 & -0.0169 \end{bmatrix} \Delta x(t) + \begin{bmatrix} v_1 & 0 \\ 0 & v_2 \\ 0 & 0 \end{bmatrix} \begin{bmatrix} \Delta w_1(t) \\ \Delta w_2(t) \end{bmatrix} + \begin{bmatrix} 0.0085 + (a_{11} - v_1) & 0 & -0.0085 & 0.0065 & 0 \\ 0 & 0.0195 + (a_{22} - v_2) & 0.0084 & 0 & 0.0065 \\ 0 & 0 & 0 & 0 & 0 \end{bmatrix} f(t)$$

with $\Delta w_1 = w_1 - x_{10}, \Delta w_2 = w_2 - x_{20}$. In the benchmark study, the parameters are set as $a_{11} = a_{22} = 0$, $v_1 = v_2 = 0.01$. Then the corresponding discretized system with sampling time being $T_s = 0.1$s is

$$\begin{aligned}\Delta x(k+1) =& \begin{bmatrix} 0.9990 & 0 & 0 \\ 0 & 0.9990 & 0 \\ 0.0008 & 0.0008 & 0.9983 \end{bmatrix} \Delta x(k) + \begin{bmatrix} 0.0009995 & 0 \\ 0 & 0.0009995 \\ 0 & 0 \end{bmatrix} \begin{bmatrix} \Delta w_1(k) \\ \Delta w_2(k) \end{bmatrix} \\ &+ \begin{bmatrix} -0.0001499 & 0 & -0.0008496 & 0.0006497 & 0 \\ 0 & 0.0009495 & 0.0008396 & 0 & 0.0006497 \\ 0 & 0 & 0 & 0 & 0 \end{bmatrix} f(k) \\ \Delta y(k) =& C_d \Delta x(k) + F_d d(k) + F_f f(k). \end{aligned} \tag{6.4}$$

6.2 Benchmark setup

The complete simulation of the networked three-tank system is realized in MATLAB/SIMULINK. It consists of two parts: the simulation of the three-tank system and the simulation of the networks.

6.2.1 Simulation of three-tank system

A nonlinear model of the three-tank system is implemented based on the first principle law (6.1) in SIMULINK and the sensor and actuator faults are also simulated. Additionally, a group of component faults are defined, which are

- the leakages in three tanks: leakage in tank 1, leakage in tank 2 and leakage in tank 3, and
- the plugging in three pipes: plugging of $Q13$, plugging of $Q32$ and plugging of $Q20$.

In the following part, these faults are called as $f_6, f_7, f_8, f_9, f_{10}$ and f_{11}, respectively.

6.2.2 Simulation of networks

Two types of networks are simulated: wireless network and wired network. In the remote FD system, a wireless network is considered where bit errors are typical. While in the FD of NCSs, a wired networked is applied.

The real-time simulation of network is the current research interest. There are different tools available, e.g. NS2 [84], NIST Net [6] and Truetime [7]. NS2 provides substantial support for simulation of TCP, routing, and multicast protocols over wired and wireless networks, which concentrates on the low level simulation. NIST net network emulator is a general purpose tool for emulating a variety performance dynamics in IP network. Truetime is a Matlab/Simulink-based simulator for real-time control systems, which facilitates co-simulation of controller task execution in real-time kernels, network transmissions and continuous plant dynamics. It can describe typical features of networks through simulating communication protocols, such as transmission delays and packet dropouts. Since Truetime is Matlab/Simulink based, it can be easily integrated with existing Simulink models. Hence Truetime toolbox is applied to simulate the wired networks in the benchmark.

Table 6.2: statistical properties of the $(8,8)$ code. ^{a}: with the probability larger than 96%

	(0,0.0025]	(0.0025,0.005]	(0.005,0.0075]	(0.0075,0.01]
$\delta_{i,2}$	$< 0.8374e-3$	< 0.0017	< 0.0025	< 0.0034
$\delta_{i,4}$	$< 0.1694e-3$	$< 0.3443e-3$	$< 0.5274e-3$	$< 0.7107e-3$
$\Vert\Delta_i(k)\Vert_T{}^{\mathrm{a}}$	< 0.3557	< 0.5060	< 0.6252	< 0.7241

The wireless network is simulated with the help of Communication Blockset in SIMULINK, which provides different kinds of models of wireless communication channels and coding methods.

6.3 Implementation of the remote FD System

In this section, the remote FD system for the closed-loop system (6.4) over time-varying communication channels is implemented. The reference signals are

$$w_1(k) = 45, w_2(k) = 15$$

and they are known by the remote FD system.

The 8-bit uniform quantizer is applied for all measurements in the source encoder and the range of the each valid measurement is assumed to be $(0, 0.6)$. The unknown disturbances $d(k)$ is simulated as a uniform random number in the range of $[-0.1, 0.1]$. The simulation time is 1000s. In each simulation, one type of faults is generated at 500s as a step function.

The channel is selected to be a BSC simulated with SIMULINK. The upper bound of BER, $p_b(k)$, is set to be $\begin{bmatrix} 0.01 & 0.01 \end{bmatrix}^T$, and four reliability classes are considered, i.e.

$$(0, 0.0025], (0.0025, 0.005], (0.005, 0.0075], (0.0075, 0.01].$$

In order to illustrate the results, an $(8,8)$-code is employed. That means the 8-bit binary sequence after quantization is directly transmitted without further channel coding. By selecting $\beta = 5$ and $T = 10$, then according to (4.14), the expectation of the energy level of $\Delta_t(k)$ is approximated. In Table 6.2, the important statistical properties of the code are given.

When all the measurements are transmitted over the same channel, i.e. centralized transmission, according to Theorem 4.4 the optimal residual generator for channel applying $(8,8)$-code are with

$$L_1 = \begin{bmatrix} 0.0006 & -0.0000 & -0.0008 \\ -0.0003 & 0.0016 & 0.0007 \\ 0.0002 & -0.0001 & 0.0001 \end{bmatrix}, L_2 = \begin{bmatrix} 0.0005 & -0.0001 & -0.0008 \\ -0.0003 & 0.0016 & 0.0007 \\ 0.0002 & -0.0001 & 0.0001 \end{bmatrix},$$

$$L_3 = \begin{bmatrix} 0.0005 & -0.0001 & -0.0007 \\ -0.0003 & 0.0015 & 0.0007 \\ 0.0002 & -0.0001 & 0.0001 \end{bmatrix}, L_4 = \begin{bmatrix} 0.0005 & -0.0001 & -0.0007 \\ -0.0002 & 0.0015 & 0.0007 \\ 0.0002 & -0.0001 & 0.0001 \end{bmatrix},$$

$$W_1 = \begin{bmatrix} 8.0171 & -0.2082 & -5.0109 \\ -0.0696 & 14.5763 & 4.6398 \\ -0.1903 & 1.5287 & 9.1559 \end{bmatrix}, W_2 = \begin{bmatrix} 7.1710 & -0.3680 & -4.7255 \\ -0.1054 & 14.0571 & 4.7948 \\ -0.1266 & 1.7024 & 8.7467 \end{bmatrix},$$

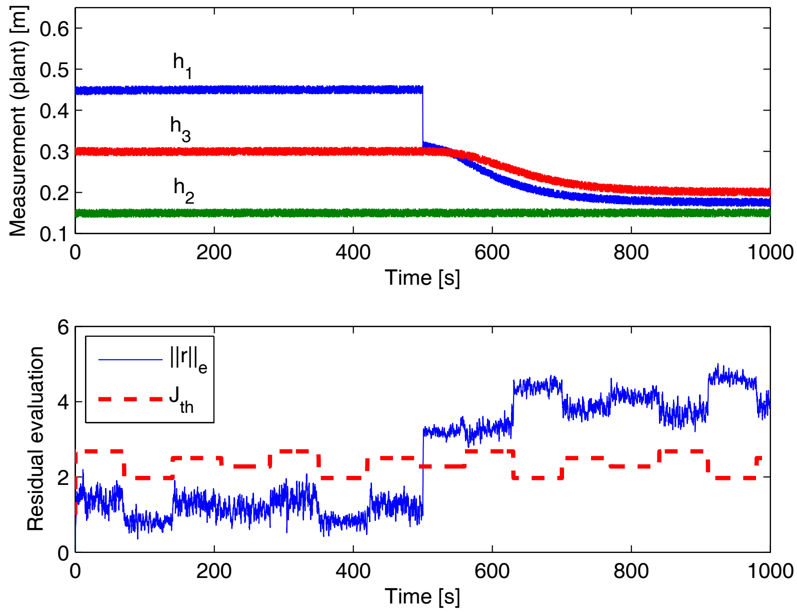

Figure 6.2: Remote FD of the scaling sensor fault in tank 1, i.e. $f_1 = 30\%$, centralized transmission. Upper figure: the measured liquid levels in tanks. Lower figure: the solid line is the evaluated residual signal and the dash line is the threshold J_{th}.

$$W_3 = \begin{bmatrix} 6.5308 & -0.4848 & -4.4988 \\ -0.1271 & 13.6200 & 4.9044 \\ -0.0827 & 1.8321 & 8.4101 \end{bmatrix}, W_4 = \begin{bmatrix} 5.9338 & -0.5920 & -4.2805 \\ -0.1451 & 13.1785 & 4.9899 \\ -0.0449 & 1.9521 & 8.0766 \end{bmatrix}$$

and $\gamma = 3.4059$.

Fig. 6.2 - Fig. 6.12 show the simulation results. The obtained thresholds are adaptive ones, and they are adjusted according to the reliability classes of the signals. As shown in Fig. 6.2 - Fig. 6.4, even small-size sensor faults can be detected in time. From Fig. 6.5 and 6.6, it is known that the remote FD system is not very sensitive to the pump faults, and only sufficient large pump faults can be detected. Middle-size leakage faults in tank 1 and 2 can be detected, but the leakage fault in tank 3 is insensitive; See Fig. 6.7 - Fig. 6.9. The plugging faults of middle-size are detected; See Fig. 6.10 - Fig. 6.12. The FAR is always upper bounded by 4%.

When different measurements are transmitted over different channels, i.e. decentralized transmission, according to Theorem 4.5 the optimal residual generator for channels applying $(8, 8)$-code are with

$$L_1 = \begin{bmatrix} 0.0006 & -0.0001 & -0.0009 \\ -0.0005 & 0.0019 & 0.0006 \\ 0.0002 & -0.0000 & 0.0001 \end{bmatrix}, L_2 = \begin{bmatrix} 0.0005 & 0.0000 & -0.0007 \\ -0.0003 & 0.0016 & 0.0003 \\ 0.0001 & -0.0000 & 0.0001 \end{bmatrix},$$

$$L_3 = \begin{bmatrix} 0.0005 & -0.0001 & -0.0008 \\ -0.0004 & 0.0019 & 0.0006 \\ 0.0001 & -0.0000 & 0.0001 \end{bmatrix}, L_4 = \begin{bmatrix} 0.0006 & 0.0000 & -0.0007 \\ -0.0005 & 0.0016 & 0.0003 \\ 0.0002 & -0.0000 & 0.0001 \end{bmatrix},$$

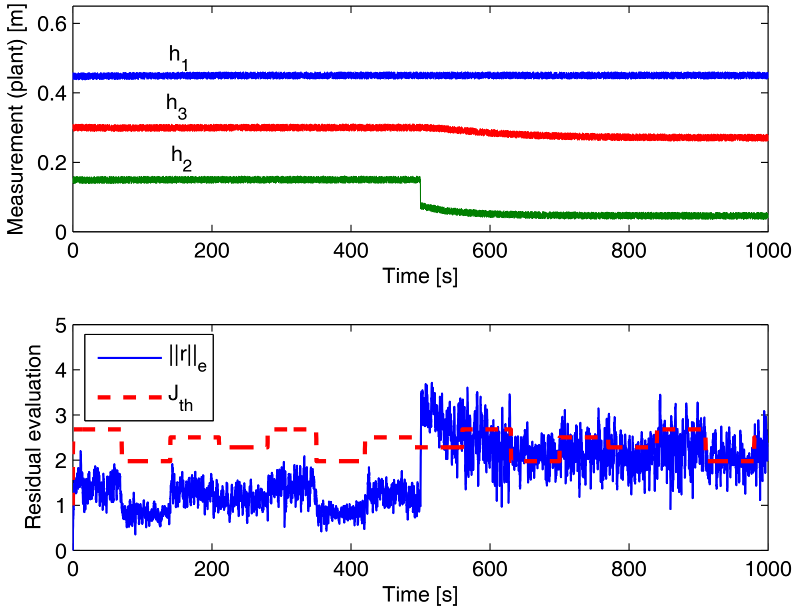

Figure 6.3: Remote FD of the scaling sensor fault in tank 2, i.e. $f_2 = 50\%$, centralized transmission. Upper figure: the measured liquid levels in tanks. Lower figure: the solid line is the evaluated residual signal and the dash line is the threshold J_{th}.

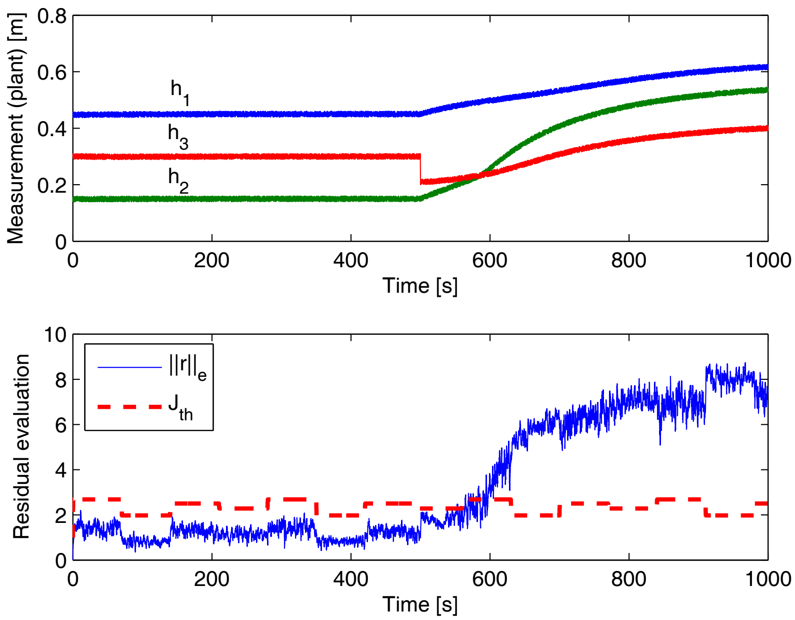

Figure 6.4: Remote FD of the scaling sensor fault in tank 3, i.e. $f_3 = 30\%$, centralized transmission. Upper figure: the measured liquid levels in tanks. Lower figure: the solid line is the evaluated residual signal and the dash line is the threshold J_{th}.

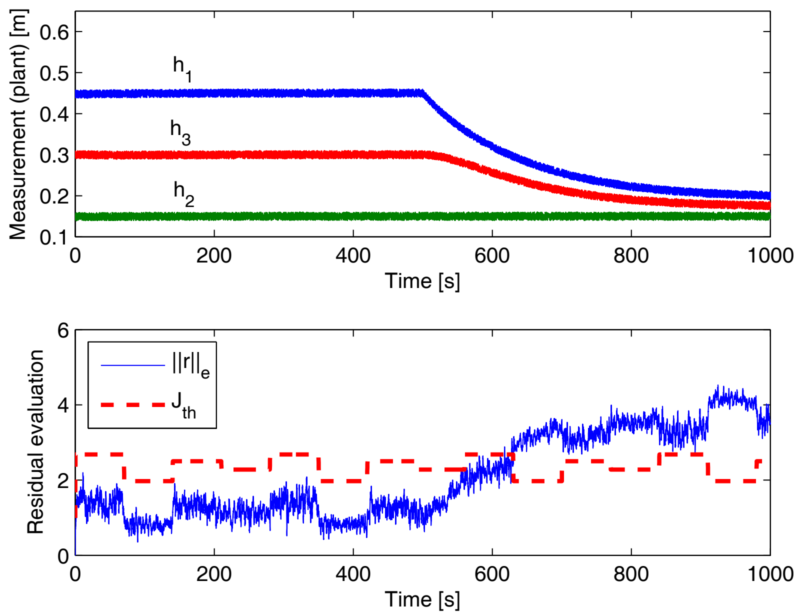

Figure 6.5: Remote FD of the scaling fault in pump 1, i.e. $f_4 = 70\%$, centralized transmission. Upper figure: the measured liquid levels in tanks. Lower figure: the solid line is the evaluated residual signal and the dash line is the threshold J_{th}.

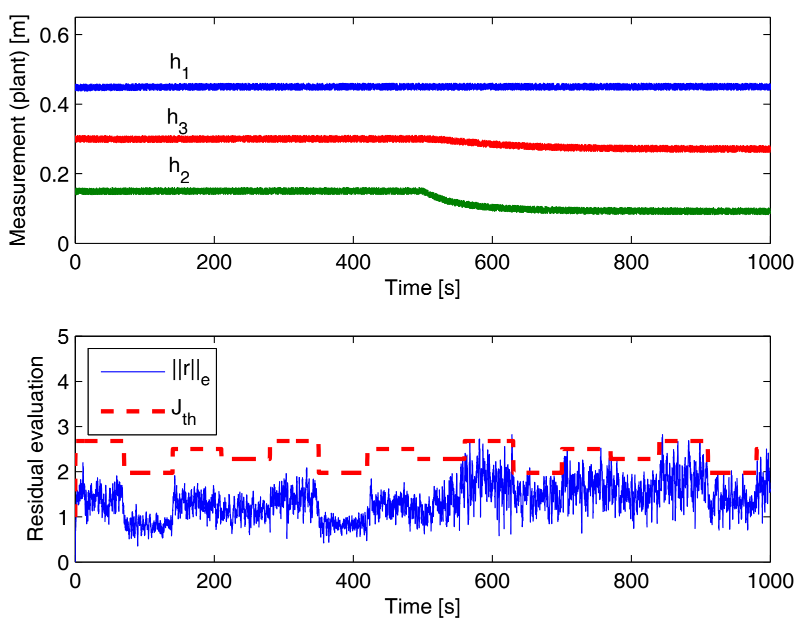

Figure 6.6: Remote FD of the scaling fault in pump 2, i.e. $f_5 = 100\%$, centralized transmission. Upper figure: the measured liquid levels in tanks. Lower figure: the solid line is the evaluated residual signal and the dash line is the threshold J_{th}.

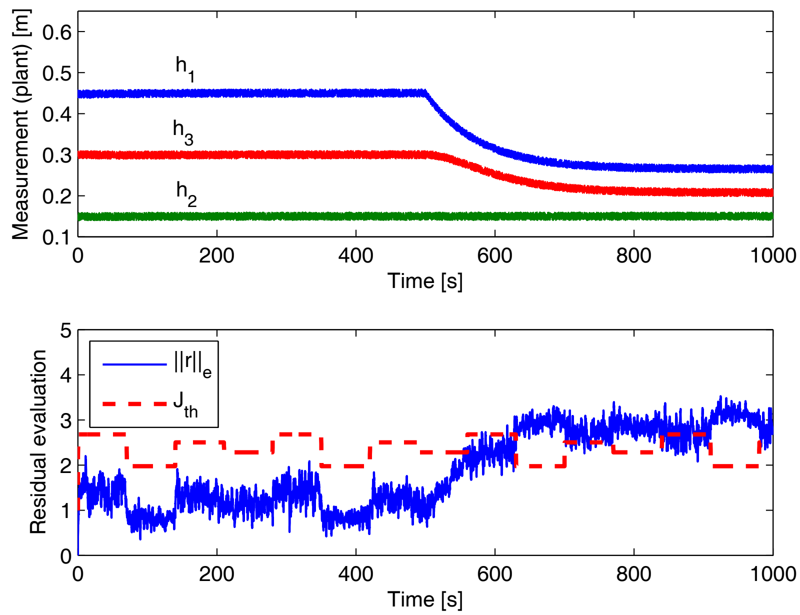

Figure 6.7: Remote FD of the scaling leakage fault in tank 1, i.e. $f_6 = 50\%$, centralized transmission. Upper figure: the measured liquid levels in tanks. Lower figure: the solid line is the evaluated residual signal and the dash line is the threshold J_{th}.

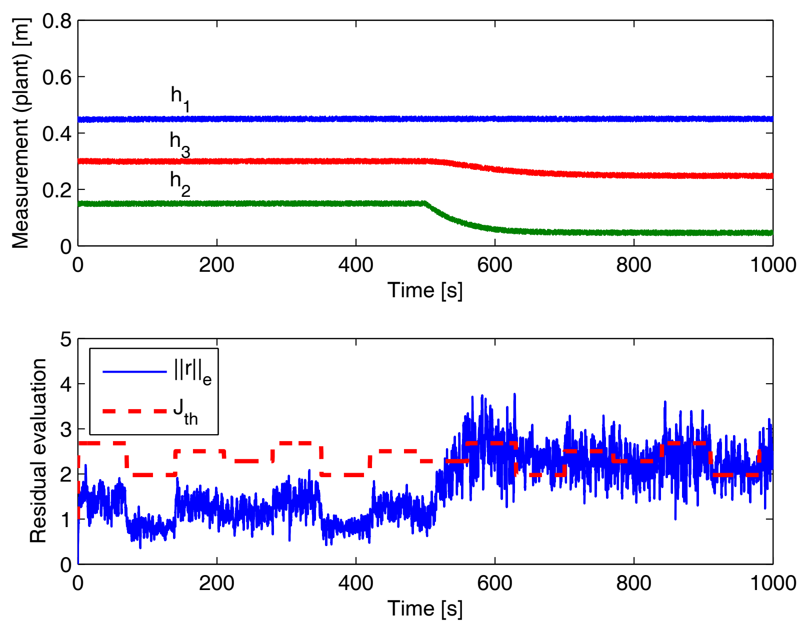

Figure 6.8: Remote FD of the scaling leakage fault in tank 2, i.e. $f_7 = 70\%$, centralized transmission. Upper figure: the measured liquid levels in tanks. Lower figure: the solid line is the evaluated residual signal and the dash line is the threshold J_{th}.

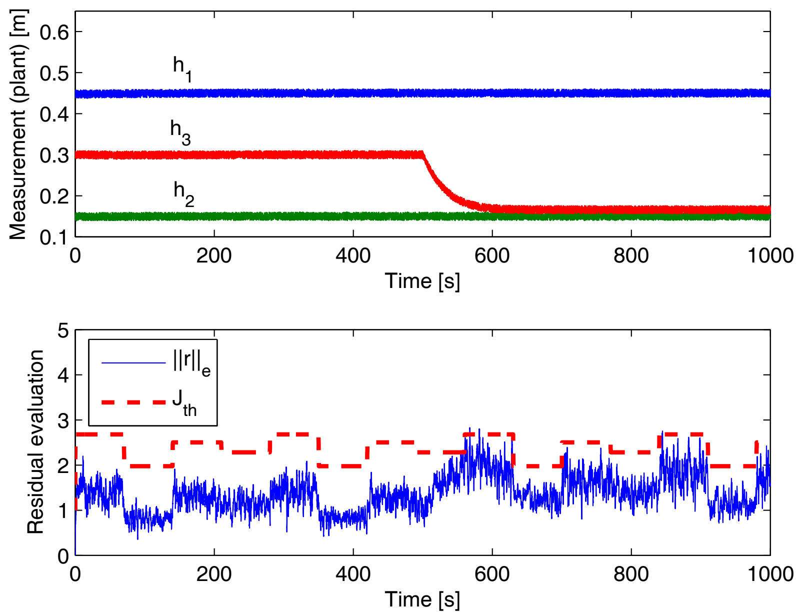

Figure 6.9: Remote FD of the scaling leakage fault in tank 3, i.e. $f_8 = 100\%$, centralized transmission. Upper figure: the measured liquid levels in tanks. Lower figure: the solid line is the evaluated residual signal and the dash line is the threshold J_{th}.

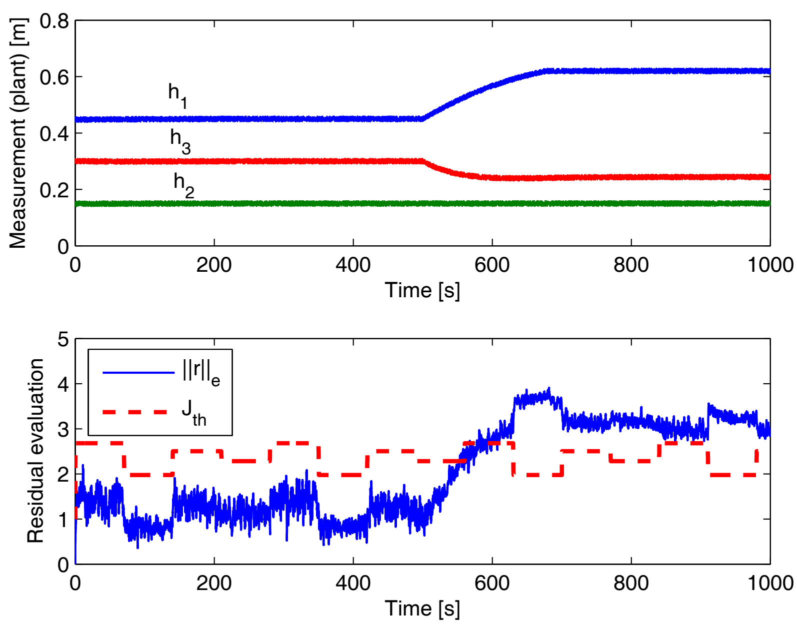

Figure 6.10: Remote FD of the scaling plugging fault in $Q13$, i.e. $f_9 = 50\%$, centralized transmission. Upper figure: the measured liquid levels in tanks. Lower figure: the solid line is the evaluated residual signal and the dash line is the threshold J_{th}.

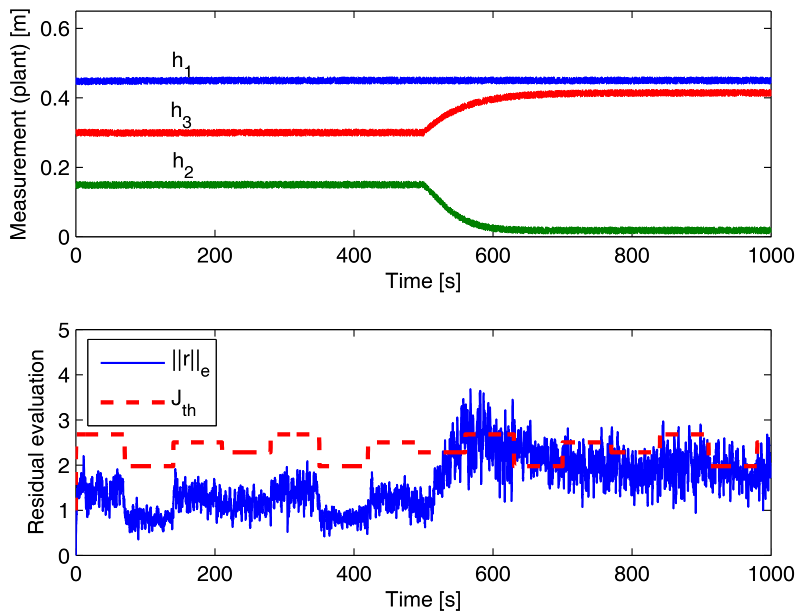

Figure 6.11: Remote FD of the scaling plugging fault in $Q32$, i.e. $f_{10} = 70\%$, centralized transmission. Upper figure: the measured liquid levels in tanks. Lower figure: the solid line is the evaluated residual signal and the dash line is the threshold J_{th}.

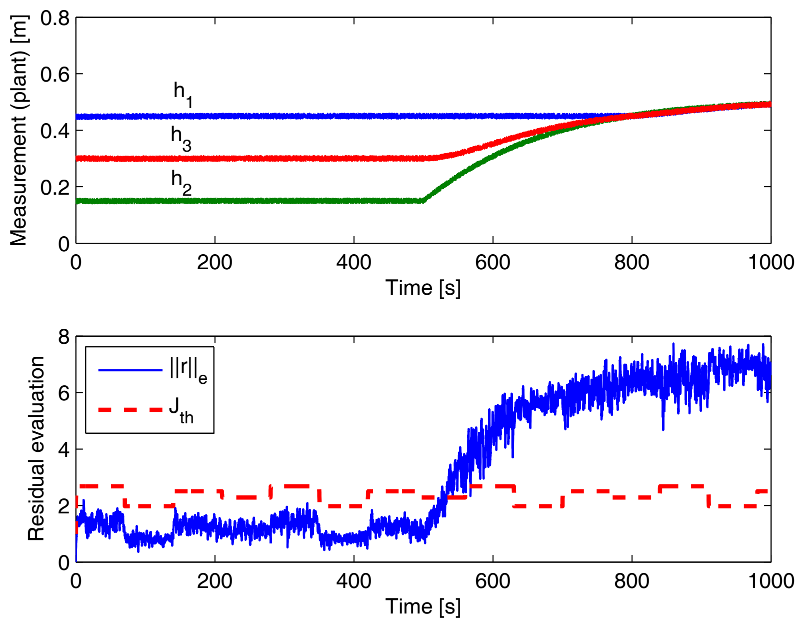

Figure 6.12: Remote FD of the scaling plugging fault in $Q20$, i.e. $f_{11} = 100\%$, centralized transmission. Upper figure: the measured liquid levels in tanks. Lower figure: the solid line is the evaluated residual signal and the dash line is the threshold J_{th}.

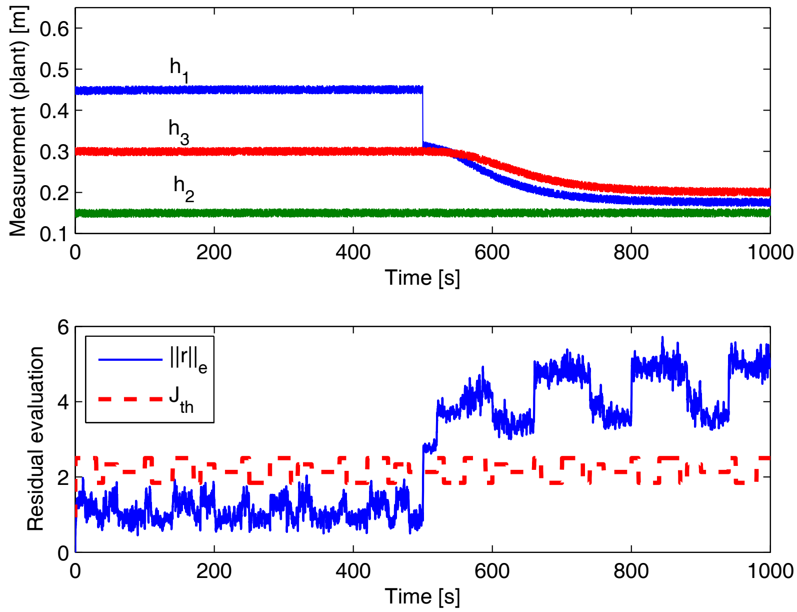

Figure 6.13: Remote FD of the scaling sensor fault in tank 1, i.e. $f_1 = 30\%$, decentralized transmission. Upper figure: the measured liquid levels in tanks. Lower figure: the solid line is the evaluated residual signal and the dash line is the threshold J_{th}.

$$W_1 = \begin{bmatrix} 8.5440 & 0.1473 & -5.4158 \\ -0.0612 & 14.3865 & 3.3906 \\ -0.3021 & 0.9741 & 9.0037 \end{bmatrix}, W_2 = \begin{bmatrix} 6.2189 & 0.5715 & -4.5564 \\ 0.0033 & 12.4878 & 0.9929 \\ -0.1993 & -0.0874 & 7.6537 \end{bmatrix},$$

$$W_3 = \begin{bmatrix} 6.5830 & 0.0239 & -5.2963 \\ -0.0711 & 14.3853 & 3.3906 \\ -0.2456 & 0.9774 & 9.0000 \end{bmatrix}, W_4 = \begin{bmatrix} 8.4795 & 0.7021 & -4.7092 \\ -0.0854 & 12.4892 & 1.0073 \\ -0.3131 & -0.0904 & 7.6661 \end{bmatrix}$$

and $\gamma = 3.0659$.

The performance of the remote FD system with decentralized transmission is similar to that of the centralized one, where the thresholds are also adaptive variables. Fig. 6.13 - Fig. 6.23 show the simulation results.

6.4 Implementation of the FD of NCSs

In this section, the closed loop system (6.4) is assumed to be networked, where $w_1(t)$ and $w_2(t)$ generated by reference generator are sent over networks and the FD system is located together with the reference signal generator. Since the three-tank system is nonlinear, w_1 and w_2 are set to be closely around the operating point, i.e.

$$w_1(t) = x_{10} + \sin(20\pi t), w_2(t) = x_{20} + \sin(20\pi t).$$

A logarithmic quantizer with $\delta_q = 0.12$ is applied. Ethernet is simulated with Truetime in SIMULINK and the probability of packet dropouts is set to be 0.1. The simulation time is 500s and all types of faults are generated at 250s as step functions. Other settings are the

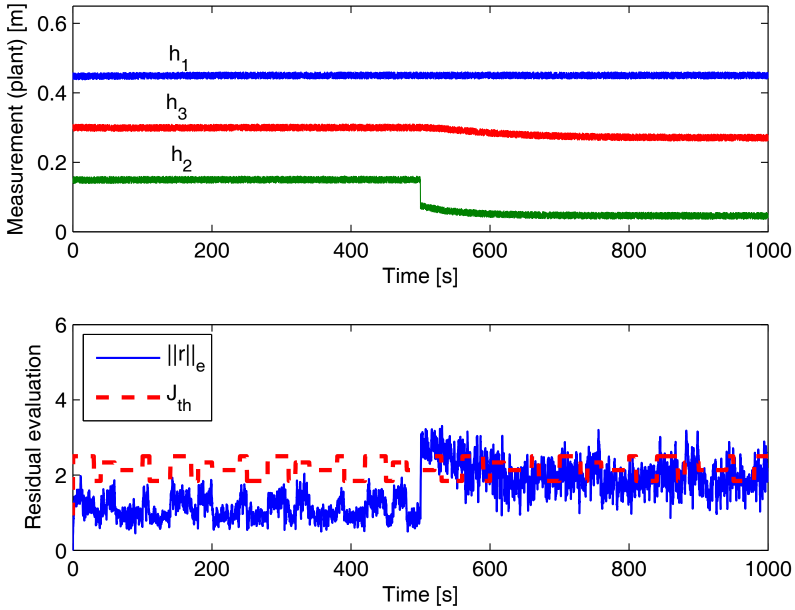

Figure 6.14: Remote FD of the scaling sensor fault in tank 2, i.e. $f_2 = 50\%$, decentralized transmission. Upper figure: the measured liquid levels in tanks. Lower figure: the solid line is the evaluated residual signal and the dash line is the threshold J_{th}.

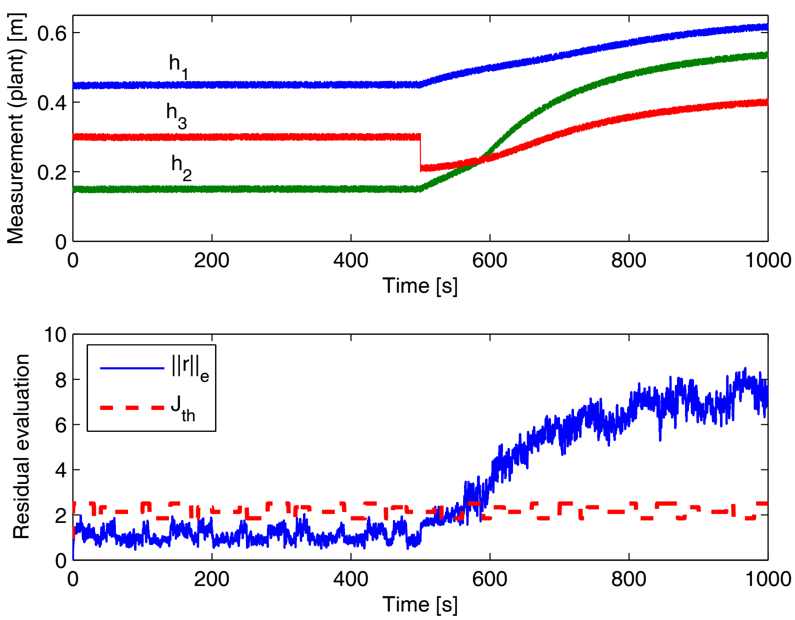

Figure 6.15: Remote FD of the scaling sensor fault in tank 3, i.e. $f_3 = 30\%$, decentralized transmission. Upper figure: the measured liquid levels in tanks. Lower figure: the solid line is the evaluated residual signal and the dash line is the threshold J_{th}.

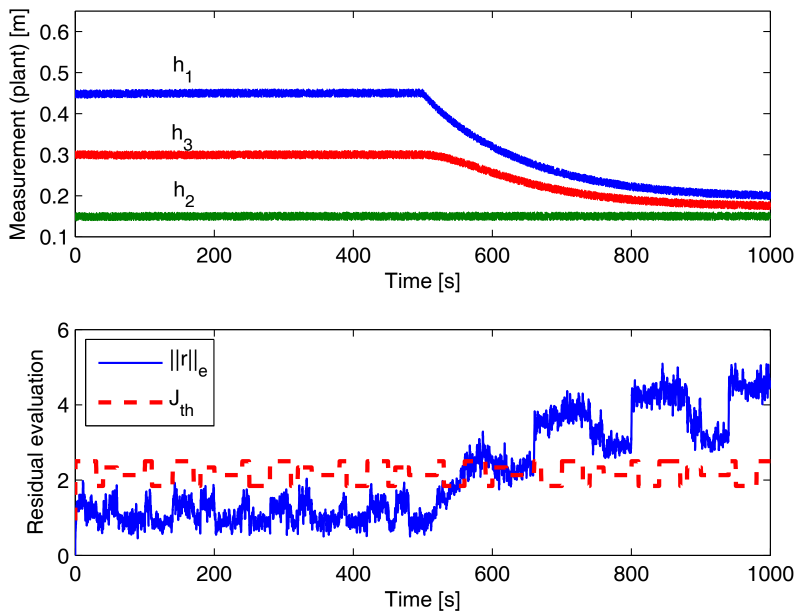

Figure 6.16: Remote FD of the scaling fault in pump 1, i.e. $f_4 = 70\%$, decentralized transmission. Upper figure: the measured liquid levels in tanks. Lower figure: the solid line is the evaluated residual signal and the dash line is the threshold J_{th}.

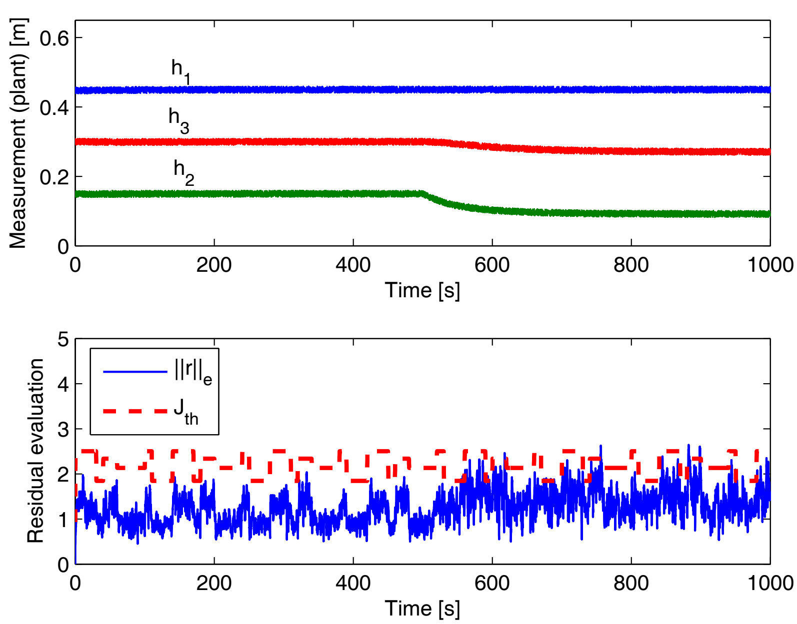

Figure 6.17: Remote FD of the scaling fault in pump 2, i.e. $f_5 = 100\%$, decentralized transmission. Upper figure: the measured liquid levels in tanks. Lower figure: the solid line is the evaluated residual signal and the dash line is the threshold J_{th}.

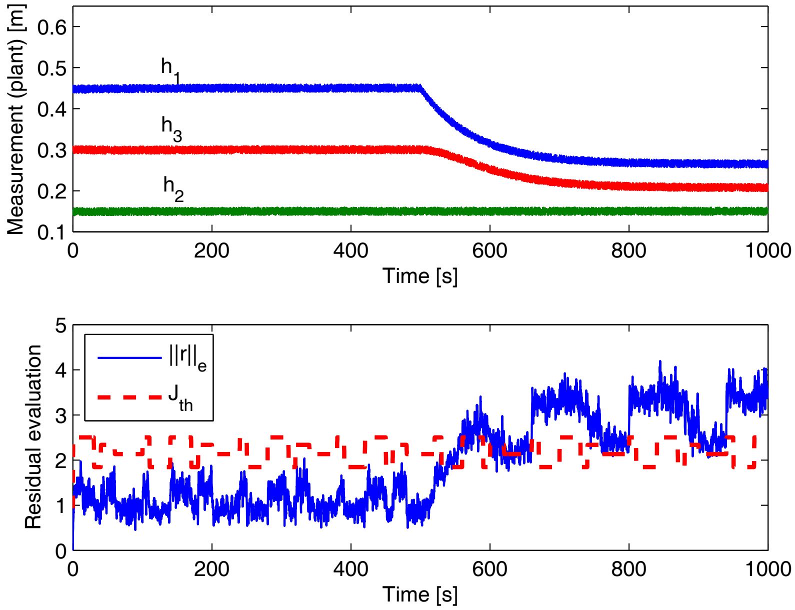

Figure 6.18: Remote FD of the scaling leakage fault in tank 1, i.e. $f_6 = 50\%$, decentralized transmission. Upper figure: the measured liquid levels in tanks. Lower figure: the solid line is the evaluated residual signal and the dash line is the threshold J_{th}.

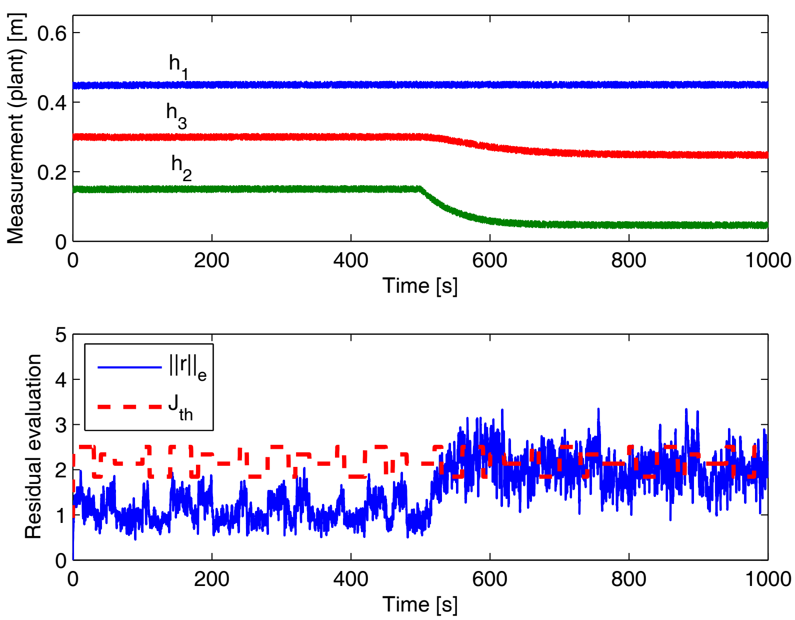

Figure 6.19: Remote FD of the scaling leakage fault in tank 2, i.e. $f_7 = 70\%$, decentralized transmission. Upper figure: the measured liquid levels in tanks. Lower figure: the solid line is the evaluated residual signal and the dash line is the threshold J_{th}.

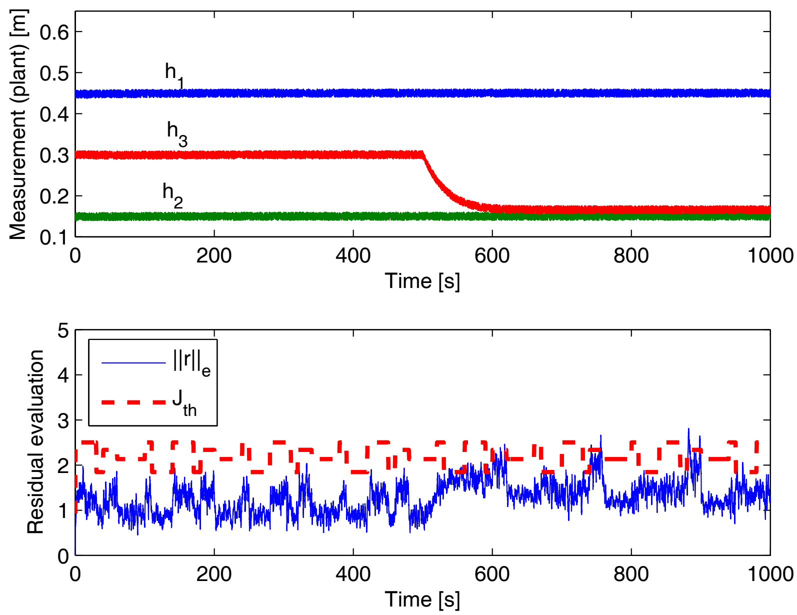

Figure 6.20: Remote FD of the scaling leakage fault in tank 3, i.e. $f_8 = 100\%$, decentralized transmission. Upper figure: the measured liquid levels in tanks. Lower figure: the solid line is the evaluated residual signal and the dash line is the threshold J_{th}.

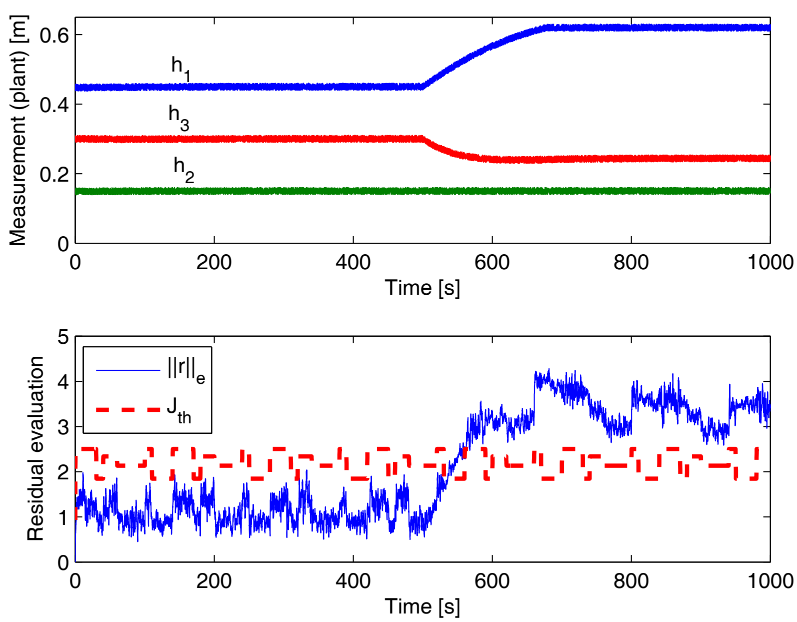

Figure 6.21: Remote FD of the scaling plugging fault in $Q13$, i.e. $f_9 = 50\%$, decentralized transmission. Upper figure: the measured liquid levels in tanks. Lower figure: the solid line is the evaluated residual signal and the dash line is the threshold J_{th}.

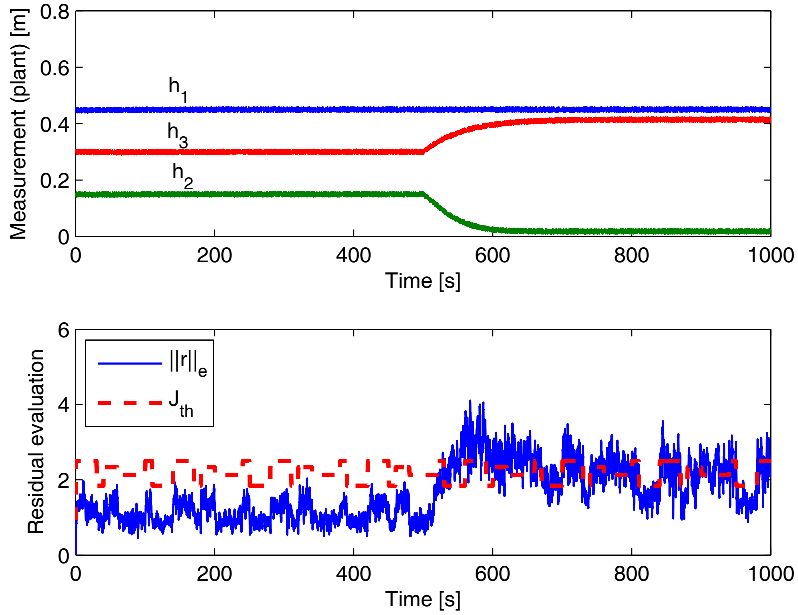

Figure 6.22: Remote FD of the scaling plugging fault in $Q32$, i.e. $f_{10} = 70\%$, decentralized transmission. Upper figure: the measured liquid levels in tanks. Lower figure: the solid line is the evaluated residual signal and the dash line is the threshold J_{th}.

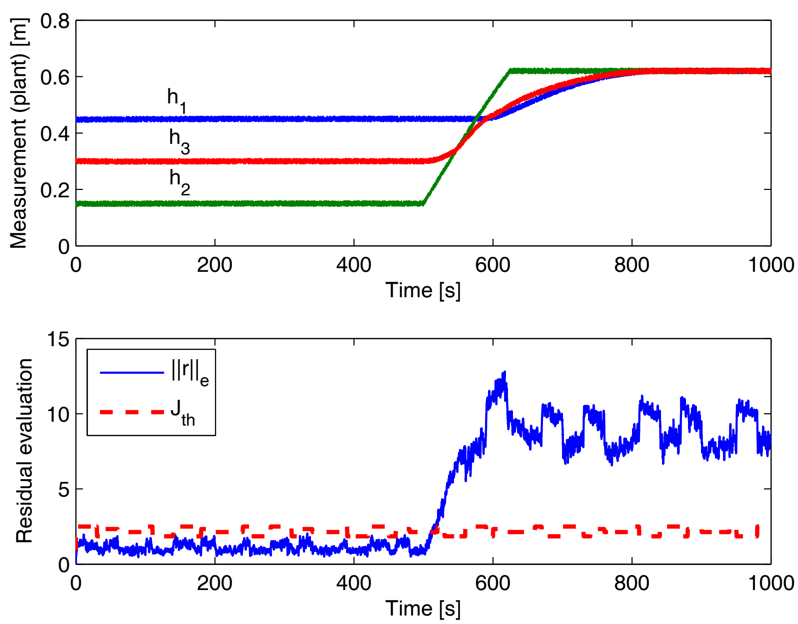

Figure 6.23: Remote FD of the scaling plugging fault in $Q20$, i.e. $f_{11} = 100\%$, decentralized transmission. Upper figure: the measured liquid levels in tanks. Lower figure: the solid line is the evaluated residual signal and the dash line is the threshold J_{th}.

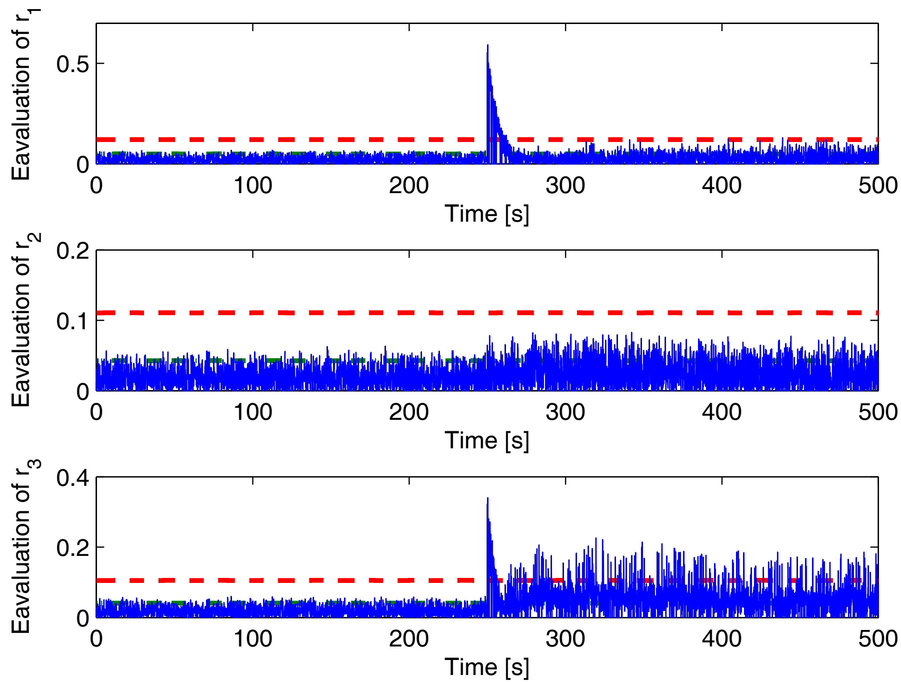

Figure 6.24: FD of NCSs: the scaling sensor fault in tank 1, i.e. $f_1 = 30\%$. The solid line is the evaluated residual signal, the dash line is J_{th} and the dash-dot line is J_e.

same with the remote FD system. From the simulation, it is known that the transmission delay is not larger than 0.001s, which is smaller than the sampling time $T_s = 0.1$s.

According to Theorem 5.3, the optimal L_1, L_2, W_1, W_2 for (6.4) are

$$L_1 = \begin{bmatrix} 0.0164 & -0.0022 & 0.0060 \\ -0.0011 & 0.0125 & 0.0031 \\ 0.0047 & 0.0026 & 0.0032 \\ -0.0831 & -0.0272 & -0.0702 \\ -0.0415 & -0.0292 & -0.0462 \end{bmatrix}, L_2 = \begin{bmatrix} 0.0154 & -0.0018 & 0.0037 \\ -0.0006 & 0.0113 & 0.0022 \\ 0.0045 & 0.0025 & 0.0029 \\ -0.0259 & -0.0081 & -0.0181 \\ -0.0128 & -0.0055 & -0.0098 \end{bmatrix},$$

$$W_1 = \begin{bmatrix} -4.0690 & -0.0718 & -2.6475 \\ -0.3527 & -3.6963 & -1.8636 \\ 2.2891 & 0.9007 & 3.1678 \end{bmatrix}, W_2 = \begin{bmatrix} -4.28560.3466 - 1.7324 \\ 0.1320 - 4.8241 - 1.4417 \\ 1.53910.21524.5486 \end{bmatrix},$$

and $L_3 = L_4 = W_3 = W_4 = 0$. Then $\gamma_{1,1} = 0.0976, \gamma_{1,2} = 0.080, \gamma_{1,3} = 0.0473, \gamma_{1,4} = 0.01$, $\gamma_{2,1} = 0.0788, \gamma_{2,2} = 0.079, \gamma_{2,3} = 0.0401, \gamma_{2,4} = 0.01$, and $\gamma_{3,1} = 0.0736, \gamma_{3,2} = 0.081, \gamma_{3,3} = 0.0312, \gamma_{3,4} = 0.01$.

Fig. 6.24 - Fig. 6.34 shows the simulation results, where all three evaluated residual signals are displayed for each fault case. The thresholds J_e are computed based on the mean values of residual signals, while J_{th} are computed according to Theorem 5.6 with $\beta = 4$ and $T = 10$. The false alarms are significantly reduced with J_{th} and FAR is guaranteed to be smaller than 6.25%. It can be seen that, the FD system is insensitive to actuator faults and leakage faults in tank 1 and tank 2. Other types of faults of small-size or middle-size can be detected in time.

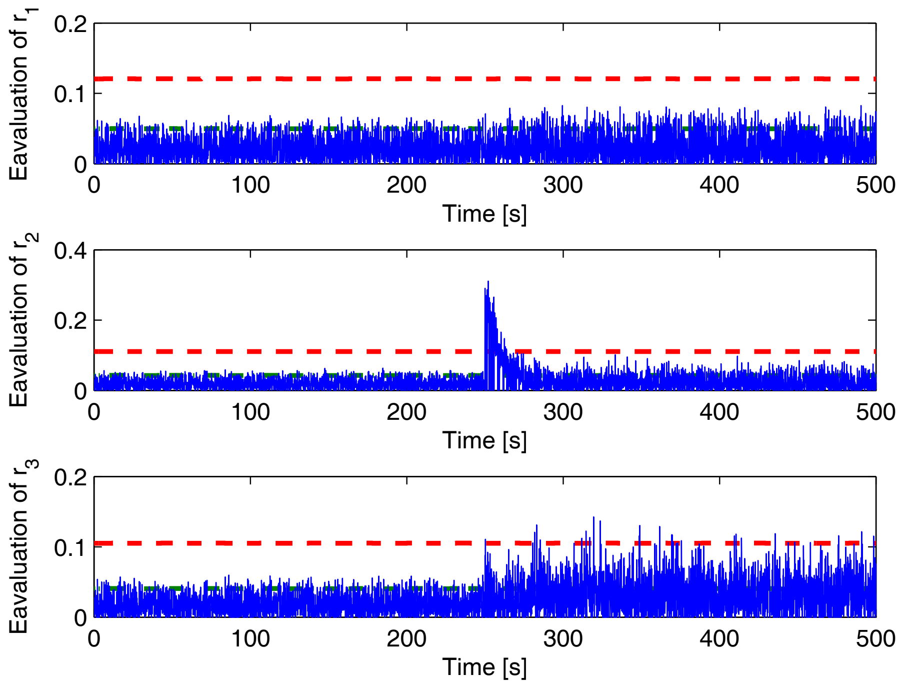

Figure 6.25: FD of NCSs: the scaling sensor fault in tank 2, i.e. $f_2 = 50\%$. The solid line is the evaluated residual signal, the dash line is J_{th} and the dash-dot line is J_e.

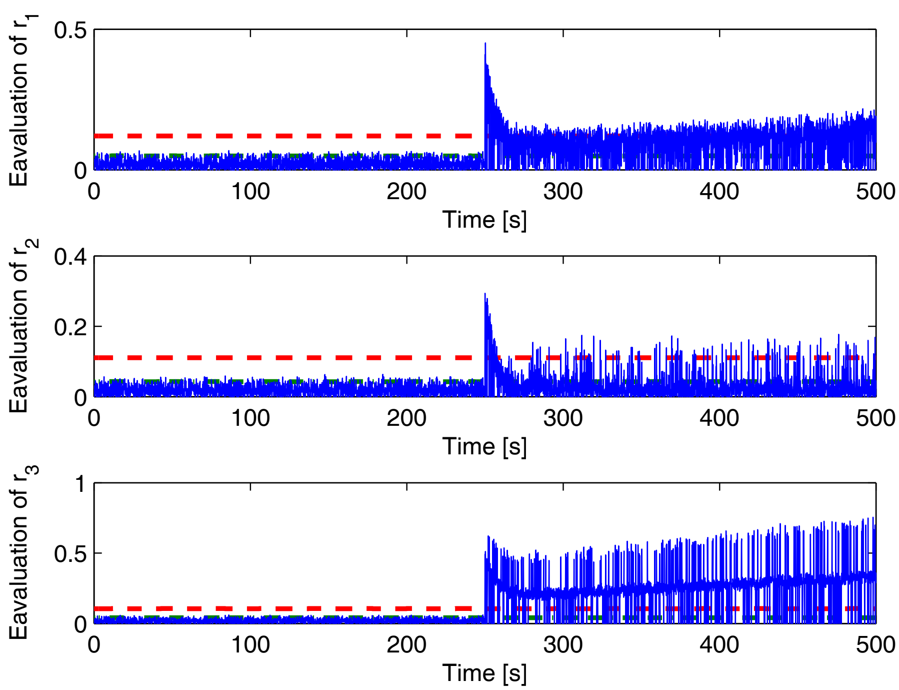

Figure 6.26: FD of NCSs: the scaling sensor fault in tank 3, i.e. $f_3 = 100\%$. The solid line is the evaluated residual signal, the dash line is J_{th} and the dash-dot line is J_e.

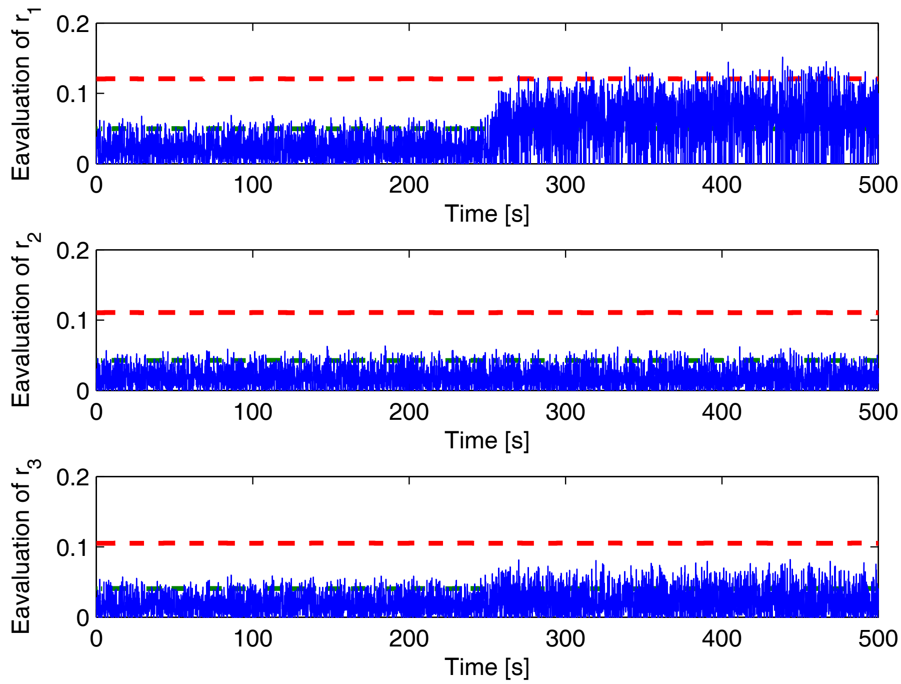

Figure 6.27: FD of NCSs: the scaling fault in pump 1, i.e. $f_4 = 100\%$. The solid line is the evaluated residual signal, the dash line is J_{th} and the dash-dot line is J_e.

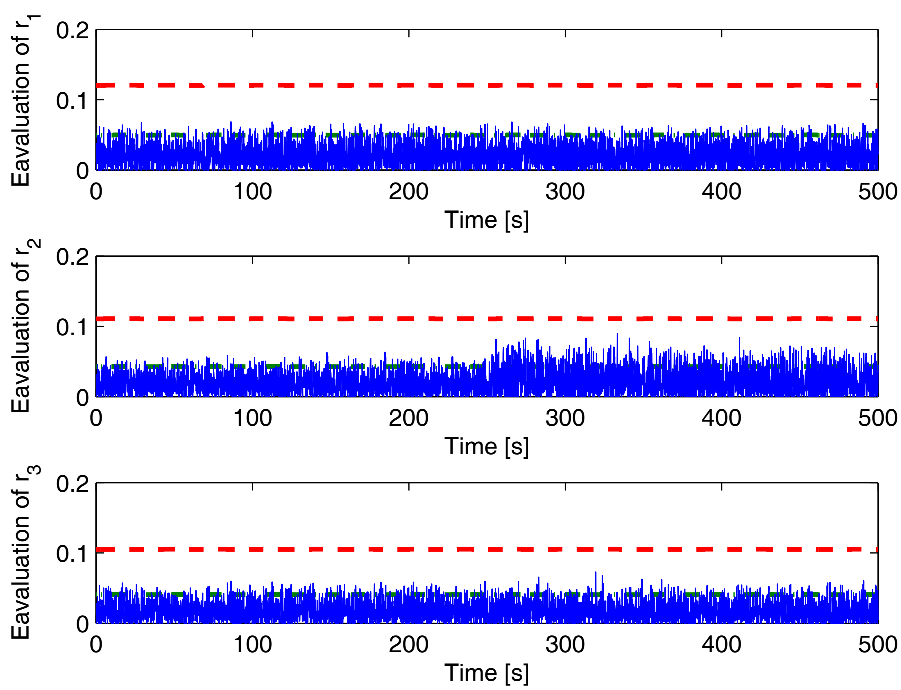

Figure 6.28: FD of NCSs: the scaling fault in pump 2, i.e. $f_5 = 100\%$. The solid line is the evaluated residual signal, the dash line is J_{th} and the dash-dot line is J_e.

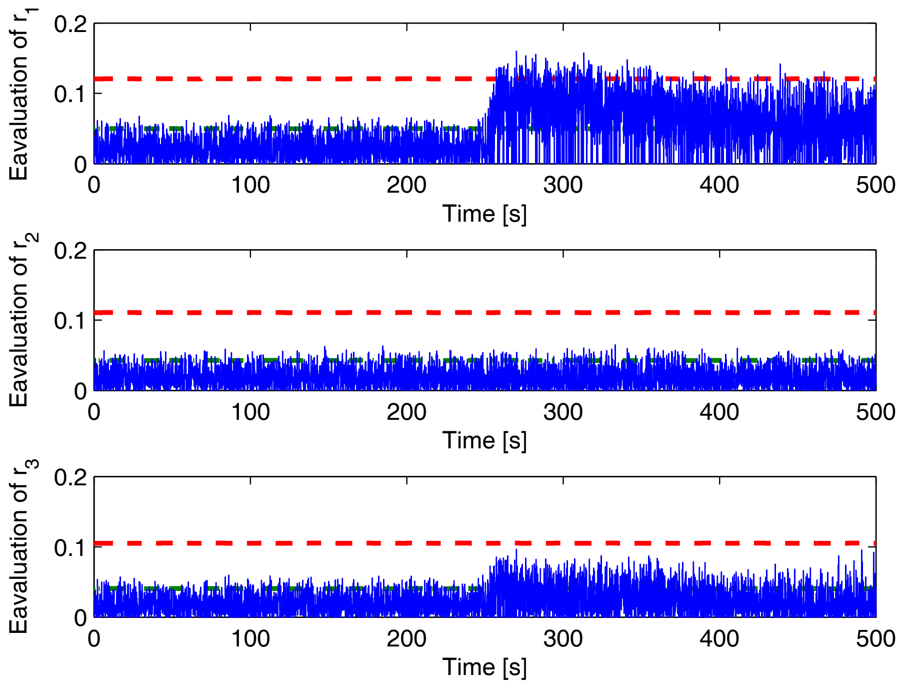

Figure 6.29: FD of NCSs: the scaling leakage fault in tank 1, i.e. $f_6 = 100\%$. The solid line is the evaluated residual signal, the dash line is J_{th} and the dash-dot line is J_e.

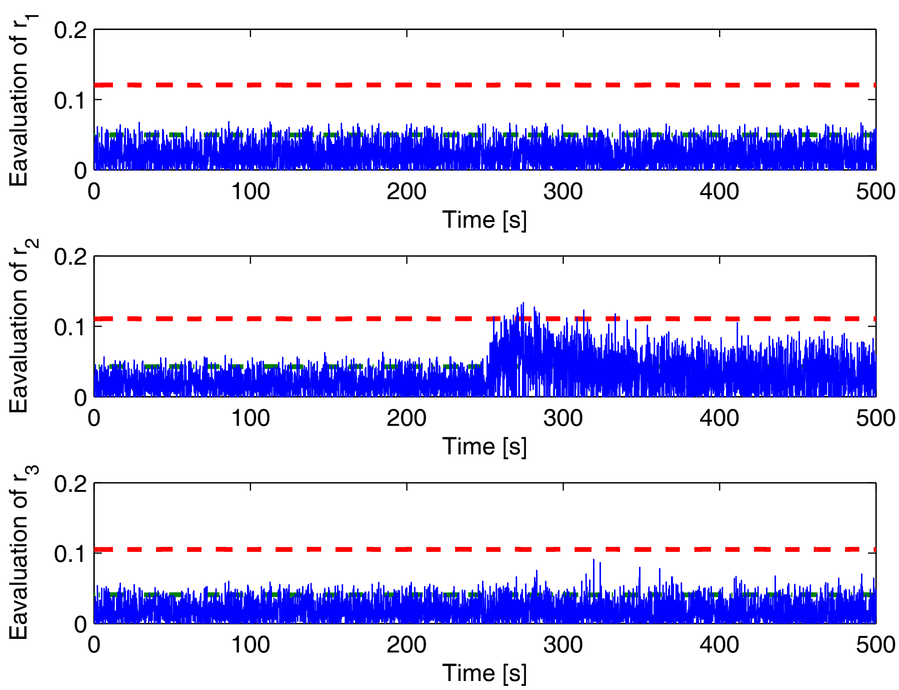

Figure 6.30: FD of NCSs: the scaling leakage fault in tank 2, i.e. $f_7 = 100\%$. The solid line is the evaluated residual signal, the dash line is J_{th} and the dash-dot line is J_e.

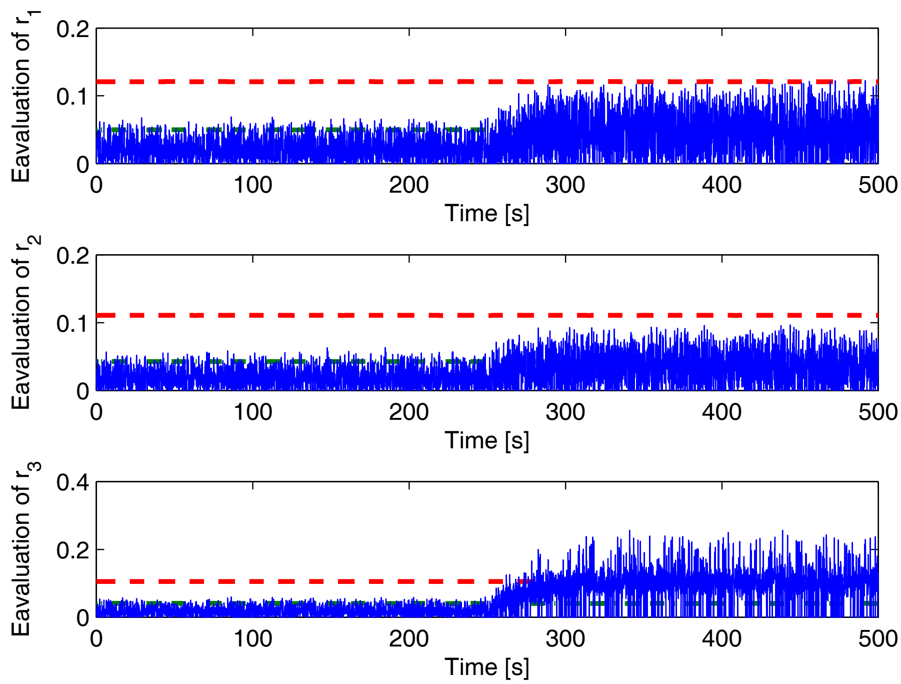

Figure 6.31: FD of NCSs: the scaling leakage fault in tank 3, i.e. $f_8 = 50\%$. The solid line is the evaluated residual signal, the dash line is J_{th} and the dash-dot line is J_e.

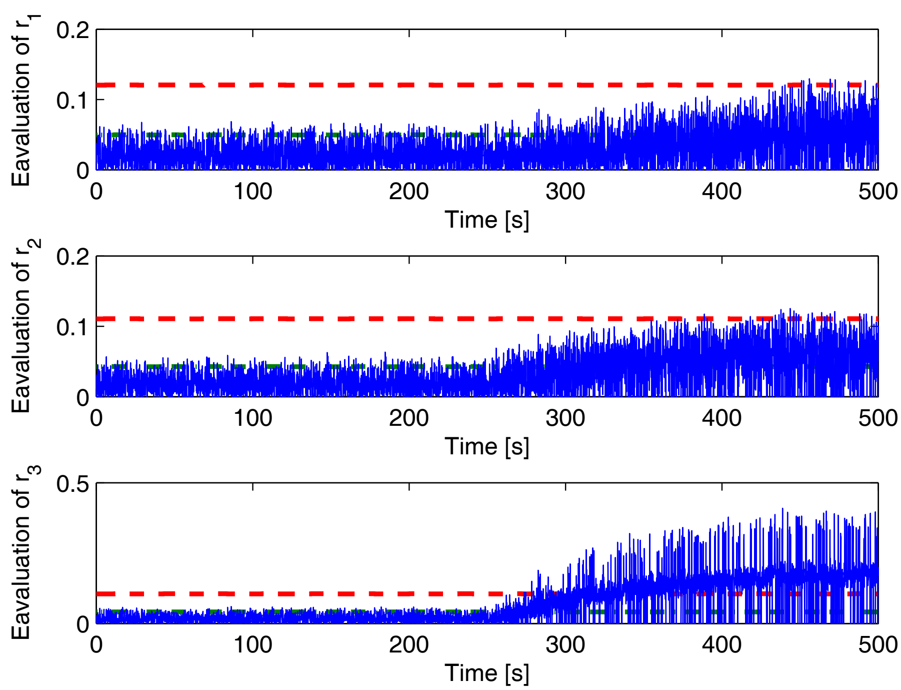

Figure 6.32: FD of NCSs: the scaling plugging fault in $Q13$, i.e. $f_9 = 50\%$. The solid line is the evaluated residual signal, the dash line is J_{th} and the dash-dot line is J_e.

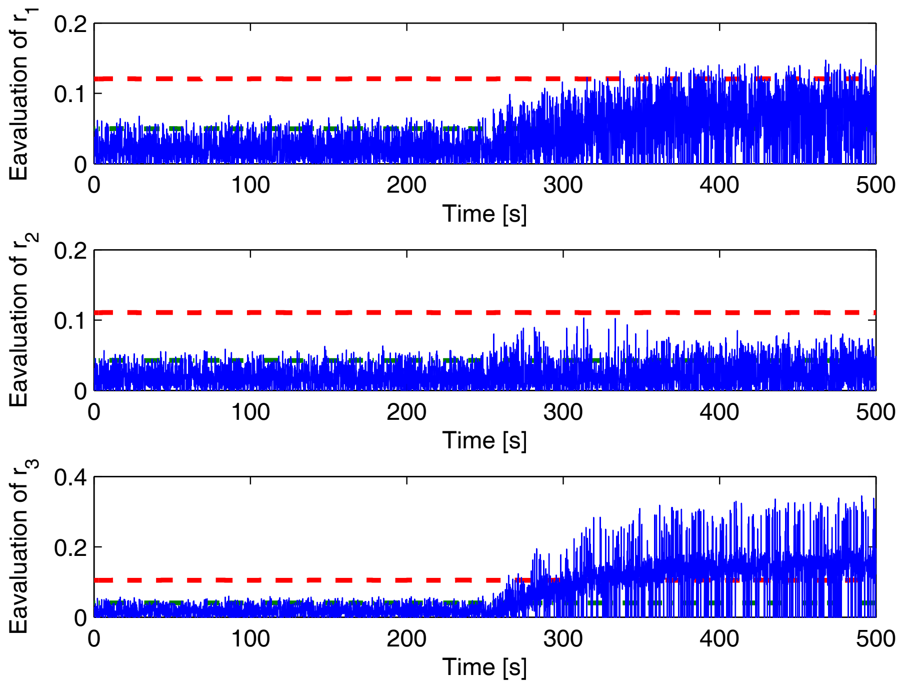

Figure 6.33: FD of NCSs: the scaling plugging fault in $Q32$, i.e. $f_{10} = 50\%$. The solid line is the evaluated residual signal, the dash line is J_{th} and the dash-dot line is J_e.

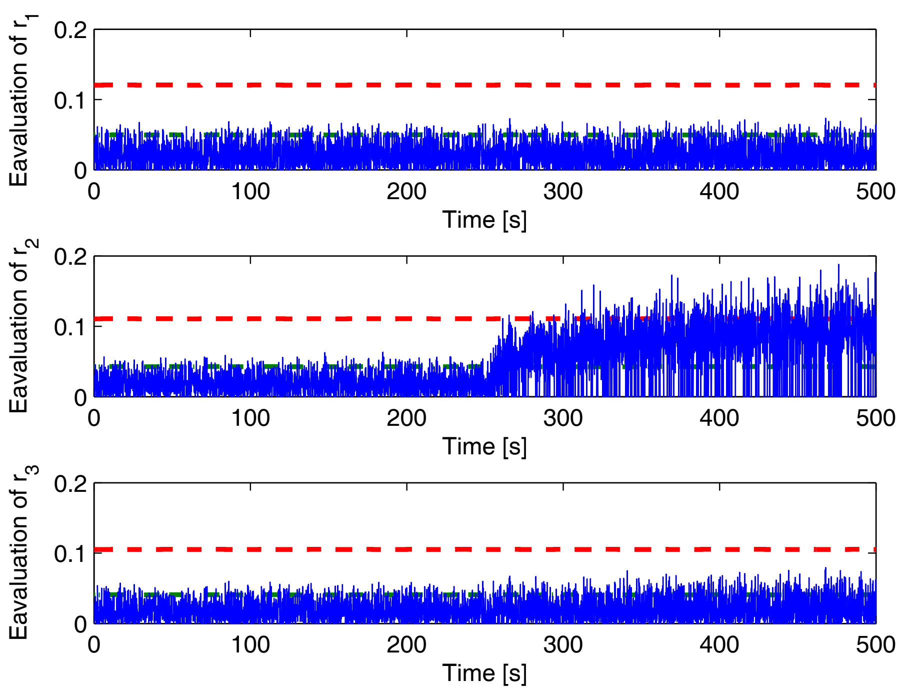

Figure 6.34: FD of NCSs: the scaling plugging fault in $Q20$, i.e. $f_{11} = 50\%$. The solid line is the evaluated residual signal, the dash line is J_{th} and the dash-dot line is J_e.

7 Conclusions and Future Work

The main concern of the presented work has been the investigation of fault detection problem, where networks have been introduced into systems. Therefore two observer-based FD schemes have been developed: the remote FD system and the FD system of NCSs. The remote FD system is suitable for detecting faults in a running technical system with known control laws, where the FD system is located at a remote site. The FD system of NCSs is for the case when the technical system itself is networked and the FD system is located together with the controller.

In order to design FD systems, the network-induced effects have been analyzed and modeled systematically from the view point of control engineering and integrated into a state-space model of technical systems. The time-varying transmission delays have been transformed into polytopic uncertainties and the quantization errors have been transformed into norm-bounded uncertainties or disturbances according to the type of the applied quantizers. The packet dropouts have been modeled as a Markov chain and then the system encountering packet dropouts has been described through an MJLS. The bit errors have been characterized as stochastic unknown inputs with constant or time-varying distribution matrices, which is achieved by analyzing the statistical properties of coding mechanisms of communication channels.

The presented optimization index and the definition of FAR are the baseline for the design of both FD schemes. The designed residual generators are going to achieve an optimal trade-off between the sensitivity to system faults and the robustness against system disturbances and network-induced effects. A model matching strategy has been applied for this purpose, where the reference model is an optimal residual generator capturing the proper fault dynamics and disturbance dynamics of the considered system. A new way to build up the reference model for MJLSs has been proposed by considering their statistical properties. The proposed residual evaluation methods for both schemes are able to guarantee the desired FAR by considering the means and variances of residual signals for the threshold computation, which are novel and different from the existing methods in literature. The variance of the technical system with stochastic parameter changing, e.g. MJLS, has been analyzed, which is ignored in the control problem but plays an essential role in the FD problem. Due to lack of knowledge of disturbances in technical systems, only the upper bounds of the means and variances have been derived in both schemes. Hence the FAR is obtained for the worst case. The design of residual generators and the computation of means and variances have been formulated as convex optimization problems and can be efficiently solved with the LMI Toolbox in MATLAB.

The designed remote FD scheme is applicable for the long distance monitoring of technical systems with centralized or decentralized data transmission via networks encountering bit errors, where a proper error control strategy is applied. Since the closed-loop dynamics of the technical system have been considered, only the measurements are required to be transmitted. This is an additional advantage towards reducing data transfer amount via networks. The influence of bit errors on control and FD system design was not yet intensively studied in literature. In the proposed scheme, the reliability information of the communication network represented by BER has been converted into structure information of the state-space form of technical systems by investigating the energy level of transmission errors caused by bit errors and quantization errors. The reliability classes have been defined to classify BERs. Based on them, the whole system has been modeled as a switching system in case of centralized transmission and a system with polytopic time-varying parameters in case of decentralized transmission, respectively. The obtained residual generator and threshold are adaptive to the reliability information of networks. The proposed scheme shall also be applicable for large systems with spatially located sensors where the decentralized data transmission is necessary.

The FD system of NCSs is suitable for monitoring of networked technical systems, where the connections between actuators, sensors and controller/FD are established with communication channels. In this scenario the design has taken transmission delays, packet dropouts and quantization errors into account. According to the packet received, four situations have been defined and the transitions between them are described by a Bernoulli process. Hence the design of FD system has been formulated in the framework of MJLSs with uncertainties. The residual generator has been designed to have network-dependent parameters. The residual signals have been evaluated separately and the obtained thresholds are adaptive variables which depend on the control inputs and packet dropouts. It is also possible to take bit errors into account in the design procedure with cost of complicated formulation and high computation efforts.

A networked three-tank system benchmark was established to test and illustrate the effectiveness of the proposed schemes. The networks were simulated with Truetime Toolbox and Communication Blockset in MATLAB/SIMULINK environment. For the demonstration of the remote FD system, a BSC wireless communication channel was employed with additional source (uniform quantizer) and channel coding mechanism. Four reliability classes were defined to characterize the quality of communication channels. With the $(8, 8)$-code, the eleven different faults, including actuator faults, sensor faults and component faults, were detected with $FAR \leq 4\%$. In the FD system of NCSs, the Ethernet provided by Truetime Toolbox was applied to connect the controller/FD, actuators and sensors, and a logarithmic quantizer was used. The faults were detected, except the one in Pump 2. The FAR was guaranteed to be below 6.25%. For different types of faults, three evaluated residual signals have different patterns, which may be useful for the purpose of fault isolation. It can be observed from the simulation results that, without considering the variances of residual signals there could be lots of false alarms, and with the proposed residual evaluation methods the amount of false alarms was significantly reduced and the FAR was upper bounded.

As possible future work, some of the obtained results can be extended. Firstly, the assumption of the initial mode distribution of Markov chain can be relaxed by developing new bounded real lemma of MJLSs, such that the variance of residual signals can be computed with any given initial distribution. Secondly, an alternative design approach of optimal residual generators can also be derived which is directly related to the unified solution proposed in [19] and does not concern the model matching problem. Thirdly, the system disturbance is assumed to be deterministic, but it can also be stochastic. Then the design of FD system becomes a pure stochastic problem and new residual generation and evaluation methods should be designed. The Kalman filter and general likelihood theory [18] could be possible methodologies. Besides, there are some works on the topic of fault tolerant or reliable control [120] over networks published very recently. In [63] the active fault tolerant scheme for system with transmission delays has been proposed. In [98] a fault tolerant control approach has been formulated in the framework of MJLSs. In [78] the adaptive fault diagnosis observer has been designed to estimate the fault shape for the purpose of fault identification and faut tolerant control of NCSs. It could be an interesting topic for future work. Another challenging research direction is to investigate the FD problem of nonlinear systems with and without networks [89], which is the one of the hottest topics in the control society.

Bibliography

[1] C. Aubrun, D. Sauter, and J. Yame. Fault diagnosis of networked control systems. *Int. J. Appl. Math. Comput. Sci.*, 18:525–537, 2006.

[2] R. Beard. *Failure accomodation in linear systems through self reorganization.* PhD dissertaion, MIT, 1971.

[3] M. Blanke, M. Kinnaert, J. Lunze, and M. Staroswiecki. *Diagnosis and fault-tolerant control.* Springer, 2003.

[4] S. Boyd, L. Ghaoui, and E. Feron. *Linear matrix inequalities in systems and control theory.* SIAM, 1994.

[5] R.W. Brockett and D. Liberzon. Quantized feedback stabilization of linear systems. *IEEE Trans. Automat. Contr.*, 45:1279–1289, 2000.

[6] M. Carson and D. Santay. Nist net – a linux based network emulation tool. *Computer Communication Review*, 33:111–126, 2003.

[7] A. Cervin, M. Ohlin, and D. Henriksson. Simulation of networked control systems using Truetime. In *Procceding of 3rd International Workshop on Networked Control Systems: Tolerant to Faults.* Nancy, France, 2007.

[8] H. Chan and Ue. Oezguener. Closed-loop control of systems over a communication network with queues. *Int. J. Contr.*, 60(3):493–510, 1995.

[9] J. Chen and R.J. Patton. Standard H_∞ filtering formulation of robust fault detection. In *Procceding of 4st IFAC Symp. SAFEPROCESS*, pages 256–261, 2000.

[10] H. Chizeck, A. Willsky, and D. Castanon. Discrete-time Markovian-jump linear quadratic optimal control. *Int. J. Control*, 43:213–231, 1986.

[11] E.Y. Chow and A.S. Willsky. Analytical redundancy and the design of robust failure detection systems. *IEEE Trans. Automat. Contr.*, 29:603–614, 1984.

[12] O. Costa and M. Fragoso. Stability results for discrete-time linear systems with Markovian jumping parameter. *J. Math. Anunal Application*, 179:154–178, 1993.

[13] O. Costa and S. Guerra. Robust linear filtering for discrete-time hybrid Markov linear systems. *Int. J. Control*, 75:712–727, 2002.

[14] O.L.V. Costa and J.B.R. do Val. Full information H_∞-control for discrete infinite Markov jump parameter systems. *J. Math. analysis and application*, 202:578–603, 1996.

[15] T.M. Cover and J.A. Thomas. *Elements of information theory.* New York: Wiley, 1991.

[16] F.A. Cuzzola and M. Morari. An LMI approach for H_∞ analysis and control of discrete-time piecewise affine systems. *Int. J. Control*, 75:1293–1301, 2002.

[17] C.E. de Souza and M.D. Fragoso. H_∞ filtering for Markovian jump linear systems. *Int. J. Syst. Sci.*, 33:909–915, 2002.

[18] S.X. Ding. *Model-based fault diagnosis techniques: design schemes, algorithms, and tools*. Springer, 2008.

[19] S.X. Ding, P.M. Frank, E.L. Ding, and T. Jeinsch. A unified approach to the optimization of fault detection systems. *Int. J. Adaptive & Control Signal Process*, 14:725–745, 2000.

[20] X. Ding and P.M. Frank. Fault detection via optimally robust detection filters. In *Procceding of 28st IEEE Conference on Decision and Control*, pages 1767–1772, 1989.

[21] X. Ding and P.M. Frank. Fault detection via factorization approach. *System and contr. Letters*, 14:431–436, 1990.

[22] X. Ding and P.M. Frank. Frequency domain approach and threshold selector for robust model-based fault detection and isolation. In *Procceding of 1st IFAC Symp. SAFEPROCESS*, pages 307–312, 1991.

[23] X. Ding and L. Guo. An approach to time domain optimization of observer based fault detection systems. *Int. J. Control*, 69(3):419–442, 1998.

[24] Y. Dong, Q. Han, and J. Lam. Network-based robust H_∞ control of systems with uncertainty. *Automatica*, 41(6):999–1007, 2007.

[25] N. Elia and S. Mitter. Stabilization of linear systems with limited information. *IEEE Trans. Automat. Contr.*, 46:1384–1400, 2001.

[26] A. Emami-Naeini, M. Akhter, and S. Rock. Effect of model uncertainty on failure detection: The threshold selector. *IEEE Trans. Automat. Contr.*, 33:1106–1115, 1988.

[27] M. Epstein, L. Shi, A. Tiwari, and R.M. Murray. Probabilistic performance of state estimation across a dropout network. *Automatica*, 44:3046–3053, 2008.

[28] J. Filipiak. *Modelling and control of dynamic flows in communication networks.* Springer, 1988.

[29] M.D. Fragoso, J.B.R. do Val, and D.L. Pinto. Jump linear H_∞-control: The discrete-time case. *Control Theory Adv. Tech.*, 10:1459–1474, 1995.

[30] P.M. Frank. Fault diagnosis in dynamic systems using analytical and knowledge-based redundancy – a survey. *Automatica*, 26:459–474, 2003.

[31] P.M. Frank, S.X. Ding, and T. Marcu. Model-based fault diganosis in technical processes. *Trans. of the Institute of Measurement and control*, 22:57–101, 2000.

[32] P.M. Frank and X. Ding. Frequency domain approach to optimally robust residual generation and evaluation for model-based fault diagnosis. *Automatica*, 30:789–794, 1994.

[33] E. Frisk and L. Nielsen. Robust residual generation for diagonsis including a reference model for residual behavior. *Automatica*, 42:437–445, 2006.

[34] E. Frisk and M. Nyberg. A minimal polynomial basis solution to reisdual generation for fault diagnosis in linear systems. *Automatica*, 37:1417–1424, 2001.

[35] M. Fu and L. Xie. The sector bound approach to quantized feedback control. *IEEE Trans. Automat. Contr.*, 50(11):1698–1711, 2005.

[36] R.G. Gallager. *Information theory and reliable communication*. New York: Wiley, 1968.

[37] H. Gao and T. Chen. H_∞ estimation for uncertain system with limited communication capacity. *IEEE Trans. Automat. Contr.*, 52:2070–2084, 2007.

[38] H. Gao, T. Chen, and J. Lam. A new delay system approach to network-based control. *Automatica*, 44(1):39–52, 2008.

[39] H. Gao, T. Chen, and L. Wang. Robust fault detection with missing measurements. *Int. J. Control*, 81:804–819, 2008.

[40] M .Garcia-Rivera and A. Barreiro. Analysis of networked control systems with drops and variable delays. *Automatica*, 43(12):2054–2059, 2007.

[41] W. Ge and C. Fang. Detection of faulty components via robust observation. *Int. J. Contr.*, 47:581–599, 1988.

[42] R.M. Gray and D.L. Neuhoff. Quantization. *IEEE Trans. Info. Theory*, 44(6):2325–2383, 1998.

[43] H. Haimovich, M.M. Seron, and G.C. Goodwin. Geometric characterization of multivariable quadratically stabilizing quantizer. *Int. J. Contr.*, 79:845–857, 2006.

[44] X. He, Z. Wang, Y.D. Ji, and D.H. Zhou. Network-based fault detection for discrete-time state-delay systems: A new measurement model. *Int. J. Adapt. Control Signal Process*, page in Press, 2008.

[45] X. He, Z. Wang, and D.H. Zhou. Network-based robust fault detection with incomplete measurements. *Int. J. Adapt. Control Signal Process*, 22:510–528, 2008.

[46] D. Henry and A. Zolghadri. Design and analysis of robust residual generators for systems under feedback control. *Automatica*, 41(2):251–264, 2005.

[47] M. Hou and P.C. Mueller. Fault detection and isolation observers. *Int. J. Contr.*, 60:827–846, 1994.

[48] M. Hou and R.J. Patton. Input observability and input reconstruction. *Automatica*, 34:789–794, 1998.

[49] L. Hu, T. Bai, P. Shi, and Z. Wu. Sampled-data control of networked linear control systems. *Automatica*, 43:903–911, 2007.

[50] M. Huang and S. Dey. Stability of Kalman filtering with Markovian packet dropouts. *Automatica*, 43:598–607, 2007.

[51] V. Ionescu and C. Oara. Spectral and inner-outer factorizations for discrete-time systems. *IEEE Transactions on Automatic Control*, 41:1840–1845, 1996.

[52] H. Ishii and T. Basar. Remote control of LTI systems over networks with state quantization. *System & Control Letters*, 54:15–31, 2005.

[53] I. Izadi, T. Chen, and Q. Zhao. Norm invariant discretization for sampled-data fault detection. *Automatica*, 41:1633 – 1637, 2005.

[54] I. Izadi, Q. Zhao, and T. Chen. Optimal design of fast rate fault detection schemes based on multirate sampled data. *IFAC Journal of Process Control*, 15:307 – 319, 2005.

[55] Y. Ji and H. Chizeck. Jump linear quadratic gaussian control: Steady-state solution and testable conditions. *Control Theory Adv. Technol.*, 6:289–318, 1990.

[56] Y. Ji, H. Chizeck, X. Feng, and K. Loparo. Stability and control of discrete-time jump linear systems. *Control Theory Adv. Technol.*, 7:247–270, 1991.

[57] Z. Jin, V. Gupta, and R.M. Murray. State estimation over packet dropping networks using multiple description coding. *Automatica*, 42:1441–1452, 2007.

[58] A. Johansson, M. Bask, and T. Norlander. Dynamic threshold generators for robust fault detection in linear system with parameter uncertainty. *Automatica*, 42:1095–1106, 2006.

[59] H. Jones. *Failure detection in linear systems.* PhD dissertaion, MIT, 1973.

[60] M.J. Khosrowjerdi, R. Nikoukhah, and N. Safari-Shad. Fault detection in a mixed H_2/H_∞ setting. *IEEE Trans. Automat. Contr.*, 50(7):1063–1068, 2005.

[61] R. Krtolica, Ue. Oezguener, H. Chan, H. Goektas, J. Winkelman, and M. Liubakka. Stability of linear feedback systems with random communication delays. *Int. J. Contr.*, 59(4):925–953, 1994.

[62] Q. Li and D.L. Mills. Jitter-based delay-boundary prediction of wide-area networks. *IEEE Journal on Selected Areas in Communications*, 9(5):578–590, 2001.

[63] S. Li, D. Sauter, C. Aubrun, and J. Yame. Stability guaranteed active fault-tolerant control of networked control systems. *J. Control Sci. and Eng.*, page in Press, 2008.

[64] W. Li and S. X. Ding. On fault detection of networked control systems. In *Proceedings of 7th IFAC Symposium on SAFEPROCESS*. Barcelona, Spain, 2009.

[65] W. Li and S.X. Ding. Remote fault detection system design with online reliability information. *Int. J. Systems Science*, accepted, 2009.

[66] W. Li and S.X. Ding. Integrated design of an observer-based fault detection system over unreliable digital channels. In *Procceding of 47th IEEE Conference on Decision and Control*, pages 2710–2715. Cancun, Mexico, December 2008.

[67] W. Li, P. Zhang, and S. X. Ding. Fault detection of networked control systems with quantized residuals. In *2nd NeCST Workshop on Networked Control Systems and Fault Tolerant Control*. Rende, Italy, November 2006.

[68] W. Li, P. Zhang, S.X. Ding, C. Chihaia, and O. Bredtmann. Fault detection over noisy channels. In *Procceding of 46th IEEE Conference on Decision and Control*, pages 5050–5055, New Orleans, USA, 2007.

[69] W. Li, P. Zhang, S.X. Ding, I.C. Chihaia, E. Goldschmidt, O. Bredtmann, and A. Czylwik. Networked fault detection systems with noisy data transmission. *at Automatisierungstechnik*, 56(1):49–57, 2008.

[70] F.L. Lian, J.R. Moyne, and D.M. Tilbury. Performance evaluation of control networks: Ehternet, controlnet, and devicenet. *IEEE Control Systems Magazine*, 21(1):66–83, 2001.

[71] D. Liberzon. Hybrid feedback stabilization of systems with quantized signals. *Automatica*, 39:1543–1554, 2003.

[72] S. Lin and D.J. Costello. *Error control coding*. Prentice Hall, 2004.

[73] J. Liu, J.L. Wang, and G.H. Yang. An LMI approach to minimum sensitivity analysis with application to fault detection. *Automatica*, 41:1995–2004, 2005.

[74] D. Llanos, M. Staroswiecki, J. Colomer, and J. Melendez. Transmission delays in residual computation. *IET Control Theory Appl.*, 1(5):1471–1476, 2007.

[75] X. Lou, A. Willsky, and G. Verghese. Optimally robust redundancy relations for failure detection in uncertain system. *Automatica*, 22:333–344, 1986.

[76] R. Luck and A. Ray. An observer-based compensator for distributed delays. *Automatica*, 26(5):903–908, 1990.

[77] R. Luck and A. Ray. Experimental verification of a delay compensation algorithm for integrated communication and control systems. *Int. J. Contr.*, 59(6):1357–1372, 1994.

[78] Z. Mao and B. Jiang. Fault identification and fault-tolerant control for a class of networked control systems. *Int. J. Innovative, Comput., Info. and Control*, 3(5):1121–1130, 2007.

[79] M.A. Massoumnia. A geometric approach to the synthesis of failure detection filters. *IEEE Trans. Automat. Contr.*, 31:839–846, 1986.

[80] D. Minoli and A. Schmidt. *Internet architecture*. Wiley, 1999.

[81] G.N. Nair and R.J. Evans. Exponential stability of finite-dimensional linear systems with limited data rates. *Automatica*, 39:589–593, 2003.

[82] J. Nilsson. *Real-time control systems with delays.* PHD Dissertation. Lund Institute of Technology, 1998.

[83] J. Nilsson and B. Bernhardsson. Stochastic analysis and control of real-time systems with random time delays. *IEEE Trans. Contr. Syst. Tech.*, 34(3):57–64, 1998.

[84] NS2. Ns2 - network simulator. www.nsnam.isi.edu, accessed Jan. 2009.

[85] M. C. DE. Oliveira, J. C. Geromel, and J. Bernussou. Extended H_2 and H_∞ norm characterizations and controller parameterization for discrete-time systems. *Int. J. Control*, 75(9):666–679, 2002.

[86] A. Papoulis. *Probability, random variables, and stochastic process.* McGraw-Hill, 1991.

[87] R. Patton, P.M. Frank, and R. N. Clark. *Issues of fault diagnosis for dynamic systems.* Springer, 2002.

[88] R.J. Patton and J. Chen. On eigenstructure assignment for robust fault diagnosis. *Int. J. Robust and Nonlinear Control*, 10(14):1193–1208, 2000.

[89] A. M. Pertew, H. J. Marquez, and Q. Zhao. H_∞ observer design for Lipschitz nonlinear systems. *Int. J. Appl. Math. Comput. Sci.*, 51:1211–1216, 2006.

[90] M.L. Rank and H. Niemann. Norm based design of fault detectors. *Int. J. Contr.*, 72(9):773–783, 1999.

[91] D. Sauter and F. Hamelin. Frequency domain optimization for robust fault detection and isolation in dynamic systems. *IEEE Trans. Automat. Contr.*, 44:878–882, 1999.

[92] D. Sauter, S. Li, and C. Aubrun. Robust fault diagnosis of networked control systems. *Int. J. Adapt. Control Signal Process*, page in Press, 2008.

[93] S. Schakkottai, A. Kumar, A. Karnik, and A. Anvekar. TCP performance over end-to-end rate control and stochastic available capacity. *IEEE Trans. Networking*, 9(4):377–391, 2001.

[94] C. Scherer, P. Gahinet, and M. Chilali. Multiobjective output-feedback control via LMI optimization. *IEEE Trans. Automat. Contr.*, 42:896–911, 1997.

[95] P Seiler and R. Sengupta. A bounded real lemma for jump systems. *IEEE Trans. Automat. Contr.*, 48:1651–1654, 2003.

[96] B. Sinopoli, L. Schenato, M. Franceschetti, K. Poolla, M.I. Jordan, and S.S. Sastry. Kalman filtering with intermittent observations. *IEEE Trans. Automat. Contr.*, 49(9):1453–1464, 2004.

[97] W. Stallings. *Data and computer communication.* Prentice-Hall, 2000.

[98] F. Tao and Q. Zhao. Synthesis of active fault tolerant control based on Markovian jump system models. *IET Control Theory and Applications*, 1:1160–1168, 2003.

[99] S. Tatikonda and S. Mitter. Control over noisy channels. *IEEE Trans. Automat. Contr.*, 49:1549–1561, 2004.

[100] S. Tatikonda and S. Mitter. Control under communication constraints. *IEEE Trans. Automat. Contr.*, 49:1056–1068, 2004.

[101] S. Tatikonda and S. Mitter. Stochastic linear control over a communication channel. *IEEE Trans. Automat. Contr.*, 49:1549–1561, 2004.

[102] Y. Tipsuwan and M. Chow. Control methodologies in networked control systems. *Control Eng. Practice*, 11:1099–1111, 2003.

[103] A. Varga. Computational issues in fault detection filter design. In *Procceding of 41st IEEE Conference on Decision and Control*, pages 4760–4765, Las Vegas, USA, 2002.

[104] J.L. Wang, G. Yang, and J. Liu. An LMI approach to H_- index and mixed H_-/H_∞ fault detection observer design. *Automatica*, 43:1656–1665, 2007.

[105] Y. Q. Wang, H. Ye, and G. Z. Wang. Fault detection of NCS based on eigendecomposition, adaptive evaluation and adaptive threshold. *Int. J. Control*, 80:1903–1911, 2007.

[106] Y.Q. Wang, S.X. Ding, H. Ye, and G.Z. Wang. A new fault detection scheme for networked control systems subject to uncertain time-varying delay. *IEEE Trans. Signal Processing*, 56:5258–5268, 2008.

[107] A. Willig. A new class of packet- and bit-level models for wireless channels. In *Proc. of 13th IEEE Intl. Symp. on Personal, Indoor and Mobile Radio Communications*. Lisboa, Portugal, September 2002.

[108] J. Wu and T. Chen. Design of networked control systems with packet dropouts. *IEEE Trans. Automat. Contr.*, 52:1314–1319, 2007.

[109] N. Xiao, L. Xie, and M. Fu. Kalman filtering over unreliable communication networks with bounded Markovian packet dropouts. *Int. J. Robust Nonlinear Control*, page in Press, 2008.

[110] L. Xie. Output feedback H_∞ control of systems with parameter uncertainty. *Int. J. Control*, 63:741–750, 1996.

[111] J. Xiong and J. Lam. Stabilization of linear systems over networks with bouned packet dropout. *Automatica*, 43:80–87, 2007.

[112] H. Ye, S. Ding, and G. Wang. Integrated design of fault detection systems in time-frequency domain. *IEEE Trans. Automat. Contr.*, 47(2):384–390, 2002.

[113] H. Ye and S.X. Ding. Fault detection of networked control systems with network-induced delay. In *Proceedings of the 8th International Conference on Control, Automation, Robotics and Vision*, pages 294–297. Kunming, China, 2004.

[114] H. Ye, R. He, H. Liu, and G.Z. Wang. A new approach for fault detection of networked control systems. In *Proceedings of the IFAC 14th Symposium on System Identification*, pages 654–659. Newcastle, Australia, 2006.

[115] L. Zhang, P. Shi, C. Wang, and H. Gao. Robust H_∞ filtering for switched linear discrete-time systems with polytopic uncertainties. *Int. J. Adapt. Control Signal Process*, 20:291–304, 2006.

[116] P. Zhang and S.X. Ding. On fault detection in linear discrete-time, periodic, and sampled-data systems. *Journal of Control Science and Engineering*, 2008:18 pages, 2008.

[117] P. Zhang, S.X. Ding, P. Frank, and M. Sader. Fault detection of networked control systems with missing measurements. In *Proc. of 5th Asian Control Conference*, pages 1258–1263, Melbourne, Australia, 2004.

[118] P. Zhang, S.X. Ding, G. Wang, and D. Zhou. Fault detection of linear discrete-time periodic systems. *IEEE Trans. Automat. Contr.*, 50(2):239–244, 2005.

[119] P. Zhang, S.X. Ding, G.Z. Wang, and D.Z. Zhou. Fault detection for multirate sampled-data systems with time delay. *Int. J. Control*, 75:1457–1471, 2002.

[120] Q. Zhao and J. Jiang. Reliable state feedback control system design against actuator failures. *Automatica*, 34:1267 – 1272, 1998.

[121] M. Zhong, S.X. Ding, J. Lam, and H. Wang. LMI approach to design robust fault detection filter for uncertain LTI systems. *Automatica*, 39:543–550, 2003.

[122] M. Zhong, H. Ye, P. Shi, and G. Wang. Fault detection for Markovian jump systems. *IEE Proc. Control Theory Appl.*, 152:397–402, 2005.

[123] K. Zhou. *Essential of robust control*. Prentice-Hall, 1998.